

THERMOKARST-POND PLANT COMMUNITY CHARACTERISTICS AND EFFECTS ON ICE-WEDGE DEGRADATION IN THE PRUDHOE BAY REGION, ALASKA

By

Emily Watson-Cook, B.S.

A Thesis Submitted in Partial Fulfillment of the Requirements

for the Degree of

Master of Science

in

Biological Sciences

University of Alaska Fairbanks

December 2022

APPROVED:

Dr. Donald A. Walker, Committee Chair

Dr. Amy L. Breen, Committee Member

Dr. Martha K. Raynolds, Committee Member

Dr. Roger W. Ruess, Committee Member

Dr. Diane Wagner, Chair

Department of Biology and Wildlife

Dr. Karsten Hueffer, Interim Dean

College of Natural Science and Mathematics

Dr. Richard Collins, *Director of the Graduate School*

Abstract

Ice-wedge thermokarst ponds are forming in many areas of the Arctic as a result of climate warming and infrastructure development. Previous research suggests that development of aquatic vegetation within these ponds may create negative feedbacks to the process of ice-wedge degradation by reducing pond-bottom temperatures and thaw depths. The objectives of this research were to characterize thermokarst-pond plant communities and to evaluate the effects of vegetation on within-pond sediment temperatures and thaw depths. Aquatic vegetation was sampled in 39 plots within 29 thermokarst ponds in the Prudhoe Bay region of Alaska. Five floristically distinct plant communities were identified: *Calliergon richardsonii* comm., *Scorpidium scorpioides* comm., *Pseudocalliergon turgescens* comm., *Hippuris vulgaris* comm., and *Ranunculus gmelinii* comm. These communities had low species diversity (mean species richness 3.2 ± 1.5 SD) and were best differentiated by the single dominant species included in plant-community names. Ordination of species composition data revealed a temperature gradient, along which high biomass was associated with low sediment temperature and shallow thaw depth. The *C. richardsonii* and *P. turgescens* moss-dominated communities had very high biomass values ($3079 \text{ g/m}^2 \pm 1895$ SD and $3135 \text{ g/m}^2 \pm 585$ SD, respectively). Examinations of temperature and thaw differences between communities were limited by sample size, as several communities were described based on only two plots each.

To evaluate the potential insulative role of pond vegetation on pond-bottom temperature and thaw depth, differences between broad vegetation types (i.e., moss, forb, sparse) rather than communities were examined. Vegetation cover, total biomass, biomass of plant functional types, and soil organic horizon thickness were sampled, along with mean thaw depth and sediment temperature. Linear mixed-effects models were used to identify vegetation-related parameters

with the highest predictive power of thaw and temperature. Mean sediment temperatures measured during 19 July – 23 August 2021 were warmest in the sparse plots ($8.9^{\circ}\text{C} \pm 0.2$ SE) compared to the forb plots ($8.2^{\circ}\text{C} \pm 0.3$ SE) and the moss plots ($6.7^{\circ}\text{C} \pm 0.4$ SE). Moss plots also had shallower late-August thaw depths (42.5 cm ± 1.3 SE) compared to forb (52.7 cm ± 1.7 SE) and sparse (52.7 cm ± 1.4 SE) plots. Vegetation cover was negatively correlated with sediment temperature, whereas vegetation cover, moss thickness, and organic layer thickness were all negatively correlated with thaw depth. The stronger relationships observed between vegetation-related factors and thaw depth compared to sediment temperature were probably affected by the short period of temperature observations within this study. Although stochastic factors likely play a role in community establishment within thermokarst ponds, additional sampling is needed across all pond ages, ice-wedge degradation/stabilization stages, and a broader range of habitats within ponds to discern if there is a clear successional trajectory for thermokarst-pond plant communities. This study provided descriptions of relatively understudied aquatic plant communities that play an important role in Arctic landscape change. Notably, very high biomass values were found in young ponds (one with an age of only 8 years) dominated by moss communities. Results indicate that aquatic plant communities with high moss biomass have high capacity for insulation that potentially reduces permafrost thaw and ice-wedge degradation, leading to ice-wedge stabilization.

Table of Contents

	Page
Abstract.....	i
Table of Contents	iii
List of Figures.....	v
List of Tables	vii
List of Appendices.....	viii
Acknowledgements	ix
1. Introduction.....	1
1.1 Climate change, ice-wedge polygons, and thermokarst ponds	1
1.2 Thermokarst-pond vegetation	3
1.3 Objectives and general outline of the study	6
2. Methods.....	6
2.1 Thermokarst-pond plant communities	6
2.1.1 Study area	6
2.1.2 Plot sampling	9
2.1.3 Biomass sampling.....	11
2.1.4 Soil sampling	12
2.1.5 Temperature measurements.....	13
2.1.6 Estimated pond age	15
2.1.7 Plant community analyses	15
2.1.7a Cluster analysis and synoptic table	16
2.1.7b Environmental gradient analysis.....	17
2.2 Temperature and thaw analyses	18
3. Results	20
3.1 Plant community analyses	20
3.1.1 Cluster analysis and synoptic table	20
3.1.2 Community descriptions	23
3.1.3 Community comparisons	37
3.1.4 Pond age	40
3.1.5 Temperature measurements.....	41
3.1.6 Environmental gradient analysis.....	44
3.2 Temperature and thaw analyses	47
4. Discussion.....	54
4.1 Thermokarst-pond plant communities	54
4.1.1 Community gradients.....	54

<i>4.1.2 Pond age and succession</i>	56
4.2 Effect of vegetation on thermal properties	59
<i>4.2.1 Role of moss in ice-wedge stabilization</i>	59
<i>4.2.2 Predictors of temperature and thaw</i>	62
4.3 Connecting community composition with thaw dynamics	64
4.4 Recommendations for future study	65
5. Conclusions	68
References	70

List of Figures

	Page
Figure 1	7
Sampling design.	
Figure 2	10
Photo of thermokarst-pond plot.	
Figure 3.	11
Photos of coring device used to collect biomass and soil samples.	
Figure 4	21
Dendrogram resulting from cluster analysis of species cover data.	
Figure 5	25
<i>Calliergon richardsonii</i> community.	
Figure 6	27
<i>Scorpidium scorpioides</i> community.	
Figure 7	29
<i>Hippuris vulgaris</i> community.	
Figure 8	31
<i>Pseudocalliergon turgescens</i> community.	
Figure 9	33
<i>Ranunculus gmelinii</i> community.	
Figure 10	37
Bar graph showing mean values of key vegetation characteristics.	
Figure 11	38
Bar graph showing mean values of key pond characteristics.	
Figure 12	39
Bar graph showing mean values of key soil characteristics.	
Figure 13	41
Occurrence of clusters and vegetation types within pond age categories.	
Figure 14	43
Mean daily water temperature over period of study (19 July – 23 August 2021) for each cluster:	

Figure 15	45
NMDS ordination of thermokarst-pond plots.	
Figure 16	48
Mean daily water temperature over period of study (19 July – 23 August 2021) for each vegetation type.	
Figure 17	Error! Bookmark not defined.
Boxplots showing (a.) mean measured sediment temperature and (b.) mean thaw depth by plot type.	
Figure 18	50
Correlations of mean sediment temperature (squared for normality) with various predictor variables.	
Figure 19	51
Correlations of mean thaw depth with various predictor variables.	
Figure 20.	52
Partial residual plots from a mixed effects model of mean sediment temperature (squared).	
Figure 21.	52
Partial residual plots from a mixed effects model of mean thaw depth.	
Figure 22.	52
Standardized effect sizes of predictor variables from models.	
Figure 23.	65
Conceptual diagram of possible function of thermokarst-pond plant communities in trajectory of thaw.	
Figure 24.	67
Occurrence of dominant vegetation types within pond age categories.	

List of Tables

	Page
Table 1.....	22
Synoptic table of fidelity (Φ), frequency (%), and mean cover (%) of taxa.	
Table 2.....	23
Key environmental variables for thermokarst-pond clusters.	
Table 3.....	40
Pond age group categories (A – D), descriptions, and number of plots.	
Table 4.....	46
Correlations of environmental variables with axes of NMDS ordination.	
Table 5.....	54
Results of mixed-effects models of mean sediment temperature and mean thaw depth.	
Table 6.....	59
Pond approximate age (yrs), total biomass (g/m ²), and aboveground net primary production.	

List of Appendices

	Page
Appendix A.....	71
Environmental data summary.	
Appendix B.....	79
Species matrix.	
Appendix C.....	80
Environmental matrix.	
Appendix D.....	82
Soils data.	
Appendix E.....	83
Biomass data.	
Appendix F.....	84
Species list.	
Appendix G.....	85
Additional plot maps of NIRPO and JS sites.	

Acknowledgements

This research was funded as part of the Navigating the New Arctic: Ice-Rich Permafrost Systems project through the National Science Foundation (NNA-IRPS, NSF Award # 1928237). Additional funding was obtained through the UAF Thesis Completion Fellowship and the UAF Student Support Fund. I would like to thank my committee members, who have provided extensive support, encouragement, and thoughtful perspective in the completion of this project: Prof. Donald “Skip” Walker (major advisor), Dr. Martha Reynolds, Dr. Amy Breen, and Prof. Roger Ruess. I would like to thank members of the NNA-IRPS project for valuable input in developing this project, including Jana Peirce, Dr. Mikhail Kanevskiy, Dr. Anna Liljedahl, Dr. Ronald Daanen, and Dr. Ben Jones. I am very thankful to Dr. Martha Reynolds and Sam Dashevsky for providing essential help and materials in the construction of the biomass/soil coring device. I would like to acknowledge Dr. John D. Madsen, who published a design of a biomass core sampler and provided useful advice on modifying the device. I would like to thank Jana Peirce for help with temperature data processing, and for high-quality field photos of thermokarst ponds. I would also like to thank Zoe Meade and Josephine Mahoney for assisting with field sampling and for making long days in cold ponds thoroughly enjoyable. I am thankful to Richard Ranft at the UAF Forest Soils Lab for help with soils analyses, and to Brian Heitz at the UAF Herbarium for help with nonvascular plant identification. I am thankful to my family, Jill Watson and Lucy Watson-Cook, for their ongoing support and enthusiasm regarding my research. I am also thankful to my partner, Brandon Ebersohl, for assisting with data processing and for ensuring that I get outside every once in a while.

1. Introduction

Ice-wedge thermokarst ponds are increasingly frequent within many Arctic landscapes (Jorgenson et al., 2006; Liljedahl et al., 2016), yet much is unknown about the vegetation found within these features and the role it plays in overall ecosystem function. This study aims to examine the plant communities that have developed in thermokarst ponds and to determine whether these plant communities influence within-pond temperatures and thaw dynamics. The area of study was within the Prudhoe Bay oilfield of northern Alaska, a region characterized by continuous permafrost, thaw lakes, ice-wedge polygons, and increasingly abundant thermokarst ponds (Walker et al., 1980; Walker et al., 2022).

1.1 Climate change, ice-wedge polygons, and thermokarst ponds

Average surface temperatures in the Arctic have increased at approximately three times the rate of the rest of the Northern Hemisphere over the past decade (AMAP, 2021). Arctic regions store as much as 50% of global soil carbon within permafrost soils, and the release of greenhouse gases following thaw provides a positive feedback that can accelerate climate warming (Schuur et al., 2015; Crowther et al., 2016). Areas with a high volume of ground ice near the upper portion of permafrost are at high risk for thaw and subsequent ground surface subsidence, which leads to the development of thermokarst terrain (Nelson et al., 2001). Ice wedges are large subsurface masses of approximately wedge-shaped ice that form as repeated thermal contraction cracking occurs and the cracks fill with water, which freezes and expands over time to increase the ice-wedge width (van Everdingen, 1998). As a result of climate warming and infrastructure development in recent years, degradation of ice wedges has occurred throughout the circumpolar Arctic (Jorgenson et al., 2006; Schuur et al., 2015; Liljedahl et al., 2016). Pond formation may also occur over time through the thaw-lake cycle involving the

process of lake formation and drainage followed by erosion (Billings & Peterson, 1980). Climate warming increases the rate of thaw-lake-cycle-associated landscape change and the abundance of drained lake basins (Jones et al., 2022).

Landscapes at Prudhoe Bay are dominated by ice-wedge polygon terrain including low-centered and high-centered polygons (Everett, 1980b). Low-centered polygons consist of a central basin, a raised rim around the basin, and a surrounding trough that is centered over the ice wedge (Kanevskiy et al., 2013). Low-centered polygons were previously the most common polygon type in the Prudhoe Bay region (Walker et al, 1980), but in recent years many low-centered polygons in the region have transitioned to high-centered polygons due to ice-wedge degradation and resulting polygon-rim erosion (Kanevskiy et al., 2022). As polygon troughs become deeper, snow and water accumulate in the depressions, and thermokarst ponds often form. Jorgenson et al. (2015) documented a 7.5-fold increase in waterbody area from 1949 – 2012 at his Prudhoe Bay study site. Walker et al. (2022) examined waterbody distribution on two sides of a heavily traveled gravel road between 1968 and 2016 and found a 7.6-fold increase in the waterbody area on the non-flooded side of the road, similar to the increase at the Jorgenson site, and an approximate 10-fold increase in the number of ponds. Rates of landform change due to ice-wedge degradation vary significantly throughout the Arctic depending on both surface and subsurface conditions including climate, disturbance, soil, ground ice content, topography, and vegetation (Kanevskiy et al., 2017). Surface water generally increases warming of sediments through radiation input and convective heating, which can accelerate the process of ice-wedge degradation (Jorgenson et al., 2015). However, recent coring of ice wedges in the Prudhoe Bay region revealed that even in areas where surface water accumulates, the buildup of vegetation, litter, and sediment can aid in the development of a thick intermediate layer (an ice-rich and

organic-rich layer of permafrost) above the ice wedge that can protect the ice wedge from further degradation (Kanevskiy et al., 2017, 2022).

1.2 Thermokarst-pond vegetation

Thermokarst-pond vegetation may play a significant role in ice-wedge stabilization, similar to processes in the terrestrial system. Arctic landscapes are already characterized by numerous water bodies because permafrost limits infiltration of water (Pienitz et al., 2008). Aquatic vegetation is likely to become increasingly dominant as surface-water cover expands. Due to high-latitude climate conditions, Arctic water bodies are subject to short growing seasons, highly variable annual temperature fluctuations, and winter freeze-up (Rautio et al., 2011; Vonk et al., 2015). Despite these extreme conditions, many Arctic lakes and ponds support robust communities of aquatic plants. Aquatic plants possess photosynthetically active parts that are either submerged in or floating on water (Cook, 1999). When rooted, submerged plants link the water column and underlying sediment by intercepting and modifying terrestrial material, while using the sediment as a nutrient source and for physical attachment (Carpenter & Lodge, 1986; Barko et al., 1991). In addition, they contribute to primary productivity, provide heterogeneous habitat for aquatic invertebrates and waterfowl, and play an important role in biogeochemical cycling by mobilizing nutrients and storing organic carbon (Barko & James, 1998; Bornette & Puijalon, 2009). As a result of continued warming, Arctic aquatic systems will likely experience changes including increased water temperatures, increased growing season length, and increased terrestrial nutrient input (Rautio et al., 2011). For most aquatic plant species, the water temperature range for optimal rates of photosynthesis is between 20 – 35 °C (Bornette & Puijalon, 2009), which is far warmer than the conditions typically found in Arctic water bodies. A review of data from shallow Arctic ponds and lakes, for example, indicates mean July water

temperatures range from 3 to 18 °C (Rautio et al., 2011). Increases in temperature have been found to promote aquatic plant growth (Lauridsen et al., 2019) and increases in net June radiation are associated with increased aquatic moss production (Riis et al., 2014). Nutrient availability tends to limit growth of aquatic plants in Arctic ponds (Mesquita et al., 2010; Riis et al., 2010), but permafrost thaw resulting from climate warming can increase the transfer of nutrients from terrestrial to aquatic systems (Schuur et al., 2008; Rautio et al., 2011). Warming trends may also lead to redistribution of water throughout Arctic landscapes, especially in areas where ice-wedge degradation has resulted in the formation of new thermokarst ponds and new drainage networks linking them (Liljedahl et al., 2016). Regional increases in surface water cover are associated with increases in cover of aquatic vegetation throughout landscapes (Magnússon et al., 2021). Abundance of aquatic vegetation is likely to increase following increased temperature, growing season length, and nutrient input, as well as expansion of available aquatic habitat, all of which may result from climate warming.

While increased temperature may initially stimulate growth, development of aquatic vegetation may ultimately lower sediment temperatures and reduce thaw within thermokarst ponds. Shallow Arctic ponds (with the exception of those that are rich in dissolved organic carbon or highly turbid) are not thought to exhibit stable summer temperature stratification of the water column when vegetation is sparse (Rautio et al., 2011). However, submerged plants in shallow aquatic systems reduce mixing by dissipating kinetic energy, thereby contributing to stratified temperature of the water column (Andersen et al., 2017). Dense aquatic vegetation can absorb and dissipate more incoming solar radiation relative to the water column and can increase vertical light attenuation, concentrating solar radiation at the top of the water column (Persson & Jones, 2008). In addition, aquatic plant biomass in shallow ponds correlates with the steepness of

the vertical temperature gradient (Dale & Gillespie, 1977). If aquatic vegetation in thermokarst ponds functions in a similar way, this may maintain lower temperatures at the sediment surface, potentially decreasing ground ice thaw. In terrestrial systems, vegetation in general preserves permafrost by lowering ground temperatures (Shur & Jorgenson, 2007), and vegetation colonization plays a role in recovery of degraded permafrost by insulating thawed soil and causing ground ice to aggrade (Shur et al., 2011). Mosses have been especially noted as associated with decreases in thaw depth and increases in recovery of permafrost (Magnússon et al., 2020). Mosses insulate soil by reducing evapotranspiration and reducing partitioning of radiation into ground heat flux (Blok et al., 2011). In thermokarst ponds, vegetation cover in areas of advanced ice-wedge degradation is dominated by aquatic mosses (Jorgenson et al., 2015). Thermokarst-pond vegetation is likely to be an important component of Arctic landscape change, given evidence for the role of aquatic vegetation in modulating feedbacks to ice-wedge degradation.

Thermokarst-pond vegetation remains relatively understudied. Previous description of aquatic vegetation in the Prudhoe Bay region focused on lake margins (Walker, 1985), due to the relative infrequency of thermokarst ponds at the time of the study. Recent increases in thermokarst ponds have occurred following ice-wedge degradation, but quantification of submerged aquatic vegetation poses unique logistical challenges in regards to sampling methodology (Madsen et al., 2007). Identifying factors that influence the process of permafrost-thaw stabilization is of particular importance given that the release of organic carbon with degradation can provide a positive feedback to climate warming (Schuur et al., 2008).

1.3 Objectives and general outline of the study

The major objectives of this study were to: 1) describe the plant communities within thermokarst ponds in the eastern portion of the Prudhoe Bay oilfield; 2) determine how these communities vary along environmental gradients; 3) quantify the factors (total percent vegetation cover, moss biomass, moss thickness, soil organic layer thickness, maximum water depth) that may influence mean sediment temperature and thaw depth within thermokarst ponds; and 4) examine relationships between plant communities and thermal properties (sediment-surface temperatures and thaw depths) of the pond bottoms. The thesis is divided into the following: Methods, Results, Discussion, and Conclusions. Each of these sections is divided into two major parts devoted to (1) thermokarst-pond plant communities and (2) temperature and thaw analyses.

2. Methods

2.1 Thermokarst-pond plant communities

2.1.1 Study area

The study took place at the Natural Ice-Rich Permafrost Observatory (NIRPO) site and the Jorgenson site (JS) (*Figure 1a*) in the eastern portion of the Prudhoe Bay oilfield, which is located along the Beaufort Sea coast of northern Alaska, USA (*Figure 1a, inset map*). The arctic climate of the Prudhoe Bay region is characterized by cold winters (-25 °C, winter mean 1991 – 2020), cool summers (6 °C, summer mean 1991 – 2020), and low precipitation (14 cm/yr, annual mean 1991 – 2020) (ACRC, 2020). Increasing trends in both temperature and precipitation have been observed since the 1980s (Walker et al., 2022). Sampling occurred during July – August 2021, a notably warm summer. Mean July temperature recorded at the nearby Deadhorse Airport was 10.9 °C which was the second warmest July (July mean 1991 – 2020 is 8.5 °C) on record

since 1968 (ACRC, 2020). Strong winds can occur year-round. In June – August, winds are typically from the north and northeast and 25% of these exceed 21.6 km/hr (Everett, 1980a). Nonacidic soils dominate the region due to wind deposition of carbonate-derived loess from the Sagavanirktok River (Walker 1985, Walker and Everett 1990).

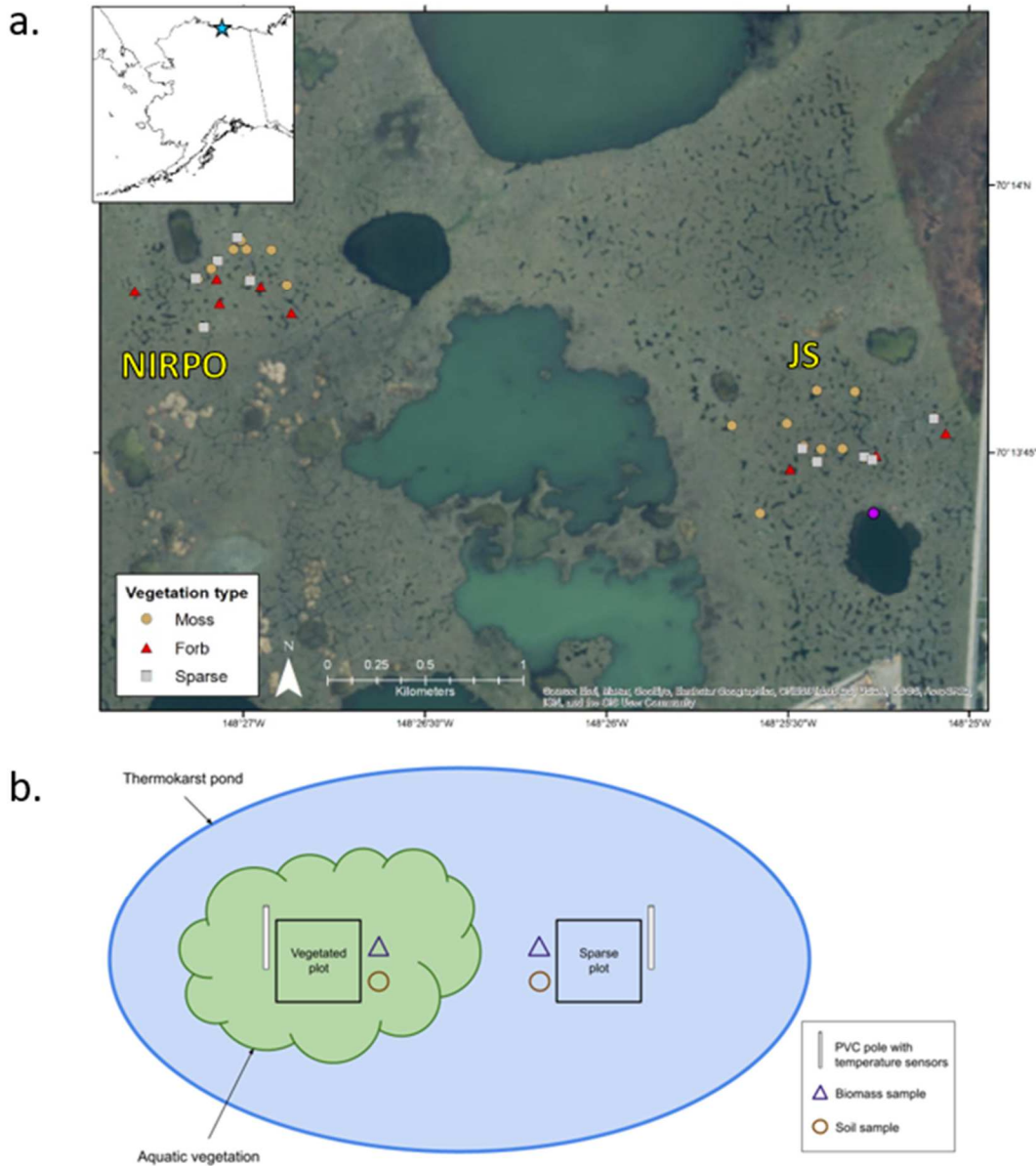


Figure 1. Sampling design, including: a. Map of study area showing both sites: NIRPO to the west and JS to the east. Points represent plots within thermokarst ponds. Purple point indicates location of temperature sensor pole in lake and inset indicates location of study area within Alaska (star). A pipeline is visible along the eastern edge of the image, and an industrial gravel pad is visible in the lower right. Lakes in the image vary in color depending on depth and substrate. Much of the area shown is dotted with small thermokarst ponds. b. Diagram of thermokarst-pond sampling scheme showing example locations of plots, sensors, and samples. Sampling included a total of 39 plots within 29 thermokarst ponds.

Descriptions and maps of the Prudhoe Bay region in the 1970s indicate the areas on older surfaces between thaw lakes and drained thaw lakes consisted primarily of relatively homogeneous landscapes characterized by low-centered polygons, low microrelief, and few thermokarst ponds (Walker et al., 1980; Walker, 1985). Continuous permafrost containing ice wedges reaches maximum depth of about 600 m in the Prudhoe Bay region, which is the greatest thickness found along the Beaufort Sea coast (Kanevskiy et al., 2011; Jorgenson et al., 2015). Sediments in northern Alaska contain an average of 11% wedge ice by volume. Although ice wedges can reach 5 m width and 4 m depth in along the Beaufort coast (Kanevskiy et al., 2017), local alluvial gravels that underlie the Prudhoe Bay region limit wedge ice depth to within about 2 m of the ground surface (Everett, 1980b). Abrupt, climate-driven increases in ice-wedge degradation began in the Prudhoe Bay region in the late 1980s as a result of warming summer temperatures and oilfield infrastructure development. Nearly 50% of examined ice wedges were continuing to degrade in the early 2010s (Kanevskiy et al., 2017). Active-layer thickness, the depth to which permafrost soil thaws annually, varies throughout the Prudhoe Bay region and has increased in the years from 1988 – 2019 (mean of 45 cm in 1988 and 70 cm in 2019) (Walker et al., 2022).

The Prudhoe Bay region is located within Bioclimate Subzone C of the Circumpolar Arctic Vegetation Map (Walker et al. 2005; Raynolds et al., 2019). Nonacidic tundra plant communities dominate the region, and are characterized by a mix of sedges, grasses, prostrate and erect dwarf shrubs, mosses, and lichens (Walker, 1985; Walker & Everett, 1991). The vegetation of ice-wedge thermokarst ponds was not examined in early descriptions of plant communities in this region because they formed a relatively minor component of the total landscape at that time. A recent study of thermokarst ponds near Prudhoe Bay in advanced stages

of ice-wedge degradation identified cover of open water, aquatic forbs (*Utricularia vulgaris* and *Hippuris vulgaris*), and aquatic mosses with calcium affinities (*Calliergon giganteum* and *Scorpidium scorpioides*) as characteristic of these features (Jorgenson et al., 2015).

2.1.2 Plot sampling

Thermokarst ponds were sampled within a study area of approximately 0.5 km² (70°14'N, 148°26'W) that included the Jorgenson Site (JS) and a portion of the NIRPO Site (Figure 1a). JS was established in 2011 to study the process of ice-wedge degradation (Jorgenson et al., 2015). NIRPO was established in 2021 in order to compare relatively undisturbed tundra to previously studied roadside areas (Walker et al., 2015, 2016, 2018). Both sites are located several kilometers north and northeast of Lake Colleen and the industrial support center near the Deadhorse Airport and are relatively undisturbed due to their distance from heavily trafficked roads. Both the JS and NIRPO sites contain large areas of well-developed ice-wedge polygons and thermokarst ponds (Jorgenson et al., 2015; Walker et al., 2022).

To sample thermokarst-pond vegetation, a total of 39 vegetation plots within 29 ponds were established: 20 at NIRPO and 19 at JS (Figure 1a). Ten ponds (five at each site) contained paired plots, with one plot located in a vegetated area of the pond and one located in a sparsely vegetated portion of the pond (Figure 1b). The remaining 19 ponds contained one vegetated plot each. Vegetated plot locations were sampled using the “centralized replicate” sampling approach (Mueller-Dombois & Ellenberg, 1974), which involved sampling 1-m² plots in the central portions of common plant communities found within thermokarst ponds. Replicate samples were obtained from areas in other ponds with similar vegetation. All plots had a mean water depth of greater than 15 cm. Sparsely vegetated plots (hereafter “sparse plots”) were positioned within

relatively unvegetated areas of ponds at least 1 m² in size. Plots were categorized into three broad types based on the dominant vegetation type: moss, forb, and sparse. Plots were square and encompassed an area of 1 m².

To examine community composition, the percentage cover of all plant species within each 1-m² plot was visually estimated using a square quadrat, which was divided with strings into 25 smaller squares (each representing 4% cover) which functioned as a visual aid (*Figure 2*). Total cover often exceeded 100% in dense stands due to overlapping canopy layers. Voucher specimens from all species found within a plot were collected. Nomenclature followed the Flora of North America (Flora of North America Editorial Committee, 1993). Within-pond vegetation was consistently rooted in the sediment and floating within the water column. The mean thickness (vertical depth) of various layers of plants (i.e., moss, forbs, emergent plants, submerged plants) within a plot was determined from the mean of three measurements using a



Figure 2. Photo of thermokarst-pond plot (21A-36) showing 1-m² plot and square quadrat, which was used as a visual aid in percent cover estimation. Photo by EWC.

meter stick. If a particular layer (i.e., moss, forb, etc.) was absent, the thickness of that layer was considered zero.

The maximum and mean within-plot water depths (based on five measurements) were measured during 23 – 24 August 2021. Thaw depth (the depth from the top of pond sediments to the top of the frozen permafrost layer) was measured at the same time in five within-plot locations with a thaw probe and meter stick. The pond dimensions were measured at the widest portion of the pond and along a line perpendicular to the maximum width.

2.1.3 Biomass sampling

To quantify aboveground biomass within thermokarst ponds, samples were collected outside each plot but within a similar homogenous area of vegetation as the plot (*Figure 3b*). Pond vegetation was always rooted, and the samples included all vegetation growing above the pond bottom within the water column. Samples were collected in late August, near the end of the growing season. A polyvinyl chloride (PVC) coring device modeled after a previously described aquatic biomass sampler (Madsen et al. 2007) was used to collect samples (*Figure 3*). The dimensions were altered from the Madsen design, and a 15.24-cm diameter steel stovepipe was

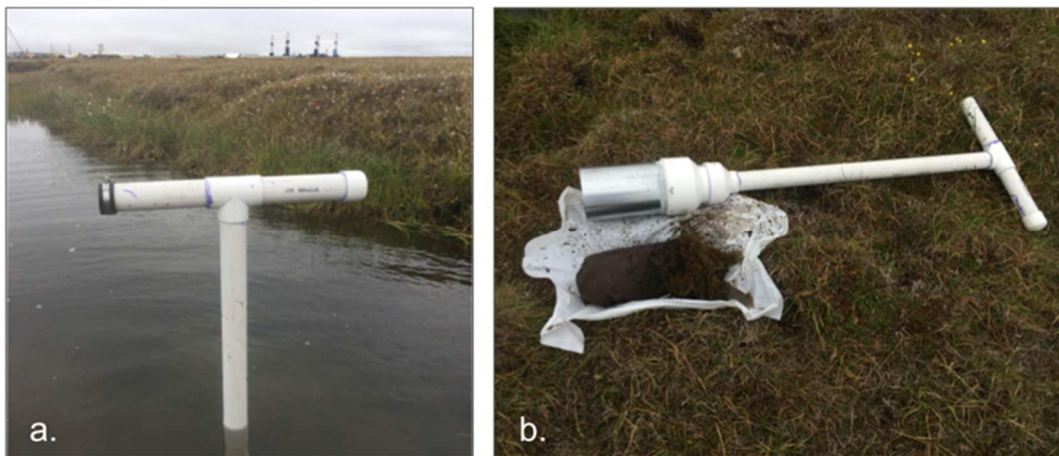


Figure 3. Photos of coring device used to collect biomass and soil samples, showing (a.) corer inserted into pond sediment with cap sealing the open handle, and (b.) intact core sample removed from the device post-extraction. Photos by EWC.

added to the end to provide a sharp coring edge, allowing the device to effectively cut through dense vegetation by rotating the corer while pushing it downward (*Figure 3b*). The corer was sealed with PVC cement, forming an air-tight tube except for the end of one handle, and a cap was placed over this handle after the corer was inserted into the sediment (*Figure 3a*). This allowed an intact sample to be removed with negative vacuum pressure holding the sample in the metal stove pipe. The sample was released from the device by removing the cap.

Each sample represented a circular coring area of 182 cm². To extract samples, the entirety of the vegetation layer was cored, as well as a small amount of the sediment layer since the additional material helped to hold the sample in the corer. Once the core was removed, a sample of aboveground biomass was obtained by cutting the core at the sediment-water interface. Samples were washed thoroughly in both the field and lab and kept cool before being sorted and dried. The samples were dried at 65 °C until a constant mass was obtained (approximately one week). Biomass samples were then sorted into the following plant functional types (PFTs): moss, forb, graminoid, and shrub. Material that was too fragmented or decomposed to identify as a particular PFT was considered litter. In this study, live and dead biomass was not differentiated due to the difficulty of differentiating live and dead mosses (particularly when these grow in a dense, continuous mat).

2.1.4 Soil sampling

To examine soil characteristics, pond sediment samples were collected adjacent to each plot during late July (*Figure 1b*) using the same coring device described above. The corer was inserted to the top of the frozen resistive permafrost layer to obtain soil cores. The thickness of the litter layer, organic horizon, and mineral horizon were measured in the field. A book of soil color chips (Munsell Color, 1975) was used to determine the hue, value, and chroma of the

mineral horizon. From the organic and mineral horizons, soil-can collections of known volume (180 cm³) were made to determine soil moisture (both gravimetric and volumetric) and bulk density. Additional collections were made from the same layers to ensure adequate material for analyses. Following collection, samples were kept frozen until they were analyzed in the UAF Forest Soils Laboratory. Soil moisture and bulk density were calculated using wet and dry sample weights (Peters, 1965; Gardner, 1986). Subsamples were dried at 65 °C until they reached a constant mass (approximately three weeks). The samples were homogenized using a mortar and pestle, and the gravel fraction was removed using a 2-mm sieve. Soil pH was determined using the saturated-paste method (McLean, 1982) and an Oakton 810 Series pH meter. The loss-on-ignition method was used to measure percent soil organic matter (SOM) (Page et al., 1982), which involved combusting samples in a furnace at 550 °C for seven hours. The Bouyoucos hydrometer method (Bouyoucos, 1936) was used to determine percentage of sand, silt, and clay for each sample.

2.1.5 Temperature measurements

To measure water and sediment temperatures, small temperature sensors (“iButton”, Maxim/Dallas Semiconductor Corp., Sunnyvale, CA, <http://www.maxim-ic.com/>) were installed within ponds. The sensors were taped to (3/4 in) PVC pipe poles that were stabilized with 3/8 in rebar. The sensors were placed in three locations: at the water surface (floating to allow for variation in water depth during the field season), at the sediment surface, and at the top of the submerged vegetation layer. In several cases of duplication, one of the three sensors was omitted. For example, if the moss layer was floating at the level of the water surface, one sensor was used to measure the temperature of both the water surface and the top of the submerged vegetation layer.

A total of 40 PVC poles were installed at the two study sites. At NIRPO, 15 poles were co-located with vegetation plots and five were co-located with sparse plots (*Figure 1b*). On the PVC poles that were co-located with sparse plots, iButtons were also placed at the water surface and at the sediment surface. Since sparse plots lacked a distinct submerged vegetation layer, the third iButton was placed at the same height above the sediment as that of the “above vegetation” sensor on the vegetated pole in the same pond. This allowed for direct comparison of temperatures in vegetated and sparsely vegetated areas. At JS, 14 poles were co-located with vegetation plots, and five poles were again co-located with sparsely vegetated plots. An additional pole was installed in a lake just south of the site (*Figure 1a*) with iButtons at the sediment and water surfaces, for comparison of temperatures in the small ponds with those of a larger lake. At both NIRPO and JS, one sensor was installed to measure air temperature. At JS, this was located on the PVC pole at plot 21A-03 at a height of 35 cm above the water surface (115 cm above the sediment), and at NIRPO this was located on the pole marking the east end of transect T6 at a height of 1 m. These sensors were attached to the PVC pole using wire and tape. A small plastic cup, which was cut to allow air flow, was placed around the sensor to limit the effects of direct sunlight.

iButton sensors were set to record measurements every 60 minutes. To waterproof the sensors, they were sealed with rubber coating, placed into the finger of a tied nitrile glove, and then placed in small, jewelry-sized plastic bags (which were not waterproof, but aided in securing the sensors to poles). Wire and duct tape were used to secure sensors to PVC poles. One sensor per pole was used to measure water surface temperature, and these were secured underneath a small square of insulation foam in order to limit the influence of direct sunlight on water surface temperature measurements.

Temperature data were downloaded from sensors and truncated such that 1) temperature data from before installation and after removal was taken out and 2) all sensor data was cut to the same time period. The resulting time period of temperature data began on 7/19/21 at 18:00 and ended on 8/23/21 at 08:00, a period of 34 days and 14 hours.

2.1.6 Estimated pond age

An attempt was made to determine the age of each pond based on the first time it was visible on aerial photos that were obtained from NV5 GeoSpatial in Anchorage, AK, through BP Exploration Alaska BPXA for a previous study (Walker et al. 2022). This photo record contained annual high-resolution (1:6000 to 1:20.000 scale) images that covered the Colleen Site (another site in the Prudhoe Bay region) for nearly all years between 1968 and 2021 (Walker et al., 2022, Supp. File S1). Most of these photos also covered the NIRPO and Jorgenson sites, but neither site was covered in years 1973 and 1988 – 1996. The age of a pond was determined from the date that the pond area was clearly covered by water. Because of the missing years of photos, pond ages were organized into four age groups of approximately 20 years each (Age group A: 1968 and earlier; B: 1969 – 1987; C: 1988 – 2007; D: 2008 – 2021), with Age Group C including the nine years of missing photos.

2.1.7 Plant community analyses

The objectives of the plant community analyses were to: 1) describe and analyze the plant communities within thermokarst ponds in the eastern portion of the Prudhoe Bay oilfield, and 2) determine how these communities vary along selected environmental gradients. All analyses were conducted using the program PC-ORD v7.08 (McCune & Mefford, 2018).

2.1.7a Cluster analysis and synoptic table

A hierarchical agglomerative cluster analysis of species-cover data was used to group plots into floristically distinct units based on species similarity, using the flexible beta group linkage method ($\beta = -0.25$), and Sørensen's distance measure (McCune & Grace, 2002). Multi-response permutation procedures (MRPP) were used to test for differences in species composition between resulting clusters. MRPP is a nonparametric alternative to discriminant analysis that does not assume multivariate normality or homogeneity of variance. Sørensen's distance measure was used, and the resulting association coefficient (A) represents chance-corrected within-group agreement (McCune & Grace, 2002).

A synoptic table summarized species information for each cluster (vegetation unit). Included in this table were the following numerical descriptors: fidelity, frequency, and dominance. *Fidelity* is a metric of a species' concentration within a given cluster and is used to determine diagnostic (characteristic) species of plant communities. The Phi coefficient of association (Φ) is a measure of fidelity that is independent of the sample size of each cluster (Tichý et al. 2006):

$$\Phi = \frac{N \cdot n_p - n \cdot N_p}{\sqrt{n \cdot N_p \cdot (N-n) \cdot (N-N_p)}},$$

where N = number of plots in the dataset, N_p = number of plots within a given cluster, n = number of occurrences of a species in the dataset, and n_p = number of occurrences of a species within a given cluster. *Frequency* is the percentage of plots of a given cluster in which the given species occurs. *Dominance* was measured as the mean percentage cover of a species in plots of a particular group. The following cutoffs were used to determine diagnostic, constant, and

dominant species for the groups: fidelity $\Phi \geq 0.25$ (high fidelity $\Phi \geq 0.5$), frequency $\geq 40\%$, and mean cover $\geq 2\%$.

2.1.7b Environmental gradient analysis

Ordination arranges plots spatially based on the similarity of species composition of the plots. To examine how plots and species varied along environmental gradients, a non-metric multidimensional scaling (NMDS) ordination was produced using the program PC-ORD v 7.08 (McCune & Mefford, 2018). Plots with similar species composition appear close together in the ordination. The NMDS ordination technique was chosen because it is robust to the presence of zero values and lacks an assumption of multivariate normality (Minchin, 1987). Relationships of the plots and species composition to environmental gradients can be shown in a variety of ways: 1) correlation of environmental variables with axis scores, 2) joint-plot diagrams with vectors showing the direction and strength of correlations of environmental variables within the ordination space, and 3) overlays showing patterns (e.g., contours of equal scores) of environmental variation or species variation within the ordination space. The package ggplot2 (Wickham, 2016) in the program R v 4.0.3 (R Core Team, 2020) was used to graph the ordination with biplot diagrams indicating the direction and strength of environmental variables with $r^2 \geq 0.2$ (McCune & Grace, 2002). Kendall's tau rank correlation coefficient (τ) for nonparametric data was used to describe the ordination axes based on correlated environmental factors. The τ cutoffs for display in the biplot were $|\tau| \geq 0.3$ for significant correlations and $|\tau| \geq 0.5$ for highly significant correlations.

One-way analysis of variance (ANOVA) was used to compare vegetation and environmental factors among clusters. Pairwise post hoc tests using Bonferroni adjustment were used to test for homogeneity of variance and normality of response variables. The following

vegetation-related variables were examined for differences in cluster means: total biomass (log transformed for normality), moss thickness (log transformed), total vegetation cover (log transformed), and species richness. Differences in cluster means of the following environmental variables were also examined: thaw depth (measured in August), water depth (August), sediment temperature, and pond width.

2.2 Temperature and thaw analyses

To determine how vegetation of thermokarst ponds influenced within-pond sediment temperatures and thaw depths, linear mixed-effects models were used. For these analyses, plots were grouped according to vegetation type (i.e., moss, forb, sparse) rather than plant community type in order to increase the sample size available for comparison (two community types contained only two plots). To test for differences in mean sediment temperature among vegetation types, a linear mixed-effects model was used with plot type (i.e., moss, forb, sparse) as a fixed factor. Site was included as a random factor to account for the effect of site identity (i.e., transect). Akaike information criterion (AIC) values were used to evaluate the inclusion of random effects within models. The package lme4 was used to run mixed-effects models (Bates et al., 2015). To avoid non-independence of samples, vegetated plots which were co-located in ponds with sparse plots were omitted. One-way ANOVA was used in combination with pairwise post hoc tests using Tukey adjustment in the R package emmeans (Lenth et al., 2022) to examine differences between groups. In this case, the response variable “mean sediment temperature” was squared to meet the assumption of normality. Normality of model residuals was determined using quantile-quantile probability plots, along with homogeneity of variance between groups. To test for differences in mean thaw depth between plot type, the same methods described above were used, with mean thaw depth as the response variable, which did not need to be transformed

for normality. All statistical analyses were performed using the program R version 4.0.3 (R Core Team, 2020).

Linear regression was used to quantify the effects of vegetation and soil-related factors on mean sediment temperature and thaw depth in thermokarst ponds. As above, vegetated plots which were co-located in ponds with sparse plots were omitted to avoid non-independence of samples. Linear regression was used to test the ability of variation in moss biomass, moss thickness, total vegetation cover, maximum water depth, and organic horizon thickness to explain the variation in temperature and thaw depth. To examine relationships with temperature and thaw more accurately, these five predictor variables were then included in multiple linear regressions. Site was included as a random factor to account for unequal variance between sites. To avoid multicollinearity within models, variables required low Pearson's correlation coefficients (<0.6) and high tolerance values (>0.2).

To examine relationships between vegetation/soil and sediment temperature, the response variable mean sediment temperature (squared for normality) was used. The following continuous predictor variables were included in this model: moss biomass, moss thickness, total vegetation cover, maximum water depth, and organic horizon thickness. Quantile-quantile probability plots were used to verify that model residuals were normally distributed. To examine relationships between vegetation/soil and thaw depth within thermokarst ponds, a mixed-effects model with mean thaw depth as the response variable was used, and again site was included as a random factor. The same methods as described above were implemented (although mean thaw depth did not need to be transformed for normality) and the same predictor variables as in the previous model were included: moss biomass, moss thickness, total vegetation cover, maximum water depth, and organic horizon thickness. Mixed-effects models were run in the R package lme4

(Bates et al., 2015). The R package car version 3.0-12 (Fox et al., 2021) was used to estimate all effects and to create partial residual plots for predictor variables.

3. Results

3.1 Plant community analyses

3.1.1 Cluster analysis and synoptic table

Seven floristically distinct groups of plots were identified based on the cluster analysis (*Figure 4*). Five of the described clusters (1–5) represent aquatic plant communities defined by dominant plant species (*Calliergon richardsonii* comm., *Scorpidium scorpioides* comm., *Hippuris vulgaris* comm., *Pseudocalliergon turgescens* comm., and *Ranunculus gmelinii* comm.). Two of the clusters (6 and 7) correspond to sparsely vegetated units. All the clusters have significantly different species composition and high within-group similarity, based on results of MRPP analysis ($A = 0.62, p < 0.01$). Species composition did not significantly differ between sites (i.e., NIRPO vs. JS). There was low within-cluster similarity when plots were grouped by site ($A = 0.02, p > 0.05$). The synoptic table (*Table 1*) contains the diagnostic, constant, and dominant species for each cluster along with the corresponding fidelity (Φ), frequency, and mean cover values. A summary table of key environmental variables for each cluster (*Table 2*), and a full summary table of environmental data for each cluster can be found in *Appendix A*. Species cover data (*Appendix B*), environmental data (*Appendix C*), soils data (*Appendix D*), and biomass data (*Appendix E*) for each plot are provided.

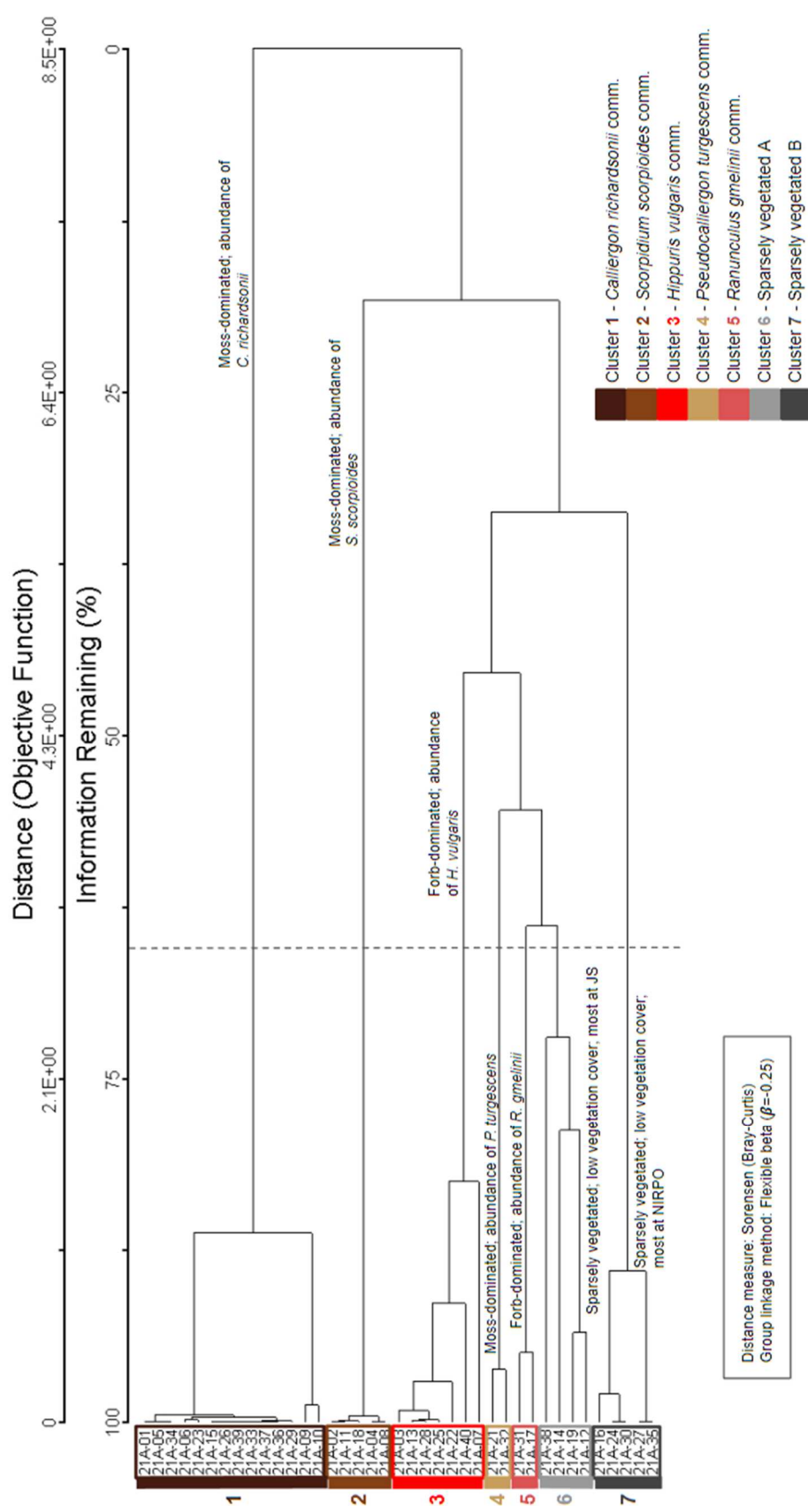


Figure 4. Dendrogram resulting from cluster analysis of species cover data from all 39 plots from thermokarst ponds in the Prudhoe Bay area, Alaska. Clusters are labeled by color and cluster characteristics are noted.

Table 1. Synoptic table of fidelity (Φ), frequency (%), and mean cover (%) of taxa in groups of thermokarst-pond plots resulting from cluster analysis. Highly diagnostic taxa ($\Phi \geq 0.50$) are highlighted in dark gray and diagnostic taxa ($\Phi \geq 0.25$) are highlighted in light gray. Fidelity values below 0.25 are omitted.
(*Single occurrence taxa that meet the fidelity cutoff $\Phi \geq 0.25$ were not considered diagnostic, as they occurred in only one plot each.)

Taxa	Growth form	Cluster		1		3		Hippuris vulgaris comm.		Scorpidium scorpioides comm.		Sparsely vegetated A		Pseudocalyngon turgescens comm.		4		Sparsely vegetated B		7		Ranunculus gmelinii comm.		5	
		n	Community	Calliergon richardsonii comm.	14	7	Mean	Φ	Freq. cover	Φ	Freq. cover	Φ	Freq. cover	Φ	Freq. cover	Φ	Freq. cover	Φ	Freq. cover	Φ	Freq. cover	Φ	Freq. cover	Φ	Freq. cover
Diagnostic taxa																									
<i>Calliergon richardsonii</i> comm.				pleurocarpous moss	0.29	100.00	92.79	-	7.14	2.03	-	80.00	3.62	-	75.00	0.08	-	100.00	0.10	-	100.00	1.60	-	50.00	0.05
<i>Calliergon richardsonii</i> (Mitt.) Kindb.				pleurocarpous moss	0.30	42.86	6.59	-	14.29	0.14	-	0.00	0.00	-	25.00	0.03	-	0.00	0.00	-	40.00	0.04	-	0.00	0.00
<i>Scorpidium cossonii</i> (Schimpet) Hedenas																									
<i>Hippuris vulgaris</i> L.	forb	-	35.71	3.64	0.56	100.00	65.14	-	20.00	0.02	-	25.00	0.25	-	0.00	0.00	-	20.00	0.20	-	20.00	0.20	-	0.04	50.00
<i>Scorpidium scorpioides</i> (Hedwig) Limpricht				pleurocarpous moss	-	7.14	0.29	-	28.57	0.73	0.61	100.00	90.40	0.35	75.00	1.75	-	0.00	0.00	-	0.00	0.00	-	0.00	0.00
<i>Carex aquatilis</i> Wahlenb.				graminoid	-	7.14	0.01	-	0.00	0.00	0.47	60.00	0.06	0.32	50.00	1.25	-	0.00	0.00	-	0.00	0.00	-	0.00	0.00
<i>Pseudocalyngon turgescens</i> comm.																									
<i>Pseudocalyngon turgescens</i> (T. Jensen) Loeske				pleurocarpous moss	-	14.29	0.01	-	28.57	0.44	-	20.00	0.02	-	0.00	0.00	0.46	100.00	71.00	-	20.00	0.02	-	0.00	0.00
<i>Hamatocaulis vernicosus</i> (Mitt.) Hedenas				pleurocarpous moss	-	14.29	0.01	-	28.57	0.03	-	0.00	0.00	-	0.00	0.00	0.55	100.00	11.50	-	0.00	0.00	-	0.00	0.00
<i>Hamatocaulis lapponicus</i> (Norrlin) Hedenas				pleurocarpous moss	-	14.29	0.36	-	0.00	0.00	-	0.00	0.00	-	25.00	0.03	0.30	50.00	9.00	-	0.00	0.00	-	0.00	0.00
<i>Scorpidium revolutum</i> (Swarz.) Rubens				pleurocarpous moss	-	28.57	0.09	-	14.29	0.01	-	0.00	0.00	-	0.00	0.00	-	0.00	0.00	0.38	60.00	0.24	-	0.00	0.00
<i>Ranunculus gmelinii</i> DC.	forb	-	7.14	0.07	-	14.29	1.43	-	0.00	0.00	-	0.00	0.00	-	0.00	0.00	-	20.00	0.02	0.61	100.00	64.50	-		
Nondiagnostic taxa																									
Taxa occurring in <i>Calliergon</i> , <i>Hippuris</i> , <i>Scorpidium</i> , Bare plots 1, and <i>Ranunculus</i> commns.																									
<i>Urticularia vulgaris</i> L.																									
Single occurrence taxa																									
<i>Pseudocalyngon</i> spp. (Limpricht) Loeske				pleurocarpous moss	-	14.29	0.10	-	0.00	0.00	-	20.00	0.10	-	0.00	0.00	-	0.00	0.00	-	0.00	0.00	-	0.00	0.00
<i>Sparganium hyperboreum</i> Laest. ex Beurl.				forb	-	0.00	0.00	0.35*	14.29	1.43	-	0.00	0.00	-	0.00	0.00	-	0.00	0.00	-	0.00	0.00	-	0.00	0.00
<i>Meesia triquetra</i> (H. Richter) Aongstr				aerocarpous moss	-	0.00	0.00	0.35*	14.29	0.43	-	0.00	0.00	-	0.00	0.00	-	0.00	0.00	-	0.00	0.00	-	0.00	0.00

Table 2. Key environmental variables for thermokarst-pond clusters, showing means for each cluster with standard deviation in parentheses. For age group, the number of plots (n) within each cluster that fall within an age category (A – D) are indicated.

	Group Community n	1 <i>Calliergon richardsonii</i> 14	2 <i>Scorpidium scorpioides</i> 5	3 <i>Hippuris vulgaris</i> 7	4 <i>Pseudocalliergon turgescens</i> 2	5 <i>Ranunculus gmelini</i> 2	6 Sparsely vegetated A 4	7 Sparsely vegetated B 5
Pond age	Age groups	C (n = 12), D (n = 2)	C (n = 3), B (n = 1), A (n = 1)	C (n = 5), B (n = 2)	C (n = 1), D (n = 1)	C (n = 2)	C (n = 4)	C (n = 5)
Mean thickness (cm)	Live moss layer	26.1 (9.9)	27.8 (16.0)	5.0 (2.7)	21.5 (4.9)	2.5 (3.5)	5.7 (2.2)	6.9 (2.9)
Depth (cm)	Mean water - Aug. Mean thaw - Aug. Maximum water - Aug.	45.9 (10.5) 44.2 (5.0) 51.1 (10.9)	54.4 (12.5) 43.4 (6.6) 62.0 (14.9)	53.6 (8.4) 50.8 (4.5) 59.9 (8.6)	32.2 (2.5) 40.1 (3.0) 36.5 (2.1)	44.8 (1.4) 53.3 (1.0) 50.5 (3.5)	56.8 (4.3) 49.4 (4.1) 61.8 (3.3)	51.3 (6.7) 55.9 (3.4) 59.8 (6.7)
Pond width (m)	Maximum width - July	16.0 (5.2)	8.5 (3.5)	16.7 (4.9)	11.9 (1.1)	11.6 (0.5)	12.2 (5.3)	17.1 (7.4)
Soil (organic horizon)	Horizon thickness (cm) Volumetric moisture (%) Bulk density (g/cm ³) Organic matter (%) pH	14.1 (5.2) 67.2 (6.0) 0.4 (0.1) 22.3 (6.5) 7.4 (0.2)	22.2 (6.4) 64.7 (3.6) 0.5 (0.1) 20.1 (6.1) 7.3 (0.3)	17.3 (5.2) 65.4 (7.0) 0.6 (0.1) 17.8 (2.2) 7.5 (0.2)	7.0 (0.0) 66.0 (1.1) 0.5 (0.0) 21.0 (4.4) 7.3 (0.0)	9.5 (0.7) 67.1 (2.7) 0.6 (0.1) 20.0 (4.0) 7.4 (0.3)	21.0 (6.0) 62.5 (1.9) 0.5 (0.0) 19.7 (3.1) 7.3 (0.1)	13.8 (5.8) 66.0 (5.3) 0.5 (0.1) 17.0 (2.3) 7.5 (0.2)
Soil (mineral horizon)	Horizon thickness (cm) Volumetric moisture (%) Bulk density (g/cm ³) Organic matter (%) pH	9.8 (5.5) 58.4 (19.5) 0.6 (0.3) 16.1 (6.9) 6.8 (2.0)	7.0 (2.6) 59.2 (9.5) 0.7 (0.3) 15.9 (2.9) 7.5 (0.2)	23.0 (6.9) 55.6 (11.4) 0.9 (0.3) 15.0 (6.1) 7.4 (0.2)	15.5 (3.5) 56.3 (8.0) 0.8 (0.2) 17.8 (6.2) 7.2 (0.1)	30.0 (11.3) 52.5 (5.6) 1.1 (0.1) 10.6 (1.3) 7.5 (0.0)	17.0 (8.2) 62.5 (10.0) 0.7 (0.1) 19.2 (5.4) 7.3 (0.2)	27.8 (5.2) 55.7 (11.7) 0.8 (0.1) 16.2 (4.0) 7.3 (0.1)
Soil texture (%)	Sand Clay Silt	40.4 (15.9) 6.5 (2.5) 45.9 (16.8)	36.8 (22.4) 5.2 (3.1) 38.0 (23.3)	45.0 (11.4) 8.0 (2.9) 47.0 (10.9)	33.6 (0.2) 6.7 (3.1) 59.6 (2.8)	36.8 (1.9) 10.6 (0.0) 52.6 (1.9)	42.1 (7.1) 8.0 (1.0) 49.9 (6.9)	42.0 (8.3) 7.7 (1.2) 50.3 (9.0)
Biomass (g/m ²)	Total Moss	3079.1 (1895.3) 3031.8 (1895.4)	1638.6 (1391.8) 1629.6 (1387.9)	166.8 (118.4) 25.5 (46.9)	3135.0 (586.5) 3129.8 (590.8)	274.9 (215.9) 40.0 (49.6)	172.0 (104.2) 124.3 (108.3)	428.3 (168.4) 243.8 (195.2)
Mean temp. (°C, 19 July – 23 Aug. 2021)	Sediment Above vegetation layer Water surface	6.5 (1.5) 9.5 (2.8) 10.6 (0.3)	6.8 (1.1) 10.3 (0.3) 10.4 (0.1)	8.2 (0.8) 10.2 (0.6) 10.6 (0.2)	6.1 (1.8) 9.6 (0.1) 10.4 (0.1)	8.7 (0.1) 10.5 (0.2) 10.6 (0.3)	9.0 (0.5) 10.4 (0.2) 10.5 (0.2)	8.7 (0.9) 8.5 (4.8) 10.6 (0.4)

3.1.2 Community descriptions

The thermokarst-pond plant communities are named informally according to the dominant species in each community. Formal naming according to the International Code of Phytosociological Nomenclature (Theurillat et al., 2020) will require more samples from a broader area. When numerical values are included in community descriptions below, they are included in the following format: (mean ± standard deviation).

It should be noted that many of the bryophyte species found within this study were taxonomically challenging. Genera within the Amblystegiaceae (e.g., *Calliergon*, *Scorpidium*, *Drepanocladus*, *Pseudocalliergon*) are notoriously difficult to identify in the field. A previous

study identified *Calliergon giganteum* within aquatic thermokarst-pond habitats (Jorgenson et al., 2015), while *C. richardsonii* was previously identified in mainly moist to wet habitats without standing water (Walker, 1985). All the *Calliergon* samples taken within this study were identified as *C. richardsonii* based on their relatively short and often branched costa (the midrib-like line of cells at the center of the leaf) and small alar regions (areas of cells, which are often inflated, at the basal corners of a leaf), but differentiation of *C. richardsonii* and *C. giganteum* is difficult. It is likely that *C. richardsonii* in this study was the same species as that previously identified as *C. giganteum*. A full species list (*Appendix F*) is provided.

***Calliergon richardsonii* community (Cluster 1, n = 14)**

Diagnostic species: *Calliergon richardsonii* ($\Phi = 0.29$), *Scorpidium cossonii* ($\Phi = 0.30$)

Constant species: *Calliergon richardsonii* (100.0%), *Scorpidium cossonii* (42.9%)

Dominant species: *Calliergon richardsonii* (92.8%), *Scorpidium cossonii* (6.6%), *Hippuris vulgaris* (3.6%)

C. richardsonii and *S. cossonii* were diagnostic, constant, and dominant species for this community type. The community was named for *C. richardsonii* based on its high frequency and high mean cover relative to that of *S. cossonii*. For both species, fidelity values ($\Phi < 0.5$) indicate that they were only moderately diagnostic of the community, likely due to their occurrence throughout other community types. *C. richardsonii*, for example, was found in at least one plot in all other clusters. Plots within this community were closely grouped within the cluster analysis with the exception of plots 21A-09 and 21A-10, in which cover of *S. cossonii* was higher than that of other plots within the cluster. These plots had *S. cossonii* cover values of 55% and 35%, respectively, while cover of *S. cossonii* did not exceed 2% in other plots.

This was the most well-represented community, occurring in 14 plots of the study: six plots at JS and eight plots at NIRPO. Characteristics of this community included abundant cover of live moss ($97.2 \pm 5.9\%$) and a continuous layer of litter below the moss layer ($100.0 \pm 0.0\%$) (Figure 5). Mean thaw depth was relatively low (44.2 ± 5.0 cm) and total biomass, which was primarily composed of moss, was high (3079.1 ± 1895.3 g/m²). Soils were mostly composed of silt and sand. Mean pH was 7.4 ± 0.2 in the organic horizon and 6.9 ± 2.0 in the mineral horizon. Mean sediment temperature (19 July – 23 August 2021) was 6.5 ± 1.5 °C and the mean difference between the mean water surface and mean sediment temperature was 4.2 ± 1.4 °C.



Figure 5. *Calliergon richardsonii* community growing within pond, at plot 21A-26. The two sensor poles on the far right correspond to a nearby sparsely vegetated plot. Photo by EWC.

Walker (1985) noted the presence of *Calliergon giganteum* among emergent aquatic vegetation, occasionally within beaded streams. Recently, Walker et al. (2022) described a

cluster of *C. giganteum* deep-water aquatic tundra plots in disturbed roadside sites in 2014. In addition, Jorgenson et al. (2015) described advanced-degradation thermokarst ponds in Prudhoe Bay as dominated by *C. giganteum*, along with *Scorpidium scorpioides* and *Utricularia vulgaris*. As mentioned above, these descriptions of *C. giganteum* were likely the species identified here as *C. richardsonii*. The Alaska Vegetation Classification (Viereck et al., 1992) described aquatic cryptogram communities dominated by various cryptogams (including *Calliergon* spp.) which were “infrequently reported” but occurred in freshwater ponds throughout Alaska.

***Scorpidium scorpioides* community (Cluster 2, n = 5)**

Diagnostic species: *Scorpidium scorpioides* ($\Phi = 0.61$), *Carex aquatilis* ($\Phi = 0.47$)

Constant species: *Scorpidium scorpioides* (100.0%), *Calliergon richardsonii* (80.0%), *Carex aquatilis* (60.0%), *Utricularia vulgaris* (40.0%)

Dominant species: *Scorpidium scorpioides* (90.4%), *Calliergon richardsonii* (3.6%)

Plots within this community grouped closely together within the cluster analysis. *S. scorpioides* was a highly diagnostic ($\Phi > 0.5$), constant, and dominant species for this community type. *C. aquatilis* was a moderately diagnostic and a constant species. *C. richardsonii* was a constant and a dominant species in this community and occurred in all but one plot. *U. vulgaris* was a constant species and occurred at trace cover (0.1%) in two plots. One unidentified species in this community, grouped into *Pseudocallieron* spp., had a relatively high fidelity ($\Phi = 0.42$) within the community, but was not considered to be diagnostic because it only occurred in one plot.

All plots within this community were from the Jorgenson site (JS). Site characteristics included abundant cover of live moss ($94.0 \pm 11.5\%$), a continuous layer of litter cover below the moss layer ($100.0 \pm 0.0\%$), and higher mean marl cover than any other community ($15.0 \pm 33.5\%$). Total biomass was relatively high ($1638.6 \pm 1391.9 \text{ g/m}^2$), although lower than that of

other moss-dominated communities (*Figure 6*). Mean thaw depth was low (43.4 ± 6.6 cm) relative to sparse and forb clusters but higher than other moss clusters. Mean water depth was relatively high (54.4 ± 12.5 cm) and maximum pond width was relatively low (8.5 ± 3.5 m). Soils were mostly composed of silt and sand. Mean pH was 7.3 ± 0.3 in the organic horizon and 7.5 ± 0.2 in the mineral horizon (higher than any other community). Mean sediment temperature (6.8 ± 1.1 °C) was comparable to that of the *C. richardsonii* and *P. turgescens* communities and lower than all others.

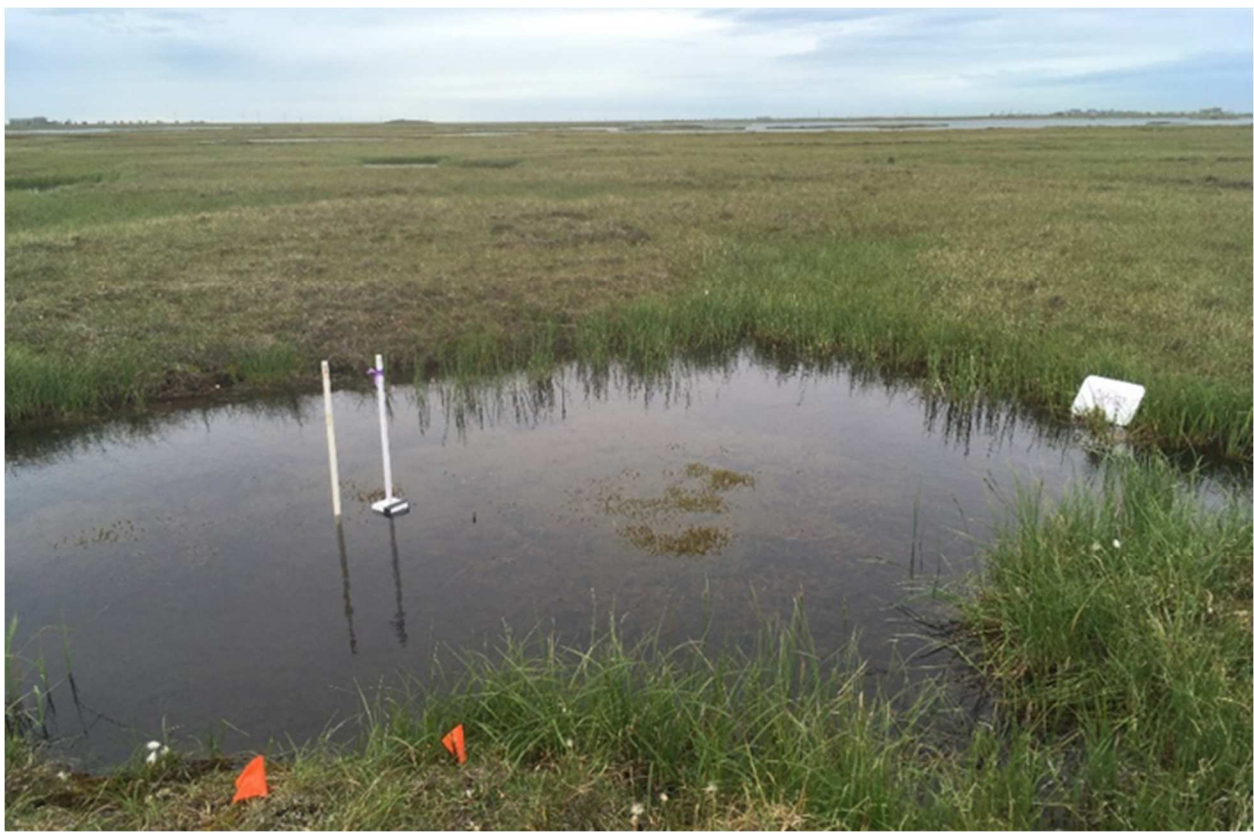


Figure 6. *Scorpidium scorpioides* community in plot 21A-02. Photo by EWC.

Walker (1985) described a wet *Carex aquatilis*-*Scorpidium scorpioides* sedge tundra (Stand Type M4) community type from Prudhoe Bay of similar species composition to the community described here. However, this type occurred in areas of shallow water (< 10 cm) and was transitional between wet sedge tundra and aquatic tundra vegetation. Walker (1985) also

described several similar aquatic emergent sites, aquatic *C. aquatilis* sedge tundra (Stand Type E1) and an aquatic *S. scorpioides* moss tundra type (Stand Type E3) that was found only in sandy polygon centers with deep water (up to 100 cm) near the Sagavanirktok River dunes. It is likely that the submerged, thermokarst-pond *S. scorpioides* community described here became more common throughout the Prudhoe Bay region with the progression of ice-wedge degradation and the development of thermokarst ponds. The Alaska Vegetation Classification (Viereck et al., 1992) described aquatic cryptogram communities dominated by various cryptogams (including *Scorpidium scorpioides*).

***Hippuris vulgaris* community (Cluster 3, n = 7)**

Diagnostic species: *Hippuris vulgaris* ($\Phi = 0.56$)

Constant species: *Hippuris vulgaris* (100.0%)

Dominant species: *Hippuris vulgaris* (65.1%), *Utricularia vulgaris* (2.9%), *Calliergon richardsonii* (2.0%)

H. vulgaris was a highly diagnostic ($\Phi > 0.5$), constant, and dominant species for this community type. *U. vulgaris* was also a dominant species, occurring in two of three plots, and having a relatively high 15% cover in one of those. *C. richardsonii* was a dominant species in this community and occurred in five plots, generally at low cover except for one plot where it occurred at 10% cover. *Meesia triquetra* and *Sparganium hyperboreum* had relatively high fidelity ($\Phi = 0.35$) but were not considered diagnostic because they each occurred in only one plot. Plots 21A-07 and 21A-40 did not cluster closely with the rest of the group within the cluster analysis. In plot 21A-40, *S. hyperboreum* was co-dominant with *H. vulgaris*. Plot 21A-07 was originally considered to be a sparsely vegetated plot, but clustered with this group due to relatively high cover of *H. vulgaris* (12%) and *U. vulgaris* (5%).

This community occurred in three plots at JS and four plots at NIRPO. Site characteristics included abundant cover of live forbs and litter. The herb layer was tallest in this community, while the height of the moss layer was relatively low (*Figure 7*). This community had the highest mean forb biomass ($110.0 \pm 134.4 \text{ g/m}^2$), although mean total biomass ($166.8 \pm 118.4 \text{ g/m}^2$) was low compared to other clusters (including sparse clusters). Mean thaw depth ($50.8 \pm 4.5 \text{ cm}$), water depth ($53.6 \pm 8.4 \text{ cm}$), and maximum pond width ($16.7 \pm 4.9 \text{ m}$) were relatively high. Soils were mostly composed of silt and sand. Mean pH was 7.5 ± 0.2 in both the organic and the mineral horizons. Mean sediment temperature ($8.2 \pm 0.8 \text{ }^\circ\text{C}$) was higher than that of the moss-dominated communities, but lower than the other clusters.

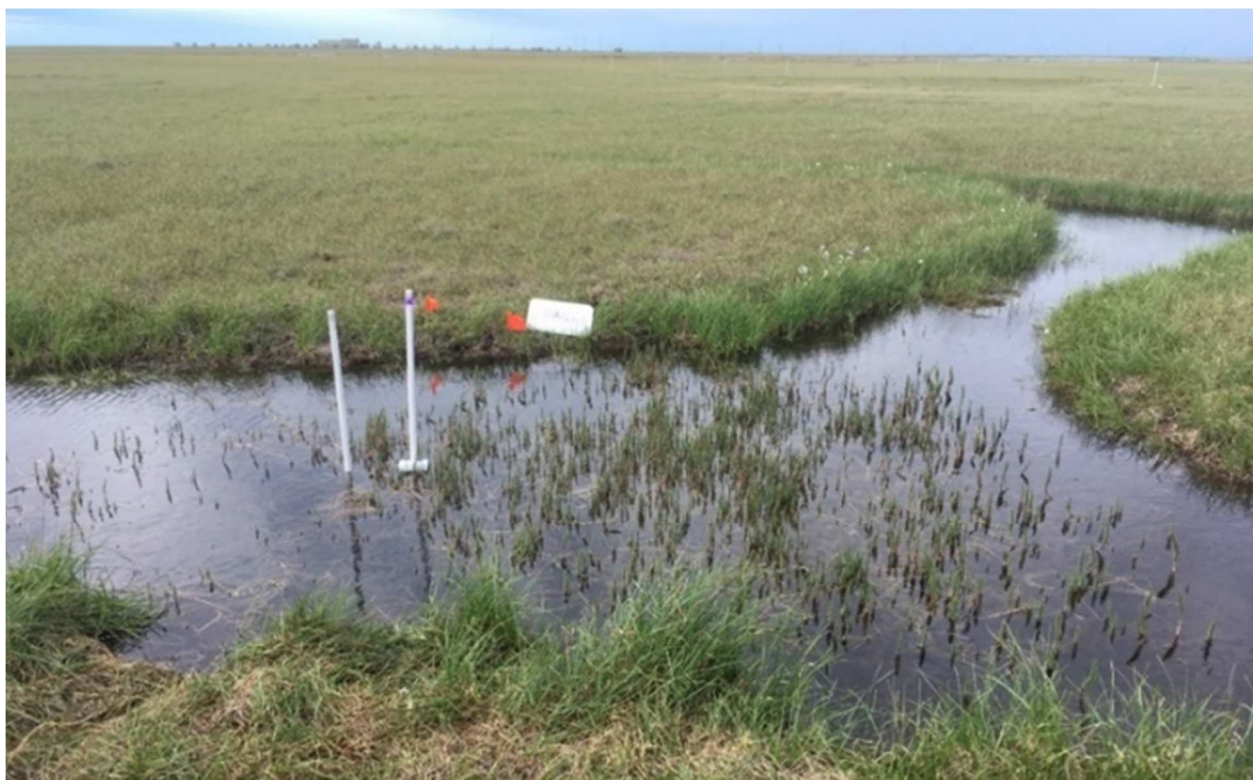


Figure 7. Hippuris vulgaris community at plot 21A-28. Photo by EWC.

Walker (1985) observed *H. vulgaris* in the Prudhoe Bay region, commonly in deep water and mainly in streams. In addition, Walker and Webber (1980) noted the presence of *H. vulgaris* in the Prudhoe Bay region within stream waters of the Tundra Stream Vegetation Complex

(Stand Types W2, E1, or E2). Within a classification of Greenland vegetation, *H. vulgaris* was included as a character species in the *Potametea* aquatic vegetation, although Daniëls (1994) noted that aquatic vegetation syntaxonomy in Greenland was poorly studied at the time. Also included as a non-important character species within the vegetation classification of Greenland was *Sparganium hyperboreum*, which was found abundantly in plot 21A-40 in this study. Jorgenson et al. (2015) noted the presence of *H. vulgaris* at a small percent cover value within advanced-degradation thermokarst ponds of Prudhoe Bay. Walker et al. (2022) identified plots at Prudhoe Bay within a *Carex aquatilis-Hippuris vulgaris* sedge marsh (Type E1). This is likely very similar to the community described here, aside from the absence of *C. aquatilis* in the deeper areas of thermokarst ponds. In addition, the Alaska Vegetation Classification (Viereck et al., 1992) described a *H. vulgaris*-dominated aquatic community occurring in tundra ponds of southeastern, south-central, western, and northern Alaska, which is similar to the community described within this study.

***Pseudocalliergon turgescens* community (Cluster 4, n = 2)**

Diagnostic species: *Pseudocalliergon turgescens* ($\Phi = 0.46$), *Hamatocaulis vernicosus* ($\Phi = 0.55$), *Hamatocaulis lapponicus* ($\Phi = 0.30$)

Constant species: *Pseudocalliergon turgescens* (100.0%), *Hamatocaulis vernicosus* (100.0%), *Calliergon richardsonii* (100.0%), *Hamatocaulis lapponicus* (50.0%)

Dominant species: *Pseudocalliergon turgescens* (71.0%), *Hamatocaulis vernicosus* (11.5%), *Hamatocaulis lapponicus* (9.0%)

P. turgescens was a moderately diagnostic ($\Phi < 0.5$), constant, and dominant species for this community type. *H. vernicosus* was highly diagnostic ($\Phi > 0.5$), constant, and dominant. This community was named for *P. turgescens* due to its greater dominance (mean cover 71.0%) than *H. vernicosus* (mean cover 11.5%) within the community. *H. lapponicus* was moderately

diagnostic ($\Phi < 0.5$), constant, and dominant, although it also had low mean cover (9.0%)

relative to *P. turgescens*. *C. richardsonii* was a constant species and occurred at trace cover values (0.1%) in all plots.

This community was described based on only two plots, one at JS and one at NIRPO, so further sampling will be needed to verify community characteristics. Site characteristics included abundant cover of live moss and very low litter cover relative to other communities. Average thickness of the live moss layer was lower than that of other moss-dominated communities, but this may be due to relatively low mean water depth (32.2 ± 2.6 cm), and thus less depth within the water column for the moss layer to extend (Figure 8). Mean biomass (3135.0 ± 586.5 g/m²) was highest in this community and was mostly composed of moss. Mean thaw (40.1 ± 3.0 cm) and water (32.2 ± 2.6 cm) depths were lowest relative to other clusters. Soils were mostly

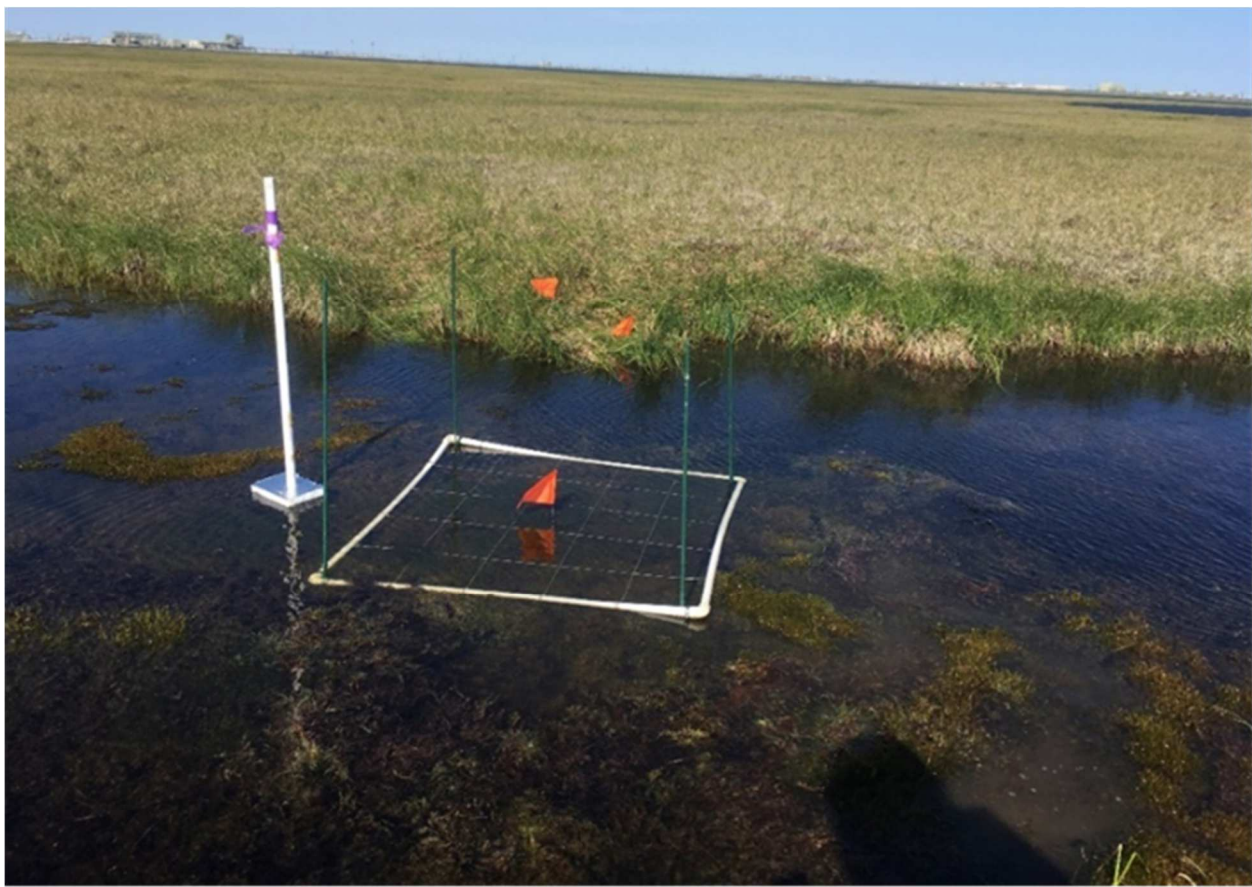


Figure 8. *Pseudocalliergon turgescens* community at plot 21A-21. Photo by EWC.

composed of silt and sand. Mean pH was 7.3 ± 0.0 in the organic horizon and 7.2 ± 0.1 in the mineral horizon. Mean sediment temperature (6.1 ± 1.8 °C) was lowest relative to other clusters and the mean temperature difference between water surface and sediment (4.4 ± 1.9 °C) was greatest.

Walker (1985) collected *P. turgescens* (formerly *Scorpidium turgescens* and *Calliergon turgescens*) within wet to moist tundra in the Prudhoe Bay region although this species was not included in community descriptions at the time, likely indicating its infrequency. Recently, *P. turgescens* specimens from southern Siberia were identified by Pisarenko (2020), who noted that this was a rare species that grew in wet areas and occurred dominantly in highland swamps of the region. Within the Prudhoe Bay region, Walker et al. (2022) noted the presence of *P. turgescens* within undisturbed moist tundra (type U3) in the 1970s and within heavily dusted and flooded polygon centers (type M2d) in 2014.

***Ranunculus gmelinii* community (Cluster 5, n = 2)**

Diagnostic species: *Ranunculus gmelinii* ($\Phi = 0.61$)

Constant species: *Ranunculus gmelinii* (100.0%), *Utricularia vulgaris* (50.0%), *Hippuris vulgaris* (50.0%), *Calliergon richardsonii* (50.0%)

Dominant species: *Ranunculus gmelinii* (64.5%), *Utricularia vulgaris* (33.5%)

R. gmelinii was a highly diagnostic ($\Phi > 0.5$), constant, and dominant species for this community type. *U. vulgaris* was both a constant and a dominant species, and it occurred in only one of two plots but had a high cover value within the plot (67.0%). Additional constant species included *H. vulgaris* and *C. richardsonii*, both of which occurred in one plot.

This community was described based on only two plots, one at JS and one at NIRPO, so further sampling will be needed to verify community characteristics. Site characteristics included abundant cover of live forbs and a continuous layer of litter cover (Figure 9). Mean height of the

herb layer was lower than that of the *H. vulgaris* community, but higher than that of all other types. Average thickness of the live moss layer was lowest in this community. Mean biomass was relatively low ($274.9 \pm 215.9 \text{ g/m}^2$), and mostly composed of forbs and litter. Mean thaw depth ($53.3 \pm 1.0 \text{ cm}$) was the second highest of any cluster, after the Sparsely vegetated B group. Mean water depth ($44.8 \pm 1.4 \text{ cm}$) was relatively shallow, and maximum pond width ($11.6 \pm 0.5 \text{ m}$) was less than that of all groups except the *S. scorpioides* community. Soils were mostly composed of silt and sand, but had a high proportion of clay ($10.6 \pm 0.0\%$) relative to other communities. Mean pH was 7.4 ± 0.3 in the organic horizon and 7.5 ± 0.0 in the mineral horizon. Mean sediment temperature was relatively high ($8.7 \pm 0.1 \text{ }^\circ\text{C}$) and closest to that of the two sparsely vegetated clusters. The mean difference between water surface and sediment

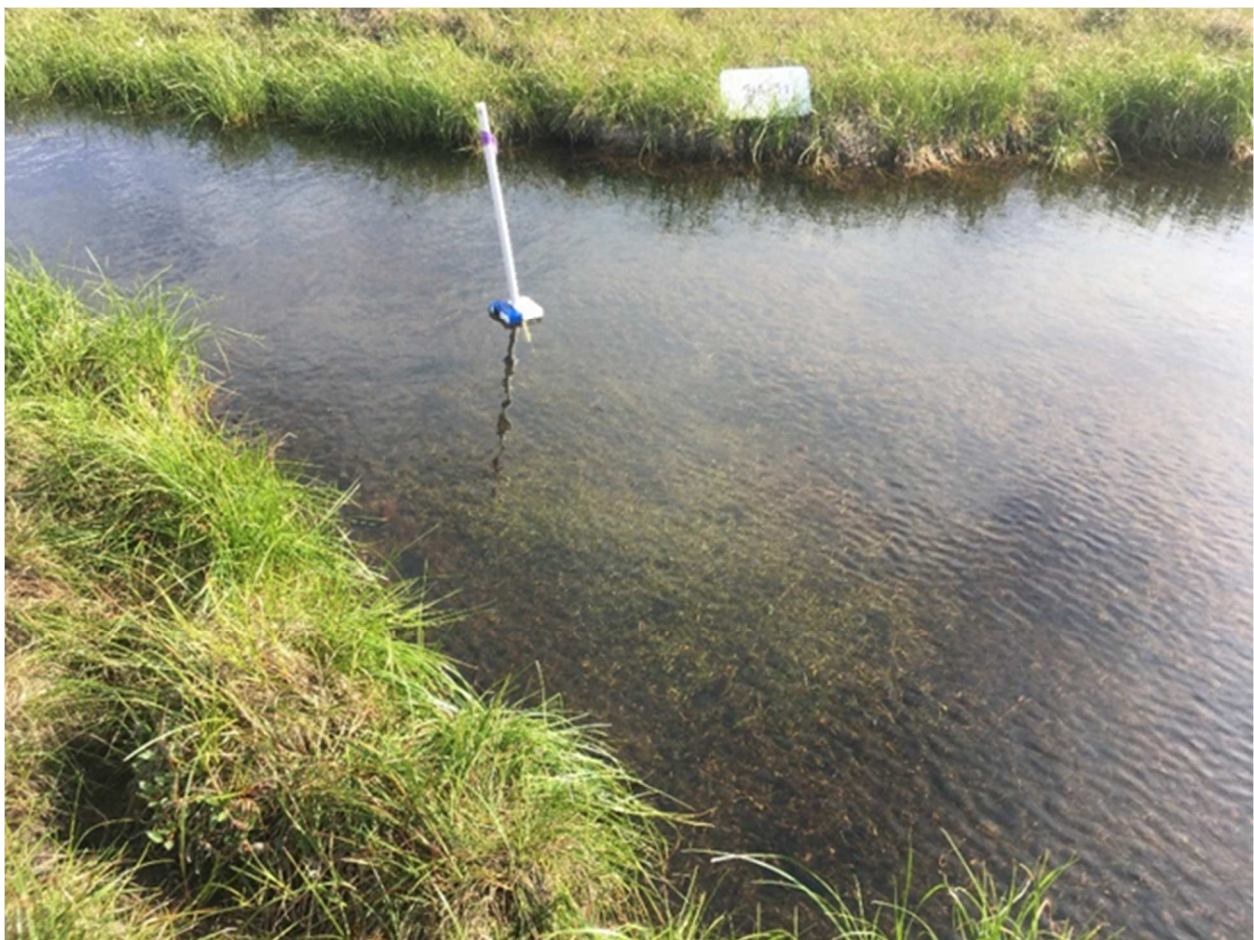


Figure 9. *Ranunculus gmelinii* community at plot 21A-31. Photo by EWC.

temperature (1.9 ± 0.4 °C) was greater than both sparsely vegetated clusters, but less than all others.

In the Prudhoe Bay region, Walker (1985) noted the rare presence of *R. gmelinii* on bare, wet mud within drained pond areas. Mucina et al. (2016) discussed a similar *Ranunculetalia* community within the class *Potamogetonetea*. This community was described as rooted and either submerged or floating, and found in mesotrophic and eutrophic Eurasian freshwater bodies. In addition, the Alaska Vegetation Classification (Viereck et al., 1992) described aquatic plant communities dominated by *R. gmelinii* occurring within shallow ponds and flooded gravel pits in south-central, western, and northern Alaska.

While *R. gmelinii* was the only diagnostic species within the community described above, it should be noted that *U. vulgaris* was present at a greater cover within one of the two sampled plots. Additional sampling may allow for the differentiation of *U. vulgaris*-dominated communities from those that are dominated by *R. gmelinii*. Within descriptions of very wet *Carex aquatilis* graminoid meadow communities (Stand Type E1), Walker (1985) included *U. vulgaris* as a present taxa, although this community occurred in shallow water (< 30 cm deep) compared to those of thermokarst ponds.

Plots within the following two clusters were selected based on their lack of vegetation to provide comparison with vegetation plots. Brief descriptions of the characteristics of these two clusters are included here. These are intended to provide comparisons with other clusters, rather than proposed descriptions of plant communities.

Sparsely vegetated type A (Cluster 6, n = 4)

Diagnostic species: *Scorpidium scorpioides* ($\Phi = 0.35$), *Carex aquatilis* ($\Phi = 0.32$)

Constant species: *Scorpidium scorpioides* (75.0%), *Calliergon richardsonii* (75.0%), *Utricularia vulgaris* (50.0%)

Dominant species: N/A

No species met the mean cover value cutoff ($> 2\%$) for dominant species. *S. scorpioides* was a diagnostic and constant species and occurred in three plots within the cluster. *C. aquatilis* was also diagnostic and occurred in two plots. Additional constant species included *C. richardsonii* and *U. vulgaris*. The plots within this group did not cluster closely within the cluster analysis.

This cluster included three plots at JS and one plot at NIRPO. Site characteristics included abundant mean cover of litter ($82.5 \pm 12.6\%$) and dead moss ($8.6 \pm 7.5\%$), as well as the highest mean bare soil cover of any group ($17.6 \pm 8.7\%$). Mean height of the herb layer was highest in this cluster (13.4 ± 16.9 cm), likely due to the presence of emergent *C. aquatilis* in two plots. Mean height of the shrub layer, which was exclusively composed of standing dead shrubs, was the highest of any cluster (6.3 ± 1.9 cm). Mean biomass (172.0 ± 104.2 g/m²) was relatively low and mostly composed of dead moss and litter. Mean thaw depth (49.4 ± 4.1 cm) and mean water depth (56.8 ± 4.3 cm) were both relatively high. Soils were mostly composed of silt and sand. Mean pH was 7.3 ± 0.1 in the organic horizon and 7.3 ± 0.2 in the mineral horizon. Mean sediment temperature (9.0 ± 0.5 °C) was high and the mean difference in water surface and sediment temperature (1.5 ± 0.6 °C) was low.

Sparsely vegetated type B (Cluster 7, n = 5)

Diagnostic species: *Scorpidium revolvens* ($\Phi = 0.38$)

Constant species: *Calliergon richardsonii* (100.0%), *Scorpidium revolvens* (60.0%), *Scorpidium cossonii* (40.0%)

Dominant species: N/A

S. revolvens was a diagnostic and constant species, although it occurred in only three plots within the cluster. *C. richardsonii* was a constant species and occurred in all plots within the cluster. *S. cossonii* was a constant species and occurred at trace cover value (0.1%) in two plots. No species met the mean cover value cutoff ($> 2\%$) for dominance.

This cluster primarily included four plots at NIRPO and one at JS. Characteristics included abundant mean cover of litter and high mean cover of bare soil, as well as the highest mean cover values of dead moss and total standing dead material of any cluster. Mean thickness of the dead moss layer was highest in this cluster. Biomass was mostly composed of moss and litter, and mean biomass ($428.3 \pm 168.4 \text{ g/m}^2$) was lower than that of the three moss-dominated communities but higher than all other clusters. Mean thaw depth ($55.9 \pm 3.4 \text{ cm}$) was high, and maximum pond width ($17.1 \pm 7.4 \text{ m}$) was relatively wide. Soils were mostly composed of silt and sand. Mean pH was 7.5 ± 0.2 in the organic horizon and 7.3 ± 0.2 in the mineral horizon. Mean sediment temperature ($8.7 \pm 0.9 \text{ }^\circ\text{C}$) was high, as was the mean difference between water surface and sediment temperature ($1.9 \pm 0.9 \text{ }^\circ\text{C}$).

3.1.3 Community comparisons

Mean total biomass and mean moss thickness were much higher in the moss-dominated communities (*Figures 10a,b*, brown bars) relative to the forb-dominated communities (red bars) and sparsely vegetated communities (gray bars). The *S. scorpioides* and *C. richardsonii* communities had greater moss thickness than all forb communities and sparse groups (*Figure 10b*). Total percent vegetation cover was higher among well vegetated clusters than the sparsely vegetated groups (*Figure 10c*) as expected given that these areas were selected based on their

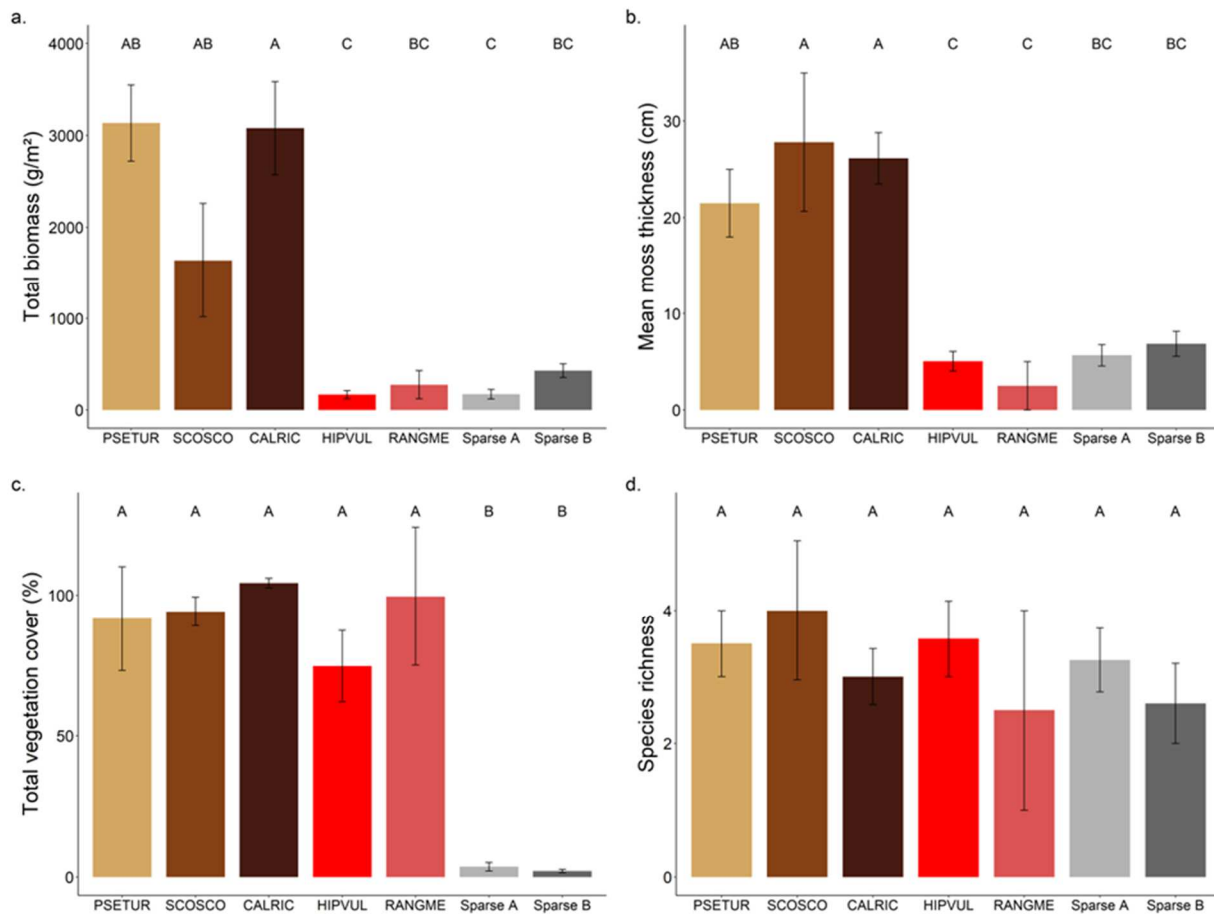


Figure 10. Bar graph showing mean values of key vegetation characteristics grouped by cluster: PSETUR (light brown, n = 2), SCOSCO (medium brown, n = 5), CALRIC (dark brown, n = 14), HIPVUL (red, n = 7), RANGME (pink, n = 2), Sparse A (light gray, n = 4), Sparse B (dark gray, n = 5). Error bars show standard error, and groups are colored by cluster (with moss clusters in brown, forb in red/pink, and sparse in gray). Variables shown include (a.) total biomass (g/m²), (b.) mean moss thickness (cm), (c.) total vegetation cover (%), and (d.) species richness. Letters above bars indicate significant ($p < 0.05$) differences in group means, based on one-way ANOVA and pairwise post hoc tests (with Bonferroni adjustment).

relative lack of vegetation cover. Species richness did not differ among clusters and was consistently low (*Figure 10d*), with richness not exceeding six species in any given plot (mean richness 3.2 ± 1.5 SD).

Mean thaw depths were shallowest in the moss-dominated plots and greatest in the Sparse B group but comparable to thaw depths in the forb-dominated communities. The moss-dominated communities generally had less thaw (*Figure 11a*). Mean water depths varied between 32.2 cm (PSETUR) and 56.8 cm (Sparse A), but did not differ among clusters (*Figure*

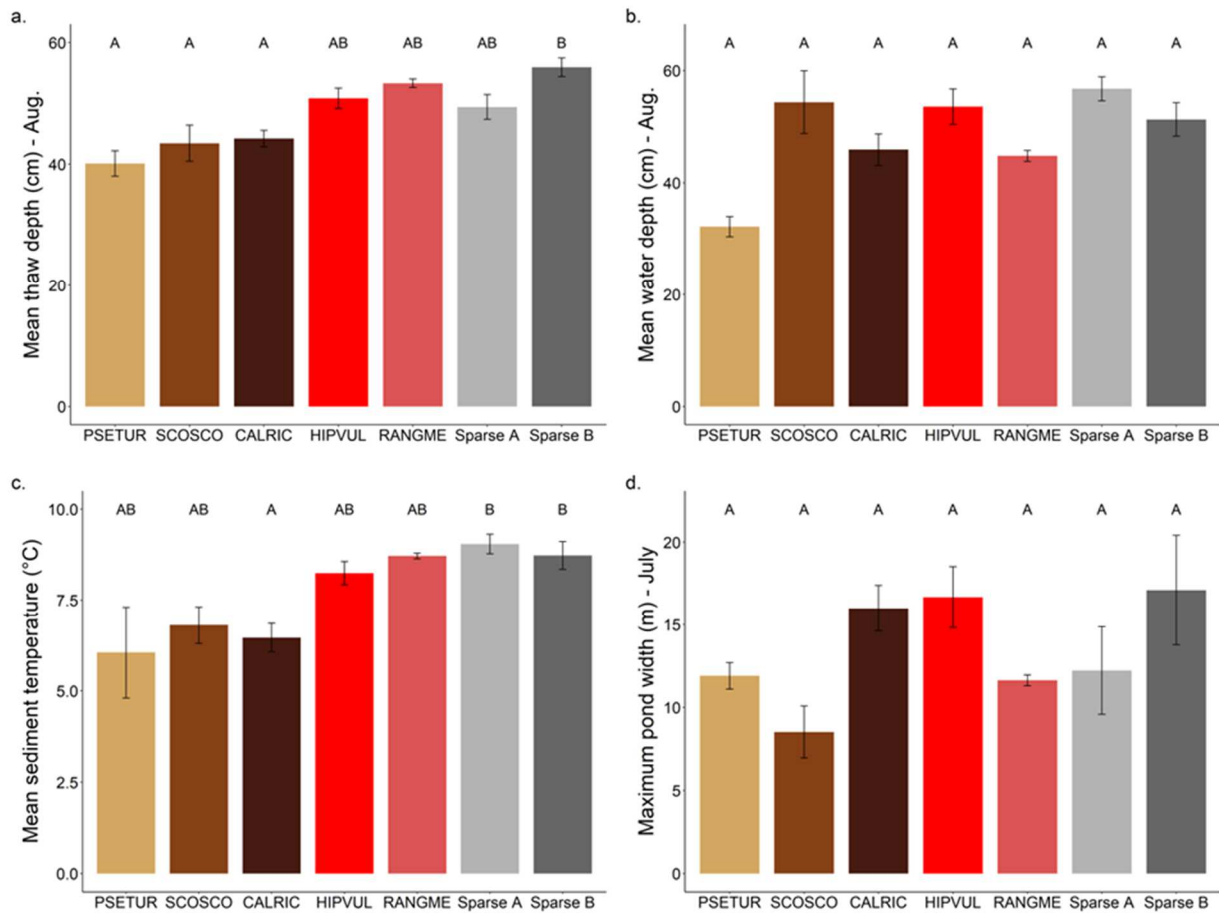


Figure 11. Bar graph showing mean values of key pond characteristics grouped by cluster: PSETUR (light brown, n = 2), SCOSCO (medium brown, n = 5), CALRIC (dark brown, n = 14), HIPVUL (red, n = 7), RANGME (pink, n = 2), Sparse A (light gray, n = 4), Sparse B (dark gray, n = 5). Error bars show standard error, and groups are colored by cluster (with moss clusters in brown, forb in red/pink, and sparse in gray). Variables shown include (a.) mean thaw depth (cm, measured in August 2021), (b.) mean water depth (cm, measured in August 2021), (c.) mean sediment temperature (°C), and (d.) maximum pond width (m, measured July 2021). Letters above bars indicate significant ($p < 0.05$) differences in group means, based on one-way ANOVA and pairwise post hoc tests (with Bonferroni adjustment).

11b). Mean sediment temperatures were lower in the *C. richardsonii* community than in sparsely vegetated groups A and B, but significant differences were not apparent among other clusters (Figure 11c). Maximum pond width did not differ among clusters (Figure 11d). Differences among clusters may be obscured in this study by low sample size and high variability.

P. turgescens and *R. gmelinii* communities had low organic-horizon thickness relative to other groups. Thawed mineral-horizon thickness of the *S. scorpioides* and *C. richardsonii* communities was low, especially relative to that of the *H. vulgaris* community, *R. gmelinii* community, and Sparse B group (Figure 12a).

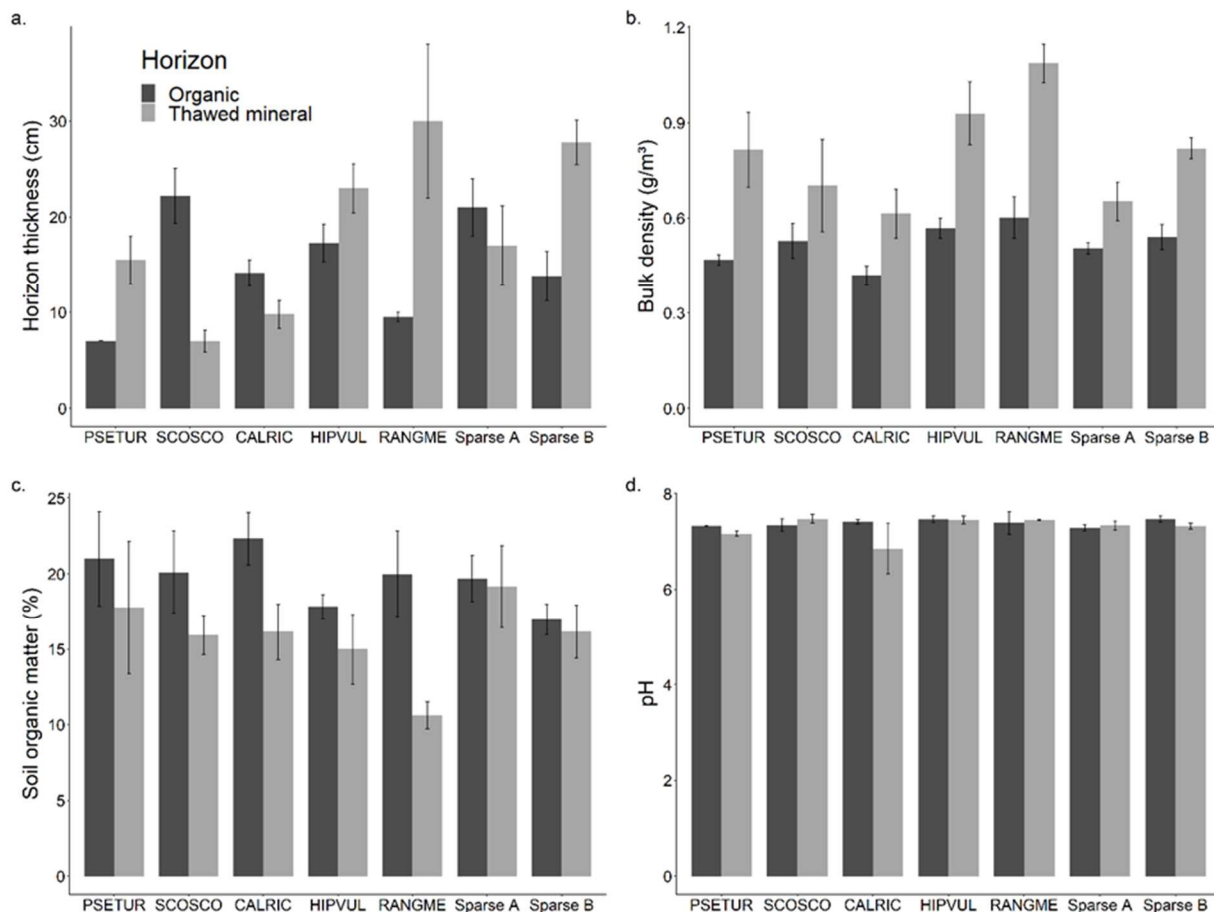


Figure 12. Bar graph showing mean values of key soil characteristics grouped by horizon and by cluster: PSETUR (n = 2), SCOSCO (n = 5), CALRIC (n = 14), HIPVUL (n = 7), RANGME (n = 2), Sparse A (n = 4), Sparse B (n = 5). Error bars show standard error, and colors indicate horizon (organic = dark gray, thawed mineral = light gray). Variables shown include (a.) horizon thickness (cm), (b.) bulk density (g/m²), (c.) soil organic matter (%), and (d.) pH.

Bulk density values in the organic horizons were consistently close to 0.5 g/m² and consistently lower than the values for the mineral horizons. The mineral-horizon bulk density of the *R. gmelinii* community (1.09 ± 0.08 g/cm³) was high relative to other clusters (Figure 12b). Percent soil organic matter (SOM) values in the organic horizon were generally around 20% in the mineral horizon, although values of the *R. gmelinii* community were lower ($10.62\% \pm 1.27$) than those of the other clusters. Mineral SOM values of most clusters generally had high standard errors (Figure 12c). Soil pH values of the mineral and organic horizons were similar (around 7.5) among all groups (Figure 12d).

3.1.4 Pond age

Most plots were located in ponds that formed during the period 1988 – 1996. Only one plot sampled was located in a pond that formed prior to 1968; three plots were in ponds that appeared between 1969 and 1987, 32 between 1988 and 2007, and three between 2008 and 2021.

Table 3. Pond age group categories (A – D), descriptions, and number of plots within each age category (n). Age group assignments for each plot are in *Appendix C*, and distribution of age classes among vegetation types is in *Table 2*.

Age group	Years	Description of time period	n
A	1968 and earlier	pre-oilfield	1
B	1969 – 1987	early oilfield, before abrupt period of thermokarst	3
C	1988 – 2007	rapid thermokarst period	32
D	2008 – 2021	recent climate warming	3

All plant communities contained ponds from the intermediate age group C (1988 – 2007). The *S. scorpioides* community contained one pond in the oldest age group, group A (1968 and earlier). The *P. turgescens* and *C. richardsonii* communities were the only clusters containing ponds in the youngest age group (D, 2008 – 2021). While most ponds at both sites were within age group C (1988 – 2007), a larger proportion of thermokarst ponds at JS were from the older age groups, with 11% of JS ponds from age group B (1969 – 1987) compared to NIRPO's 5%,

and 5% of JS ponds from age group A (1968 and earlier) compared to NIRPO's 0%. Overall, all clusters and vegetation types showed overlap in pond development age (*Figure 13*).

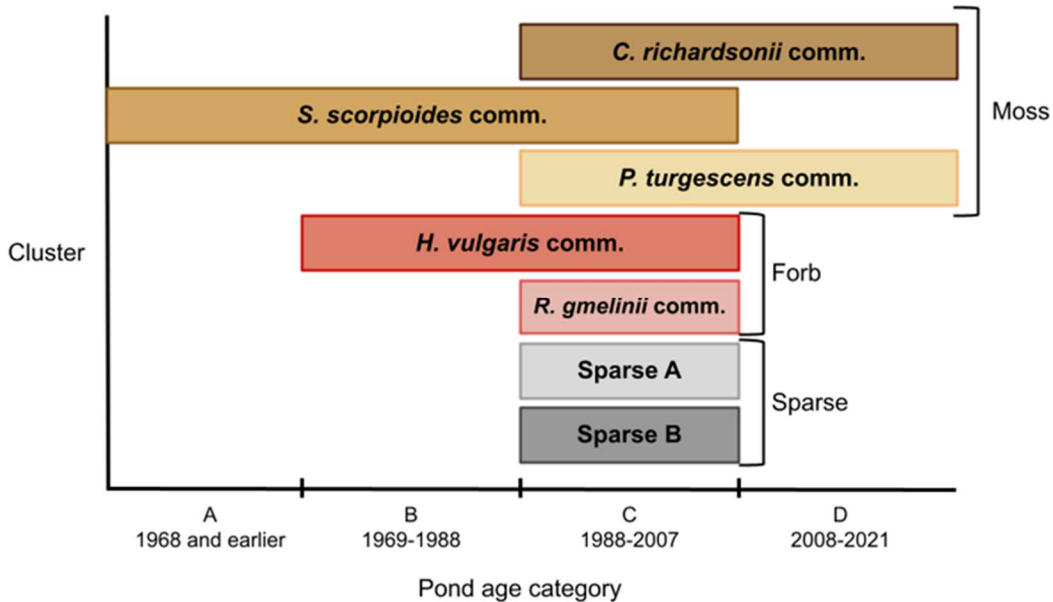


Figure 13. Occurrence of clusters and vegetation types within pond age categories. Figure shows which age categories are included within each type.

3.1.5 Temperature measurements

Mean daily temperature was determined for each sensor by calculating the mean temperature over a 24-hour period of hourly measurements, and mean sediment temperatures (19 July – 23 August 2021) were determined for each plot (*Appendices C1 and C2*) and each community cluster (*Appendix A*). Temperature differences between clusters were greater at the sediment surface relative to the water surface or submerged vegetation layer throughout the period of measurement. Mean daily water-surface temperatures ranged from a maximum of about 20 °C in mid-July to a minimum of about 5 °C in mid-August, and there was little difference among the clusters (*Figure 14a*). Mean daily temperatures above the submerged vegetation layer also ranged from about 20 °C to about 5 °C. There was little variation in temperature of the submerged vegetation layer among clusters. The Sparse A and Sparse B

clusters had higher submerged vegetation layer temperatures at certain times throughout the measurement period, while the *P. turgescens* community had lower temperatures (*Figure 14b*). Differences in temperature between clusters were most pronounced at the sediment surface. Mean daily sediment temperatures ranged from a maximum of about 15 °C in sparse clusters in mid-July to a minimum of about 4 °C in moss groups in mid-August. Moss clusters had consistently lower temperatures than sparse or forb clusters, and this difference was greater during periods of increasing temperature (e.g., approx. 25 July – 2 August) than during periods of decreasing temperature (e.g., approx.. 22 – 24 July) (*Figure 14c*). A summary of temperature data including iButton sensor IDs, plot locations, and positions within ponds (i.e., at water surface, above submerged vegetation layer, at sediment surface) can be found in Walker et al. (in preparation).

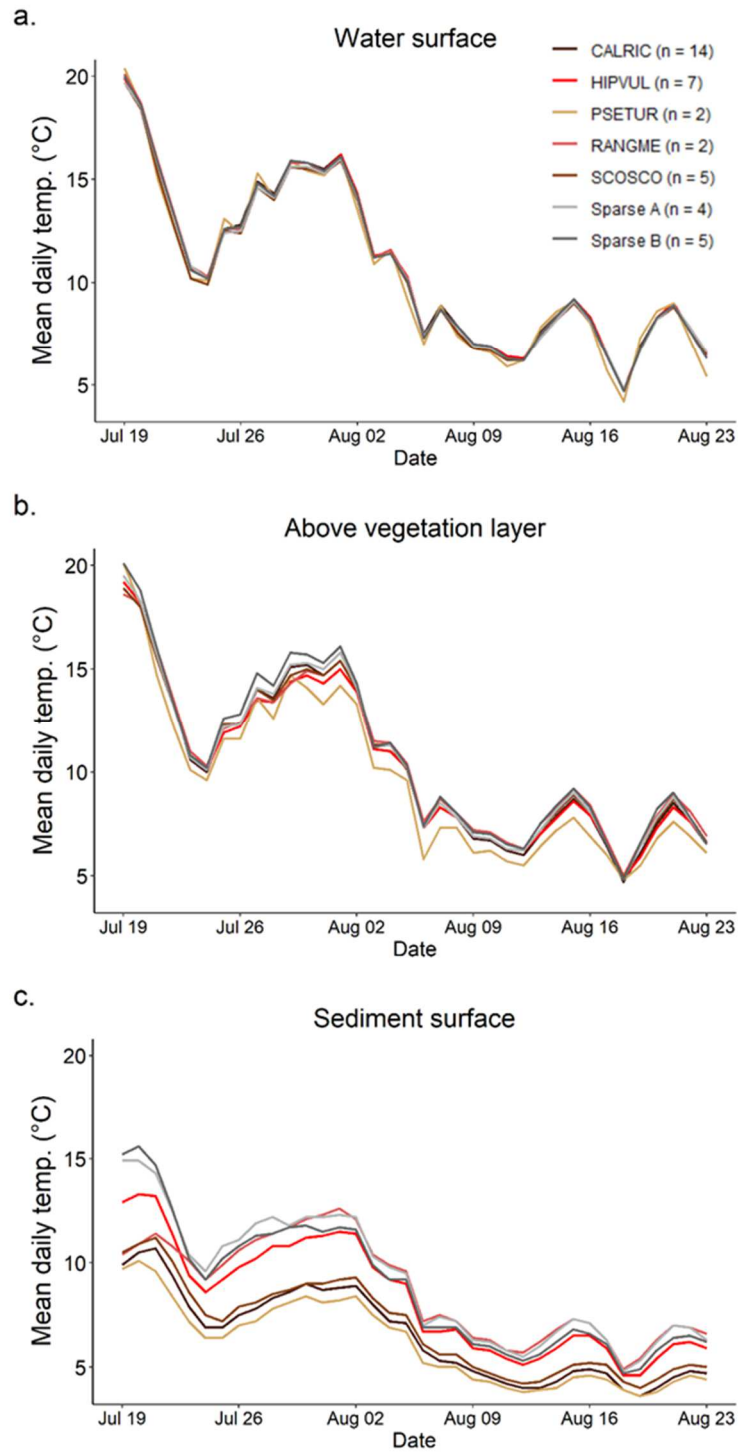


Figure 14. Mean daily water temperature over period of study (19 July – 23 August 2021) for each cluster: CALRIC (n = 14), HIPVUL (n = 7), PSETUR (n = 2), RANGME (n = 2), SCOSCO (n = 5), Sparse A (n = 4), Sparse B (n = 5). Temperatures shown are from sensors positioned (a.) at the water surface, (b.) above the submerged vegetation layer, and (c.) at the sediment surface.

3.1.6 Environmental gradient analysis

NMDS ordination of plots resulted in a three-dimensional solution with a final stress of 13.3 after 144 iterations, which explained 61% of the variation among plots. The ordination was rotated 171° by the variable “moss biomass” to improve visualization of gradients. Following rotation, Axis 1 explained 21% of the variation, Axis 2 explained 22%, and Axis 3 explained 18% (*Figure 15*). Vector biplots, the cluster of vectors at the centroid of the ordination space, indicate the direction and strength of environmental variables with relatively high linear correlations ($r^2 \geq 0.20$) with the variation in species composition. Variables were correlated with each axis based on the values of their Kendall’s tau rank correlation coefficient (τ), using a cutoff value of $|\tau| \geq 0.3$ for correlated variables and $|\tau| \geq 0.5$ for highly correlated variables (*Table 4*).

The vegetation types were generally well separated in the final rotated view, especially when all three axes were considered. Axis 1 represented a complex gradient of temperature and thaw, which was influenced by biomass. Total biomass and live moss cover were highly positively correlated with Axis 1. Moss biomass, moss thickness, litter thickness, temperature difference (water surface to sediment), and litter cover were positively correlated with Axis 1. Mean sediment temperature, mean thaw depth (in July), and bare soil cover were negatively correlated with Axis 1. Plots within the *C. richardsonii* community consistently occupied the ordination space associated with high biomass, high moss cover/biomass/thickness, and greater temperature difference from water surface to sediment. At the other end of Axis 1, the *R. gmelinii* community and sparsely vegetated A group consistently occupied the ordination space associated with high sediment temperatures, high cover of bare soil, and deep thaw.

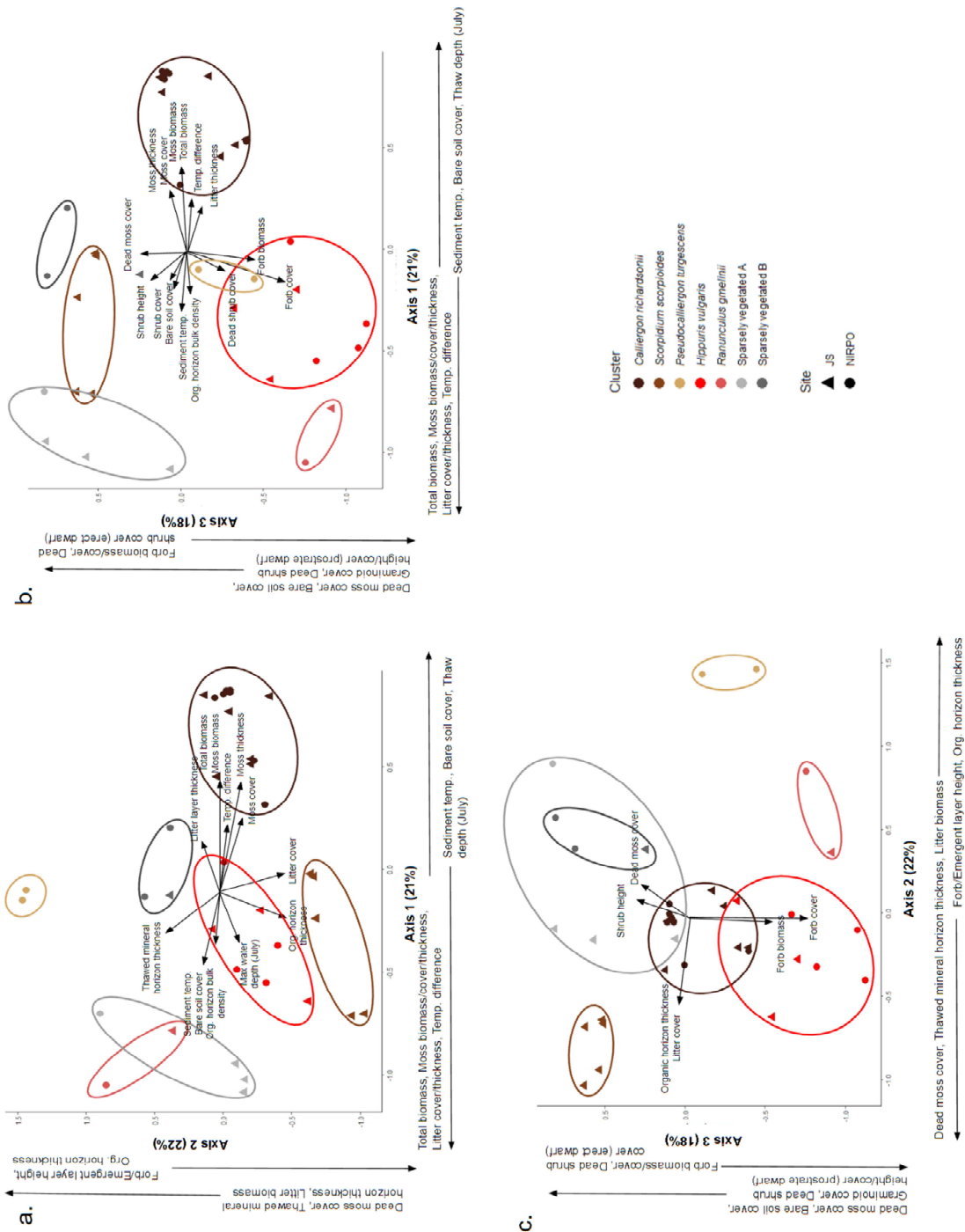


Figure 15. NMDS ordination of thermokarst-pond plots within various community clusters, showing all axes: (a.) Axes 1 and 2, (b.) Axes 1 and 3, and (c.) Axes 2 and 3. Plots are arranged spatially based on differences in species composition. Vector biplots show environmental variables ($r^2 \geq 0.2$), and variables correlated each to axis ($|t| > 0.3$) are indicated along the axis.

The variables positively correlated with Axis 2 included litter biomass, dead moss cover, and thawed mineral horizon thickness. Organic horizon thickness and forb/emergent vegetation layer thickness were negatively correlated with Axis 2, but no variables were highly correlated with Axis 2. The *P. turgescens*, *R. gmelinii*, and, to a lesser extent, both sparsely vegetated groups occupied the ordination space along Axis 2 associated with high litter biomass, thawed mineral horizon thickness, and dead moss cover. The *S. scorpioides* community occupied the ordination space associated with high organic layer thickness and emergent/forb layer height.

Table 4. Correlations of environmental variables with axes of NMDS ordination. Cutoff values for correlations are $r^2 \geq 0.2$ for inclusion in biplot, $|\tau| \geq 0.3$ for correlation with axes, and $|\tau| \geq 0.5$ for high correlation with axes. Values meeting these cutoffs are indicated in light gray.

		Axis 1		Axis 2		Axis 3	
		r^2	τ	r^2	τ	r^2	τ
% Cover (Live/Dead)	Erect dwarf shrub (D)	0.061	-0.219	0.001	-0.042	0.198	-0.340
	Prostrate dwarf shrub (D)	0.150	-0.285	0.031	0.182	0.136	0.310
	Deciduous shrub (D)	0.150	-0.285	0.031	0.182	0.136	0.310
	Erect forbs (L)	0.136	-0.298	0.003	-0.193	0.580	-0.619
	Erect forbs (D)	0.012	-0.118	0.028	-0.019	0.191	-0.345
	Non-tussock graminoid (L)	0.102	-0.227	0.005	-0.279	0.053	0.345
	Non-tussock graminoid (D)	0.077	-0.267	0.047	0.046	0.085	0.404
	Moss (L)	0.457	0.500	0.065	-0.208	0.011	0.066
	Moss (D)	0.017	-0.146	0.120	0.353	0.227	0.300
	Bare soil	0.202	-0.326	0.009	0.229	0.132	0.373
Mean thickness (cm)	Litter	0.049	0.305	0.362	-0.293	0.002	-0.133
	Shrub layer	0.104	-0.288	0.068	0.187	0.234	0.399
	Emergent layer	0.016	0.141	0.122	-0.324	0.008	-0.093
	Herb layer	0.037	-0.227	0.145	-0.332	0.084	-0.287
	Live moss layer	0.331	0.425	0.059	-0.189	0.019	0.056
	Thawed mineral horizon	0.140	-0.252	0.188	0.313	0.032	-0.113
	Organic horizon	0.113	-0.236	0.395	-0.428	0.023	0.106
Organic horizon	Litter layer	0.238	0.323	0.027	0.128	0.029	-0.154
	Bulk density (g/cm ³)	0.211	-0.284	0.000	-0.011	0.005	-0.072
Mean depth (cm)	Thaw (July)	0.190	-0.334	0.010	0.178	0.006	0.099
Biomass (g/m ²)	Total	0.418	0.513	0.001	0.032	0.001	0.015
	Moss	0.414	0.470	0.000	0.011	0.001	0.091
	Forb	0.049	-0.210	0.007	-0.094	0.426	-0.585
	Litter	0.013	-0.229	0.110	0.386	0.065	0.213
Mean temp. (°C, 19 July – 23 Aug. 2021)	Sediment	0.251	-0.343	0.023	0.186	0.007	0.107
	Difference (water surface to sediment)	0.275	0.357	0.027	-0.178	0.015	-0.131

Axis 3 represented a complex gradient of forb presence, with forb-dominated communities at one end and those with high cover of graminoids, dead moss, and bare soil at the other. Axis 3 was highly negatively correlated with live forb cover and forb biomass. Dead forb cover and dead shrub (erect dwarf) cover were also negatively correlated with Axis 3. Graminoid cover, dead shrub (prostrate dwarf and deciduous) cover, dead moss cover, bare soil cover, and shrub height were positively correlated with Axis 3. The *H. vulgaris* and *R. gmelinii* communities occupied the ordination space along Axis 3 associated with high forb biomass/cover and high dead erect dwarf shrub cover. The ordination space associated with high dead moss cover, bare soil cover, graminoid cover, dead shrub height, and shrub (prostrate dwarf and deciduous) cover was occupied by the *S. scorpioides* community and both groups of sparsely vegetated plots.

3.2 Temperature and thaw analyses

Over a 35-day period (19 July – 23 August 2021), the highest mean daily pond sediment temperatures were observed in mid-July (approx. 15 °C) and the lowest were observed in mid-August (approx. 4 °C) (*Figure 16c*), which is consistent with summer air temperature trends in the region (1991 – 2020 July mean 8.5°C, August mean 6.4 °C) (ACRC, 2020). Water surface temperatures ranged from approximately 5 to 20 °C during the period of measurement, and there were no clear differences in water-surface temperatures among vegetation types (*Figure 16a*). The highest mean daily sediment temperatures were observed in sparse plots, which ranged from 4.8 to 15.3 °C. Mean daily sediment temperatures in forb plots were similar to those of the sparse plots, ranging from 4.6 to 12.5 °C. Moss plots had the lowest mean daily sediment temperatures of any plot type throughout the period of measurement, ranging from 3.7 to 10.7 °C. The periods of greatest sediment temperature difference between groups occurred during the warmest times

of the summer from 19 July through early August, and particularly at peaks in temperature curves (*Figure 16c*). Throughout the period of sampling, differences in mean daily temperature between vegetation types were less distinct above the submerged vegetation layer (*Figure 16b*) and nearly absent at the water surface.

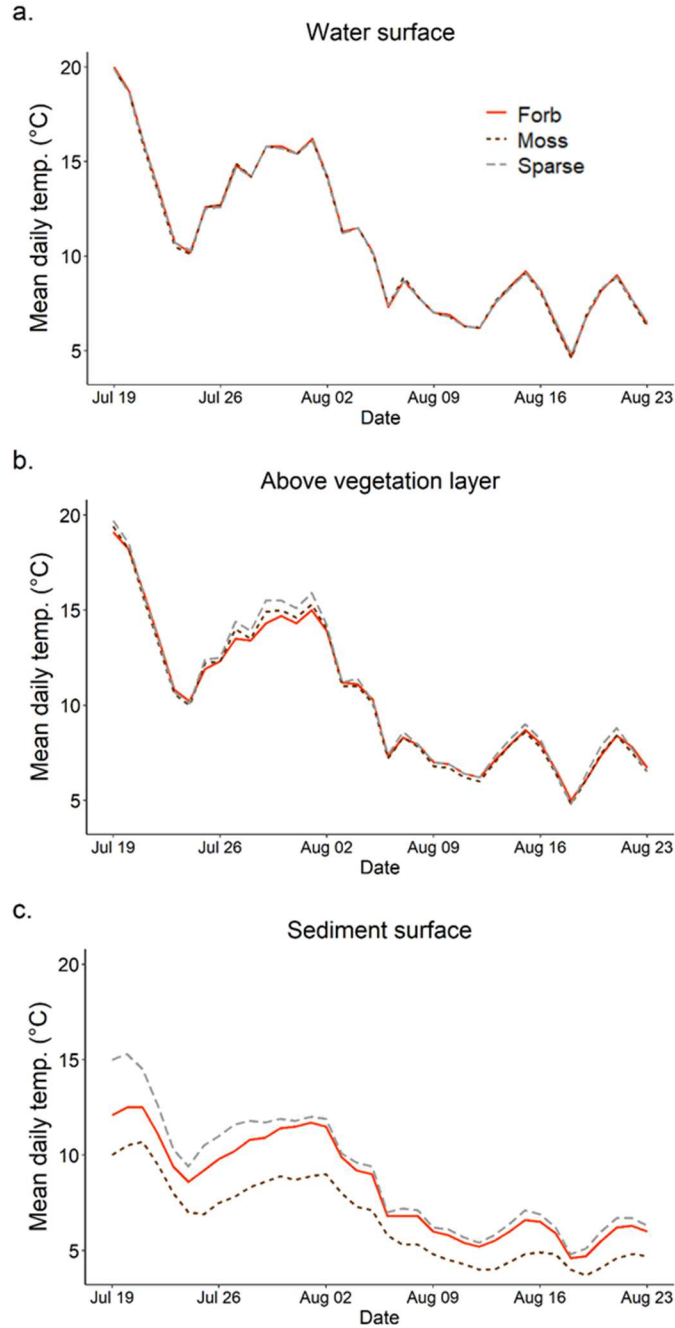


Figure 16. Mean daily water temperature over period of study (19 July – 23 August 2021) for each vegetation type: moss ($n = 12$), forb ($n = 7$), sparse ($n = 10$). Temperatures shown are from sensors positioned (a.) at the water surface, (b.) above the submerged vegetation layer, and (c.) at the sediment surface.

Differences in mean sediment temperature within thermokarst ponds varied significantly with vegetation type, with lower mean temperatures in moss-dominated plots relative to sparse and forb-dominated plots (*Figure 17a*). Mean sediment temperature was significantly lower in moss-dominated plots ($6.7^{\circ}\text{C} \pm 0.4 \text{ SE}$) relative to sparse ($8.9^{\circ}\text{C} \pm 0.2 \text{ SE}; p < 0.05$) or forb-dominated plots ($8.2^{\circ}\text{C} \pm 0.3 \text{ SE}; p < 0.05$), although mean sediment temperatures within sparse and forb-dominated plots did not differ significantly ($p = 0.34$).

Mean thaw depth also differed depending on vegetation type (*Figure 17b*). Thaw depth was significantly shallower in moss-dominated plots ($42.5 \text{ cm} \pm 1.3 \text{ SE}$) than in sparse plots ($52.7 \text{ cm} \pm 1.4 \text{ SE}; p < 0.05$) or forb-dominated plots ($52.4 \text{ cm} \pm 1.7 \text{ SE}; p < 0.05$), indicating the function of moss in subsurface insulation. Mean thaw depth did not significantly differ between sparse and forb plots ($p = 0.99$).

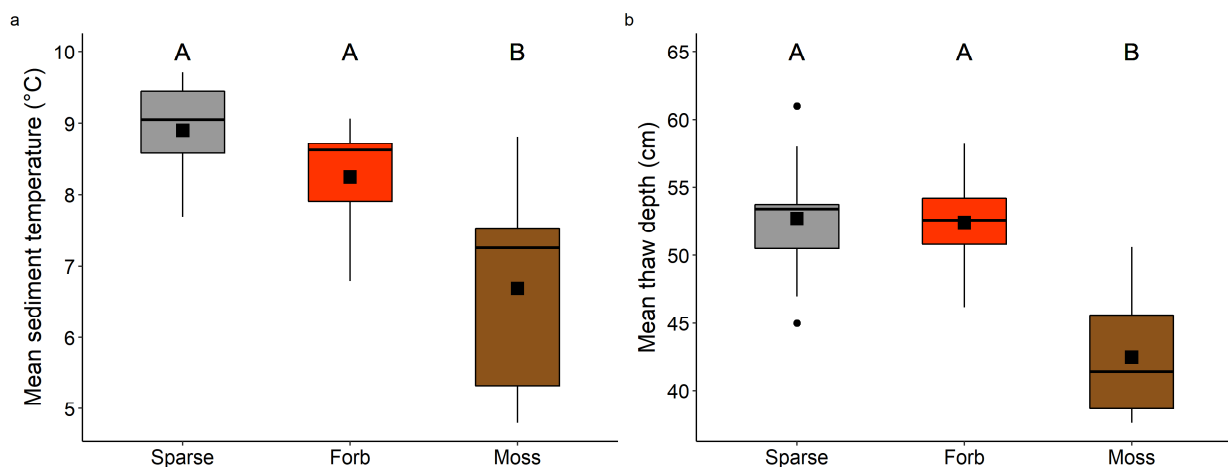


Figure 17. Boxplots showing (a.) mean measured sediment temperature and (b.) mean thaw depth by plot type: sparse ($n = 10$), forb ($n = 7$), and moss ($n = 12$). Boxes indicate interquartile range (IQR, 25 – 75th percentile), box lines indicate median, whiskers indicate values within 1.5 times IQR, circular points indicate outliers, and square points indicate mean values. Capital letters above boxes indicate significance of group differences based on one-way ANOVA and post hoc Tukey-adjusted estimates (significance at $p < 0.05$).

Vegetation-related variables were negatively correlated with mean sediment temperature and mean thaw depth. Moss thickness explained more variation in sediment temperature ($R^2=0.44$) than moss biomass ($R^2=0.26$) or total vegetation cover ($R^2=0.34$) (Figure 18a-c). Maximum water depth and organic horizon thickness were not found to be correlated with sediment temperature (Figure 18d-e). Correlations with thaw depth showed similar results, with moss thickness explaining the greatest amount of variation ($R^2=0.58$) (Figure 19b). Moss biomass ($R^2=0.39$) and total vegetation cover ($R^2=0.30$) were also negatively correlated with thaw depth (Figure 19a,c). Correlations with maximum water depth and organic horizon thickness were not found ($p > 0.05$) (Figure 19d,e).

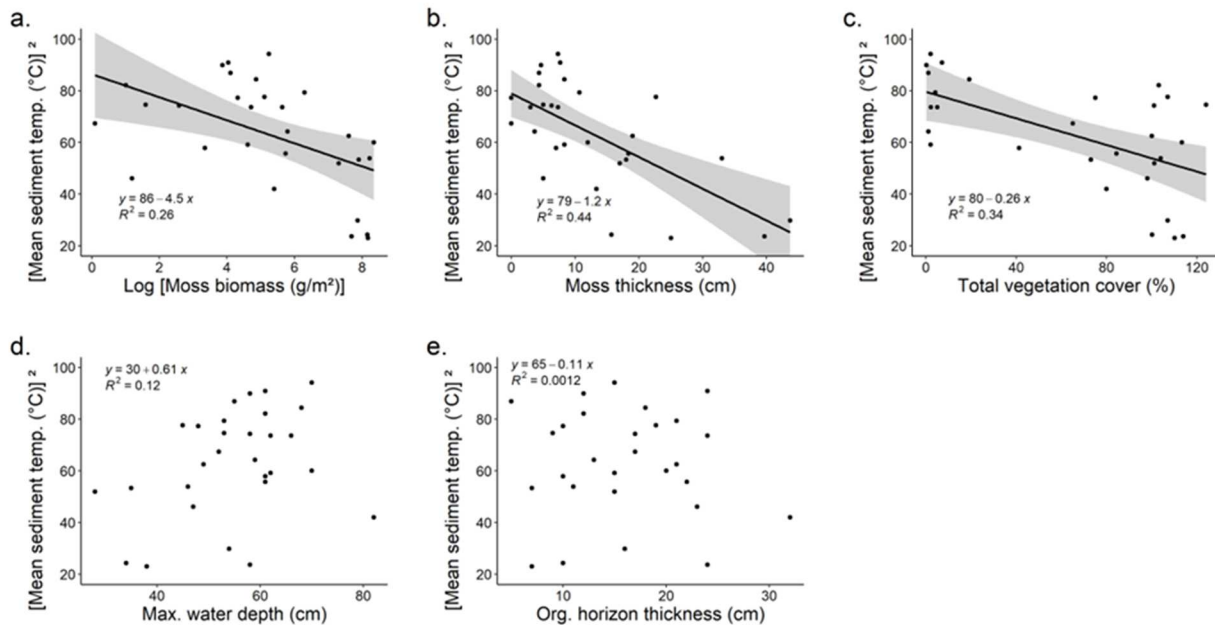


Figure 18. Correlations of mean sediment temperature (squared for normality) with various predictor variables, including (a.) log-transformed moss biomass, (b.) moss thickness, (c.) total % vegetation cover, (d.) maximum water depth, and (e.) organic horizon thickness. Equations and R^2 values are from linear regression analyses of plot data, where $n=29$. Lines indicate model estimates for statistically significant associations ($p < 0.05$), points indicate data points, and ribbons indicate upper and lower 95% confidence intervals.

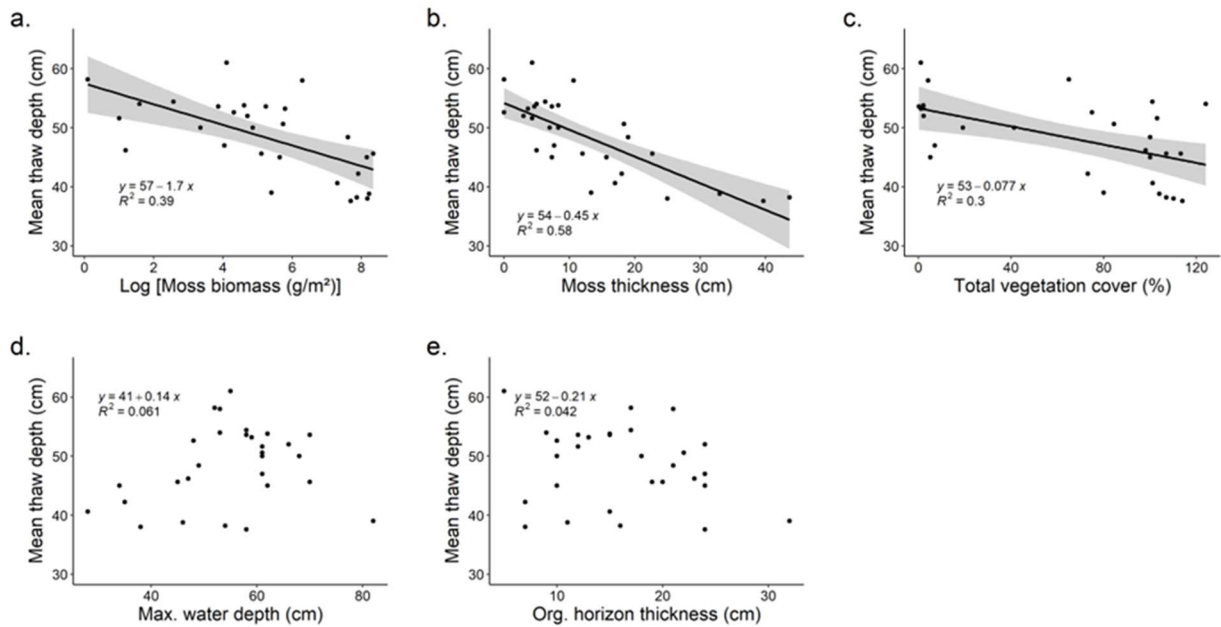


Figure 19. Correlations of mean thaw depth with various predictor variables, including (a.) log-transformed moss biomass, (b.) moss thickness, (c.) total % vegetation cover, (d.) maximum water depth, and (e.) organic horizon thickness. Equations and R^2 values are from linear regression analyses of plot data, where $n=29$. Lines indicate model estimates for statistically significant associations ($p < 0.05$), points indicate data points, and ribbons indicate upper and lower 95% confidence intervals.

Mixed-effects models showed correlations with temperature and thaw depth while accounting for the effects of multiple variables. R^2 values from models are shown within figures. Marginal R^2 is the variance a model explained only by fixed effects, while the conditional R^2 is the variance explained by the full model including random effects. Variables related to vegetation quantity and soil organic horizon were negatively correlated with sediment temperature and thaw depth, whereas water depth had no effect (*Figures 20, 21*). Total vegetation cover was negatively correlated ($p < 0.05$) with both mean sediment temperature and mean thaw depth (*Figures 20c, 21c, 22*). Organic horizon thickness was negatively correlated with thaw depth (*Figures 21e, 22*). Mean moss thickness had a negative effect on thaw depth (*Figures 21b, 22*). Water depth was not correlated with either sediment temperature (*Figures*

20d, 22) or thaw depth (*Figures 21d, 22*). Correlations of variables with thaw depth were more apparent than those with sediment temperature (*Figure 22*).

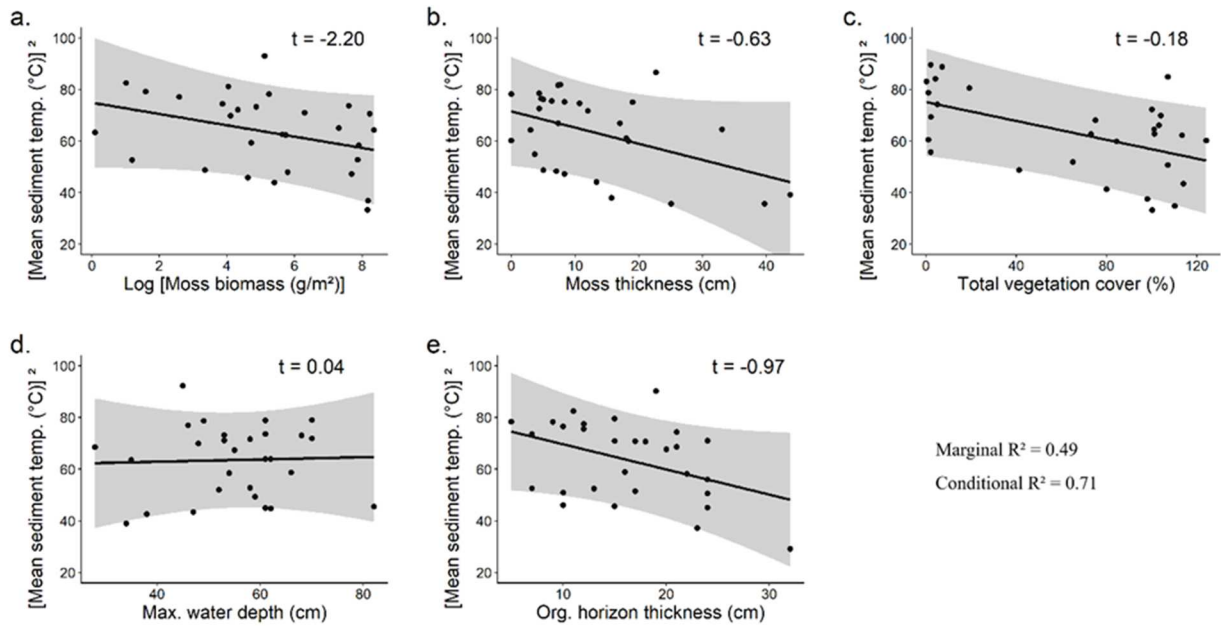


Figure 20. Partial residual plots from a mixed effects model of mean sediment temperature (squared), with site as a random effect. Plots show residuals of a particular predictor variable against residuals of the response variable, accounting for all other predictors included in the model. Predictors shown include (a.) log-transformed moss biomass, (b.) moss thickness, (c.) total % vegetation cover, (d.) maximum water depth, and (e.) organic horizon thickness. Lines indicate model estimates, points indicate data points, and ribbons indicate upper and lower 95% confidence intervals. Marginal and conditional R² values of overall model are shown, along with coefficient estimates (t) for each variable.

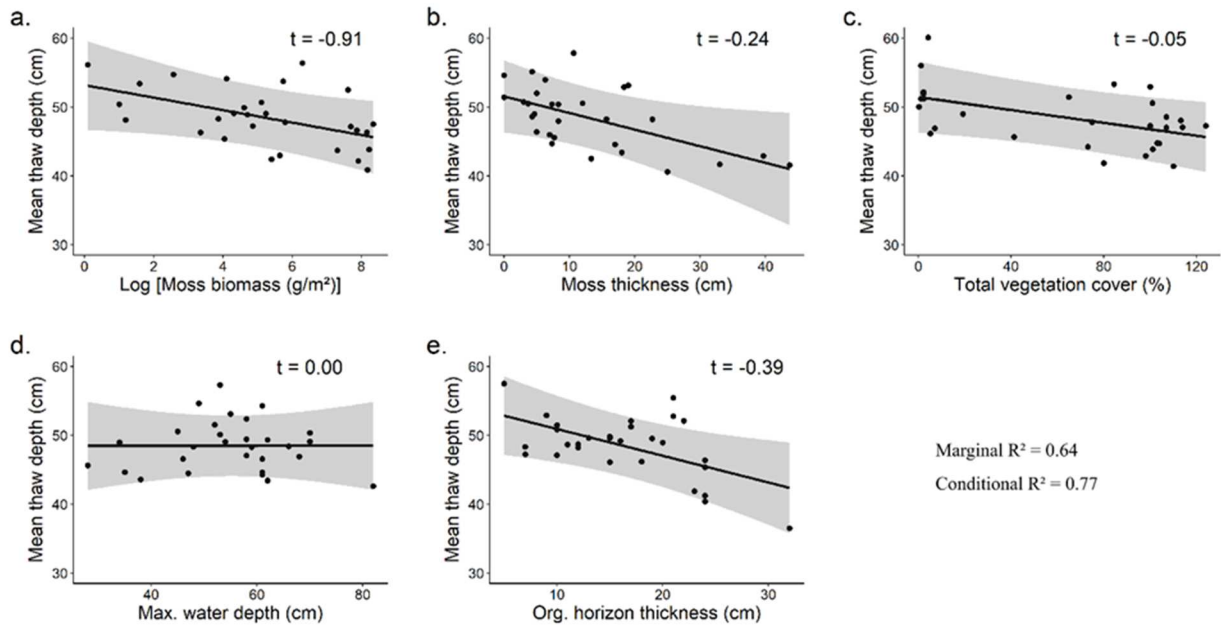


Figure 21. Partial residual plots from a mixed effects model of mean thaw depth. Plots show residuals of a particular predictor variable against residuals of the response variable, accounting for all other predictors included in the model. Predictors shown include (a.) log-transformed moss biomass, (b.) moss thickness, (c.) total % vegetation cover, (d.) maximum water depth, and (e.) organic horizon thickness. Lines indicate model estimates, points indicate data points, and ribbons indicate upper and lower 95% confidence intervals. Marginal and conditional R² values of overall model are shown, along with coefficient estimates (*t*) for each variable.

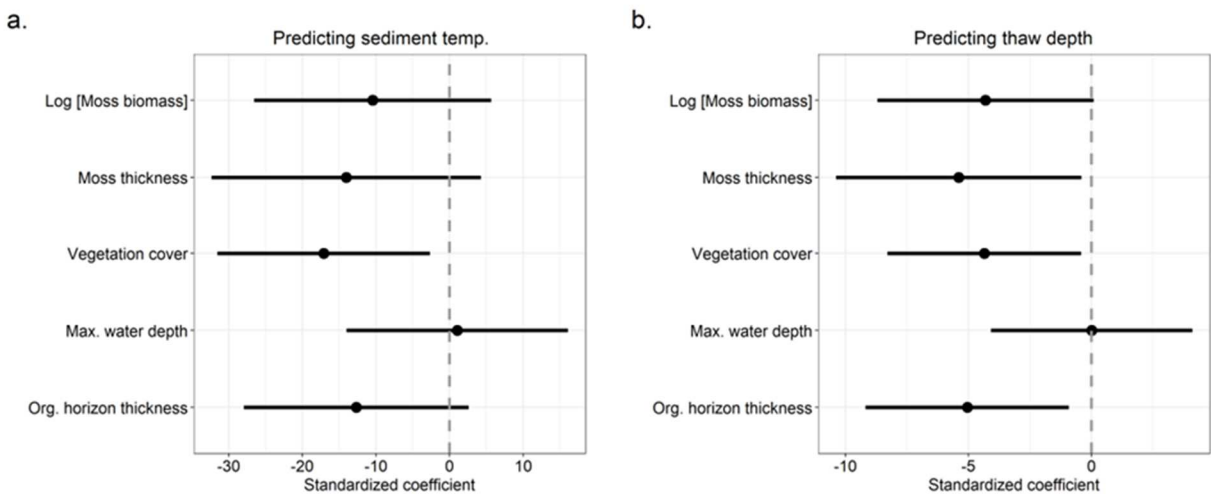


Figure 22. Standardized effect sizes of predictor variables from models of (a.) mean sediment temperature and (b.) mean thaw depth. Points indicate mean model estimates, whiskers indicate upper and lower 95% confidence intervals, and dotted line indicates a coefficient estimate of zero. Coefficients are divided by two times their standard deviation in order to improve comparison of effects (Gelman, 2008).

Table 5. Results of mixed-effects models of mean sediment temperature and mean thaw depth with all fixed predictors, including model estimate, upper and lower 95% confidence interval, test statistic, *p*-value (based on F-test using Kenward-Roger degrees of freedom approximation), and degrees of freedom. Bold values indicate significance at the *p* < 0.05 level. Also shown are the total variance (σ^2), the variance explained by the random effect of site (τ_{00}), the intraclass correlation coefficient (ICC), the number of random effect groups (N), the total number of observations (N), and the R² (both marginal and conditional) of the models.

Predictors	Sediment temp.					Thaw depth				
	Estimates	CI	Statistic	<i>p</i>	df	Estimates	CI	Statistic	<i>p</i>	df
(Intercept)	108.05	54.19 - 161.92	4.30	0.001	13.93	65.55	50.92 - 80.19	9.56	< 0.001	14.85
Log [Moss biomass]	-2.20	-5.59 - 1.19	-1.34	0.193	22.06	-0.91	-1.83 - 0.02	-2.03	0.055	22.08
Moss thickness	-0.63	-1.45 - 0.19	-1.59	0.126	22.07	-0.24	-0.47 - (-0.02)	-2.24	0.036	22.09
Vegetation cover	-0.18	-0.34 - (-0.03)	-2.43	0.024	22.24	-0.05	-0.09 - 0.00	-2.27	0.033	22.30
Max. water depth	0.04	-0.60 - 0.69	0.14	0.888	22.48	0.00	-0.18 - 0.18	0.00	0.997	22.58
Org. horizon thickness	-0.97	-2.26 - 0.31	-1.57	0.131	22.97	-0.39	-0.75 - (-0.03)	-2.25	0.034	22.74
Random Effects										
σ^2	187.56					13.97				
τ_{00}	145.36 site					8.10 site				
ICC	0.44					0.37				
N	2					2				
Observations	29					29				
Marginal R ²	0.492					0.640				
Conditional R ²	0.714					0.772				

4. Discussion

4.1 Thermokarst-pond plant communities

This study described three moss-dominated communities, two forb-dominated communities, and two sparsely vegetated units. These communities were low-diversity and generally dominated by a single species. Communities sorted out along a gradient of vegetation abundance and pond sediment temperature, along which high biomass and cover were associated with low temperature and increased stratification of the water column from water surface to sediment. This indicates that vegetation influences temperature and thaw dynamics within ponds, and that communities have differential capacities for insulation.

4.1.1 Community gradients

Gradients in community composition were largely driven by vegetation type. Along Axis 3, community clusters sorted out distinctly in the ordination space along a forb abundance

gradient according to whether they were moss- or forb-dominated (*Figure 15b, c*). In the ordination space represented by Axes 1 and 3 (*Figure 15b*), there was a general separation in the ordination space between the forb-dominated communities (*H. vulgaris* and *R. gmelinii*) and both the moss-dominated communities and sparsely vegetated clusters. However, overlap existed in regards to the *H. vulgaris* community. The moss-dominated community *P. turgescens* overlapped this community in some cases (*Figure 15a*), likely due to the presence of *P. turgescens* and *H. vernicosus* in some of the *H. vulgaris* community plots. The *C. richardsonii* community also showed overlap with the *H. vulgaris* community (*Figure 15c*), likely due to the presence of *H. vulgaris* in some plots of the *C. richardsonii* community and vice versa. The *S. scorpioides* community and both clusters of sparsely vegetated plots consistently clustered farthest away from the forb-dominated communities along Axis 3 (*Figure 15b,c*). This was likely due to their relatively low forb cover and high graminoid cover.

There were several axis correlations which represented variables that were likely not of high ecological importance within ponds. For example, cover of dead erect dwarf shrubs was negatively correlated with Axis 3, while shrub height and cover of prostrate dwarf shrubs was positively correlated with the same axis (*Table 4*). When shrubs were found within ponds, they were exclusively standing dead shrubs and occupied very low cover. The presence of submerged dead shrubs close to the sediment surface could easily have been obscured by dense vegetation in many of the moss-dominated plots. While the presence of shrubs was of interest in indicating relatively young ponds, in which submerged shrubs had not yet decomposed, shrub presence was not likely to be representative of a major compositional gradient. Graminoid cover was positively correlated with Axis 3, which was exclusively composed of *C. aquatilis*, the only graminoid found within plots. Within the Sparse A group, two plots contained *C. aquatilis*, with one having

1% cover and one having 4% cover. Graminoid cover may have been slightly higher in these sparsely vegetated areas due to a lack of competition with other aquatic species for light, space, or nutrients. In all other clusters, including the *S. scorpioides* community in which *C. aquatilis* was a diagnostic species, cover of this species did not exceed trace percentage (0.1%). In addition, *C. aquatilis* was only found within plots at the JS site. Plots containing graminoids, especially those within the *S. scorpioides* community, may have represented a variation of the *Carex aquatilis-Scorpidium scorpioides* sedge tundra (Stand Type M4) community described by Walker (1985), which was generally found in shallower waters (< 10 cm). While axis correlations with shrub and graminoid-related factors were apparent within the ordination, these growth forms were not abundant within thermokarst ponds and were not likely to represent major compositional gradients.

4.1.2 Pond age and succession

A clear successional trajectory was not apparent within this study. All clusters and vegetation types showed overlap in pond development age (*Figure 13*). It is possible that the *P. turgescens* and *C. richardsonii* communities represented an earlier stage of thermokarst-pond succession, given that these were the only clusters containing ponds in the youngest age group (D, 2008 – 2021). Age differences between clusters may also be due to differences in pond initiation between sites. A larger proportion of thermokarst ponds at JS were from the older age groups compared with NIRPO. These age differences could be a result of differences in degradation timelines between sites, with earlier initiation of pond formation at JS relative to NIRPO, rather than an indication of a successional trajectory. Further complicating the identification of a successional vegetation trajectory was the fact that some ponds (often relatively large ponds, based on observation) contained multiple communities representing

multiple vegetation types. Areas of a pond that were sparsely vegetated may have represented areas that have yet to be colonized by vegetation or are in very early stages of colonization. Overall, a successional trajectory was not clear.

While deterministic trajectories of succession have been observed in thermokarst ponds (Magnússon et al., 2020), there is likely a high degree of stochasticity in aquatic plant-community composition due to frequent small-scale disturbances that may trigger stochastic processes (Capers et al., 2010). In shallow thermokarst ponds, stochastic community assembly processes have been found to influence microbial communities within the water column (Le Moigne et al., 2020). A previous study of aquatic vegetation within ponds found plant community composition to be individualistic, largely determined by chance dispersal, and not closely associated with environmental conditions (Edvardsen & Økland, 2006). In addition, a study of three recently drained thaw lakes in the northern region of Bering Land Bridge National Preserve found that different plant species colonized each lake basin immediately following drainage. These early successional stands were nearly monospecific, but all transitioned to graminoid-dominated wetland tundra within several years (Swanson, 2022). Stochastic processes are thought to be influential in early stages of vegetation succession, and to give way to more environmentally-driven, deterministic processes in later stages (Måren et al., 2018).

The notion that species colonize newly formed thermokarst ponds largely by chance and maintain dominance by forming dense stands that shade out other species is supported by clear patterns of monospecific dominance and low species richness (mean plot richness 3.2 ± 0.2) within ponds. Within this study, the role of stochastic processes is also indicated by the high variability in species composition found within ponds of similar age, as well as the fact that many of these ponds are relatively young and may be in earlier stages of succession, during

which priority effects are of greater importance. When a particular species is able to colonize a pond area successfully, it may then maintain dominance by limiting light available for the establishment of other species. Mosses growing in dense, submerged mats can limit light and space available to other species, and even display a high risk of self-shading, wherein their own production is limited by their dominance (Riis et al., 2014). Rapid development of abundant aquatic mosses within ponds may limit the establishment of and outcompete other species following initial colonization. In five of the 14 plots within the *C. richardsonii* community, emergent *H. vulgaris* was found growing through the dense moss mat at cover values ranging from 2 – 18%. These plots were in ponds that ranged in age from 22 – 30 years, and may represent an area formerly dominated by *H. vulgaris* which was later colonized by *C. richardsonii*. Subsequent shading by the dense *C. richardsonii* moss mat may have resulted in the disappearance of most submergent *H. vulgaris* growth due to competition for light. The patterns of abundant, monospecific growth of singular species within very low-diversity plant communities that were observed here may be a result of stochastic establishment of species followed by rapid growth that inhibits the establishment of additional species in a given area.

Biomass can develop rapidly in moss-dominated thermokarst-pond communities. Surprisingly, plots within the youngest age group (D, 2008 – 2021) had notably high total biomass values and were all moss-dominated (two *C. richardsonii* plots and one *P. turgescens* plot). Aboveground net primary production (ANPP) values were calculated for these plots using total biomass values and approximate age of pond formation determined from aerial images (*Table 6*). These values ranged from approximately 268 – 428 g/m²y, which is high relative to known ANPP values of Arctic vegetation classes. For example, these values exceed ANPP ranges for sedge-moss tundra (50 – 250 g/m²y) and are comparable to those of low and tall shrub

tundra (250 – 1000 g/m²y) (Gould et al., 2003). Many of the moss species found within ponds can also occur in moist and wet tundra terrestrial plant communities (Walker, 1985), so it is possible that species from nearby terrestrial habitats may simply have persisted and proliferated as their surroundings became inundated, and that these calculated values may overestimate ANPP. Further study including a larger sample size of young ponds will be needed to obtain accurate productivity estimates. However, it remains clear that moss-dominated communities have the ability to rapidly develop biomass soon after pond formation.

Table 6. Pond approximate age (yrs.), total biomass (g/m²), and aboveground net primary production (g/m²y) of plots within the youngest age group (D, 2008 – 2021).

Plot	Community	Approx. Age (yrs.)	Total biomass (g/m ²)	ANPP (g/m ² y)
21A-09	<i>Calliergon</i> comm.	8	2146.8	268.4
21A-10	<i>Calliergon</i> comm.	10	4277.7	427.8
21A-32	<i>Pseudocalliergon</i> comm.	10	2720.3	272.0

4.2 Effect of vegetation on thermal properties

4.2.1 Role of moss in ice-wedge stabilization

Vegetation, especially moss, reduced sediment-surface temperatures and thaw depth. Moss-dominated areas had lower sediment temperature and thaw depth than forb-dominated or sparsely vegetated areas. Temperature is known to affect moss growth; for example, annual growth of the moss species *Drepanocladus trifarius* in Arctic ponds was found to correlate positively with mean summer temperatures (Thiemer et al., 2018). However, within this study, it is unlikely that the observed effects represented effects of temperature on vegetation. For most aquatic plant species, the temperature range for optimal rates of photosynthesis is between 20 and 35 °C (Bornette & Puijalon, 2009), which is above the maximum sediment temperature observed during the period of sampling (approximately 15 °C). Lower mean sediment

temperatures and greater vertical temperature stratification in moss-dominated plots indicated that mosses insulated the sediment surface and reduced within-pond mixing. While sediment temperatures differed by plot type, differences in water-surface temperatures between vegetation types were not observed throughout the period of sampling (*Figure 16a*). This is consistent with results of previous studies regarding the effects of pond vegetation on temperature, which found that submerged aquatic vegetation increased temperature stratification within the water column (Andersen et al., 2017). In shallow ponds of northern Alaska, Leffingwell (1919) observed a similar effect of vegetation, noting that blankets of algae preserved underlying ice well into spring and summer by reducing radiative and convective heating. In this case, it is less likely that mosses were preferentially growing in areas of lower sediment temperature and more likely that vegetation itself was influencing temperature.

Although thermal conductivity of moss is generally positively correlated with volumetric water content (O'Donnell et al., 2009), potentially reducing the summer insulative properties of aquatic mosses, the results of this study indicated an insulative function of submerged aquatic mosses, despite their high water-content. This is consistent with previous studies (Jorgenson et al., 2015; Kanevskiy et al., 2022). The ability of terrestrial mosses to insulate the ground surface and reduce thaw depth has also been empirically shown in studies of Arctic terrestrial vegetation (Gornall et al., 2007). Experimental removal of terrestrial mosses was found to increase ground heat flux in the Siberian Arctic (Blok et al., 2011). A study of patterned-ground features found that experimental removal of vegetation led to warmer summer soil temperatures and deeper thaw, while removal in combination with terrestrial moss addition led to cooler summer soil temperatures and shallower thaw (Kade & Walker, 2008). Over the period of summer-temperature measurements, areas of moss maintained mean daily sediment temperatures that

were consistently lower than forb or sparse areas. Every 10 cm increase in moss thickness resulted in a decrease in sediment temperature of approximately 3.5 °C. This temperature differential was greatest during the end of July, when summer temperatures in the region are highest on average (1991 – 2020 July mean 8.5 °C, the warmest month) (ACRC, 2020).

The large quantity of vegetation found in moss-dominated areas contributed to the low temperatures and thaw observed in these areas. Moss-dominated plots had significantly higher mean total biomass ($2741.4 \text{ g/m}^2 \pm 1771.7 \text{ SD}$) and total vegetation cover ($100.7\% \pm 10.7 \text{ SD}$) relative to forb (biomass $185.4 \text{ g/m}^2 \pm 144.8 \text{ SD}$, cover $87.8\% \pm 26.0 \text{ SD}$) and sparse plots (biomass $306.3 \text{ g/m}^2 \pm 181.9 \text{ SD}$, cover $4.4\% \pm 5.6 \text{ SD}$). In this study, every 1000 g/m² of moss biomass resulted in a decrease in sediment temperature of approximately 3.7 °C, and a decrease in thaw depth of approximately 5.1 cm (*Figures 18a, 19a*). Biomass of submerged vegetation has been found to reduce mixing and increase temperature gradients within the water column (Dale & Gillespie, 1977; Andersen et al., 2017). In addition, mosses decompose slowly and are well adapted to conditions of low light, temperature, and nutrients (Kallio & Karenlampi, 1975; Riis & Sand-Jensen, 1997; Riis et al., 2010), all of which may account for the ability of these moss-dominated areas to develop greater quantities of vegetation relative to forb-dominated areas. Thus, areas dominated by mosses are more likely to display ice-wedge stabilization.

Given the importance of mosses in stabilizing ice wedges, determining why dense moss develops in some thermokarst ponds and not others will be important in predicting trajectories of degradation. The factors controlling vegetation type within thermokarst ponds remain poorly described, but aquatic-plant-community composition is known to be influenced by environmental conditions (Akasaka & Takamura, 2011), succession (Li et al., 2017; Magnússon et al., 2020), spatial processes such as dispersal, and stochasticity due to frequent small-scale

disturbances (Capers et al., 2010). Identifying the factors that determine whether a thermokarst pond becomes dominated by mosses, forbs, or sparse vegetation will aid in predicting which ice wedges may stabilize and which may continue to degrade.

4.2.2 Predictors of temperature and thaw

Vegetation and sediment organic-matter thickness influence the process of ice-wedge degradation within thermokarst ponds by decreasing sediment temperature and thaw depth. Vegetation cover was the only predictor within the model that was significantly correlated with both sediment temperature and thaw depth. A previous study of ice-wedge degradation at the JS study site also identified a negative correlation between sediment surface temperature and vegetation cover, and a positive correlation between sediment temperature and water depth (Jorgenson et al., 2015). Correlations between thaw or temperature and water depth were not found within this study, which may be due to differences in scope of sampling. Here, sampling was specifically done within relatively deep thermokarst ponds (mean maximum plot water depth of all plots $55.5\text{ cm} \pm 11.2\text{ SD}$), while sampling by Jorgenson et al. (2015) included areas with relatively low water depth (all mean water depths $< 20\text{ cm}$) in addition to advanced-degradation thermokarst ponds (mean water depth approximately 60 cm). Inclusion of relatively shallowly flooded polygon troughs may reveal water-depth correlations which are obscured within this deep-water sampling scheme.

Correlations between predictor variables and thaw depth are more apparent than those with sediment temperature and are more indicative of long-term changes in permafrost below ponds. Temperature data were temporally limited in this study, given the relatively short 35-day sampling period. Although a relationship between vegetation cover and sediment temperature was observed, seasonal differences and long-term effects were not captured within these

temperature measurements. Measurements of thaw depth, resulting from the full summer's temperatures > 0 °C, provide a more direct indication of potential insulative effects of vegetation. Thaw depth was negatively correlated with moss thickness, vegetation cover, and organic horizon thickness, indicating that these factors represented negative feedbacks to ice-wedge degradation. The development of vegetation cover and the buildup of organic material can contribute to the formation of a thick intermediate layer above an ice wedge, which is a key determinant of a wedge's vulnerability to thermokarst (Kanevskiy et al., 2017). In addition, vegetation can directly insulate thawed soil and cause ground ice to aggrade (Shur et al., 2011; Magnússon et al., 2020).

Although the general relationships between temperature and thaw that were identified in this study may be common throughout similar areas within the North Slope region, the quantitative relationships found here may not be representative of those found in other Arctic regions. The progression of ice-wedge degradation varies throughout the Arctic depending on subsurface ice content (Kanevskiy et al., 2017), disturbance due to infrastructure (Raynolds et al., 2014; Kanevskiy et al., 2022), vegetation composition (Nauta et al., 2015), terrain (Liljedahl et al., 2016), hydrology (Abolt et al., 2020), and the interactions between these factors. The correlations between vegetation and thaw identified within this study represent a relatively small study area within the nonacidic tundra of the Prudhoe Bay region and may vary throughout the Arctic. For example, in areas of acidic tundra where *Sphagnum* mosses (which were absent in the nonacidic study area) dominate thermokarst ponds in advanced stages of permafrost recovery (Magnússon et al., 2020), rates of stabilization may be faster due to the ability of *Sphagnum* as an ecosystem engineer to create conditions that favor increased *Sphagnum* growth (van Breemen,

1995). Studies of the effects of thermokarst-pond vegetation on ice-wedge degradation in other Arctic regions will help to resolve these relationships at a broader spatial scale.

Relationships between vegetation and permafrost thaw have important implications for trajectories of landscape change. This study indicated that aquatic vegetation within thermokarst ponds created negative feedbacks to ice-wedge degradation by decreasing sediment temperatures and reducing subsurface thaw. In addition, vegetation cover, moss thickness, and sediment organic horizon thickness were the factors with the largest effects on thaw dynamics, and moss-dominated areas displayed the lowest temperatures and thaw depths. Continued warming is likely to result in increases in temperature, nutrient input, and growing season length within aquatic systems (Rautio et al., 2011), all of which are likely to create favorable conditions for increased aquatic plant growth (Schuur et al., 2008; Riis et al., 2010; Lauridsen et al., 2019). Given these findings on the effects of vegetation on temperature and thaw, thermokarst-pond vegetation may play a major role in promoting ice-wedge stabilization if these effects are able to offset the many positive feedbacks to climate warming.

4.3 Connecting community composition with thaw dynamics

Given the observed differences in insulation capacity between communities and vegetation types, understanding the determinants of community composition within thermokarst ponds is of interest in predicting trajectories of thaw. A simplified conceptualization based on findings of this study summarizes the potential role of broad plant community types (i.e., moss, forb, sparse) in landscape change (*Figure 23*). Forb-dominated and sparsely vegetated areas of vegetation appear to have a low capacity for insulation, thus ponds dominated by these types may experience continued thaw of underlying ice wedges and adjacent permafrost. A study of an unvegetated thermokarst pond found it to be a significant source of methane (Beckebanze et al.,

2022), as did a study involving thermokarst pond formation following a shrub removal experiment (Nauta et al., 2015). Continued permafrost thaw can release large amounts of organic carbon, perpetuating further climate warming (Schuur et al., 2008). In contrast, areas dominated by moss accumulate large quantities of vegetation and soil organic matter that decrease the amount of solar radiation absorbed by sediments. This is likely to have a negative effect on permafrost thaw and increase the likelihood of ice-wedge stabilization. Areas where ice-wedge stabilization has occurred are less likely to degrade in the future due to the formation of a thicker intermediate layer overlying the ice wedge (Kanevskiy et al., 2017).

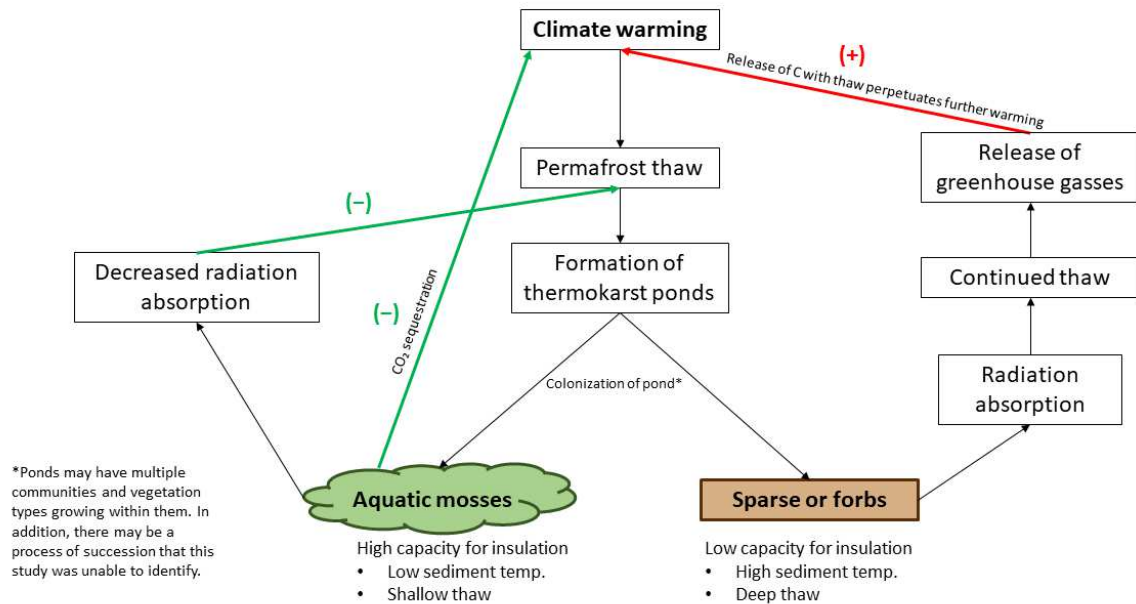


Figure 23. Conceptual diagram of possible function of thermokarst-pond plant communities in trajectory of thaw. Red arrow indicates positive feedback, green indicates negative.

4.4 Recommendations for future study

Results of this study did not identify clear environmental conditions, other than temperature and thaw depth, associated with species composition or possible successional paths for these communities. The study focused on relatively homogeneous plant communities that occur in relatively deep ponds. Shallowly flooded pond edges and polygon troughs were

generally not sampled. The range of pond ages was also rather narrow, as 28 of the 39 sampled communities were in ponds that formed between 1988 and 2007. Nutrient availability (Schneider, 2007), water transparency (Sculthorpe, 1967), littoral slope (Duarte & Kalff, 1986), and connectivity (Akasaka & Takamura, 2011) have been found to influence aquatic vegetation, and these factors were not addressed in this study. In addition, dispersal may play an essential role in thermokarst-pond plant colonization. Most aquatic plant species can propagate vegetatively, and can be dispersed by flooding (Bornette & Puijalon, 2009). Yearly runoff following snowmelt may be an important method of dispersal for aquatic plants in the Prudhoe Bay region. Waterbirds are also known to disperse aquatic plant propagules (Green et al., 2002). Evidence of waterfowl (i.e., feathers, feces) was abundant in proximity to ponds sampled within this study. Geese, gulls, and phalaropes were seen in and around ponds, and extensive evidence of grazing of *Carex aquatilis* and *Eriophorum angustifolium* along pond margins was observed.

A targeted study of vegetation succession within ponds may aid in resolving trajectories of community development. Several studies have examined vegetation succession within thermokarst ponds in the Siberian Arctic. Magnússon et al. (2020) proposed a successional trajectory involving the transitions from open water to sedges to *Sphagnum* mosses. Within that study, young ponds (those that had formed since 2010) were found to have very low moss cover relative to older ponds. Similarly, Li et al. (2017) found very little cover of moss in newly formed ponds following a nine-year shrub removal experiment as compared with older, naturally formed ponds in the same area. In both cases, mosses were assumed to represent a later stage of succession. Results of this study were not consistent with the proposed open water to sedge to moss successional process. *Sphagnum* mosses were absent in this study and generally uncommon throughout the Prudhoe Bay region which has a high soil pH due to loess deposition from the

Sagavanirktoq River (Walker, 1985; Walker & Everett, 1991). In this study, moss communities occurred in ponds of every age class, from oldest to youngest (*Figure 24*), and abundant moss growth was observed within recent formed (≤ 10 years old) ponds. Sedges were not abundant within plots sampled in this study although they occurred frequently around pond margins. It is likely that the deep water within our plots inhibited extensive sedge growth, and sedges are often dominant in early stages of pond formation when water depths are shallower.

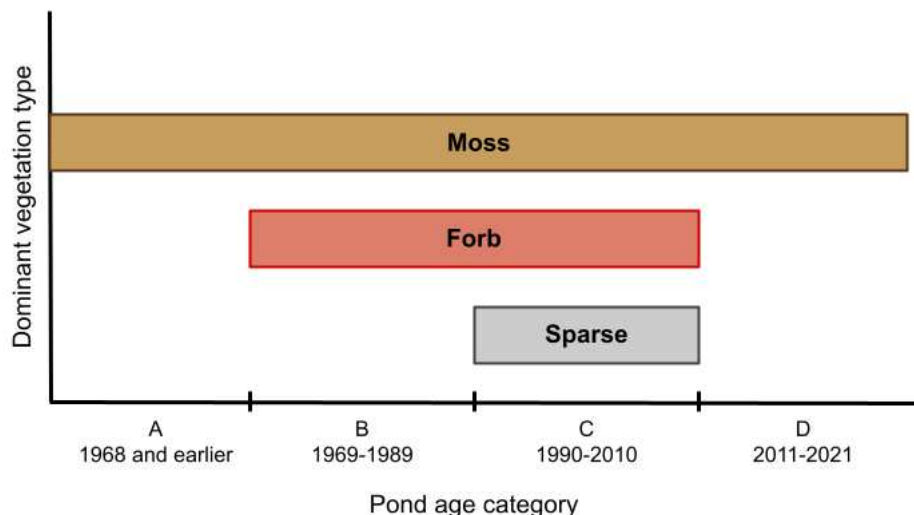


Figure 24. Occurrence of dominant vegetation types within pond age categories. Dominant types include moss ($n = 12$), forb ($n = 7$), and sparse ($n = 10$). Figure shows which age categories are included within each type.

A more thorough analysis of the exact year when ponds formed using a complete record of aerial photos may reveal trends which are obscured by the broad age categorizations used in this study. In addition, targeted study of ponds of various ages would be beneficial. Several ponds present at the Jorgenson Site in 1949 were still present in 2021. These ponds were generally deep and located at the intersection of ice wedges. Study of these old ponds may prove useful to examination of aquatic vegetation succession. Use of an ice-wedge degradation-focused framework may also help to identify successional trajectories. Jorgenson et al. (2015) and Kanevskiy et al. (2017) used 4 stages of ice-wedge degradation and stabilization to structure ecological observations: initial degradation, advanced degradation, initial stabilization, and

advanced stabilization. They found transitions from drier to wetter and then drier vegetation with stabilization. Determining degradation stage requires knowledge of subsurface conditions, which is typically obtained through permafrost coring, which was beyond the scope of this vegetation study. However, twelve ponds were cored in the summer of 2021 and only one of these was found to be actively degrading at that time (Walker et al., in preparation).

Thawing of permafrost is expected to continue under conditions of sustained climate warming (Smith et al., 2022). As permafrost thaws and ice wedges degrade, thermokarst ponds will form in some Arctic regions. Results of this study showed that vegetation colonization within a particular area of a pond influences temperature and thaw within that area, although the reasons for colonization by species remain unknown. It is important to note that this study examined plots that represent only a portion of the total pond area and that some of the ponds studied, particularly those with a large area, contained multiple plant community types. Overall effects on a pond and the underlying ice wedge may depend on the proportion of plant communities that occupy a given pond. This plant community-focused study examined small, homogeneous areas of vegetation in order to describe distinct communities. Future studies should quantify the proportion of each plant community within a given pond in order gain a pond-scale perspective of thaw dynamics.

5. Conclusions

This study provides new information about relatively understudied thermokarst-pond plant communities that have become more common in many regions of the Arctic during recent climate warming. Cluster analysis of 39 sampled vegetation plots identified seven floristically distinct groups of plots, including five provisionally described plant communities (*Calliergon*

richardsonii comm., *Scorpidium scorpioides* comm., *Pseudocalliergon turgescens* comm., *Hippuris vulgaris* comm., and *Ranunculus gmelinii* comm.) and two relatively sparsely vegetated groups. All the groups had low species diversity. Ordination analysis revealed a strong positive correlation of the first axis of the ordination with moss cover, moss thickness, and total biomass, and a negative correlation with mean sediment temperature and thaw depth.

The most important finding within this study was the extraordinarily large biomass of moss in three of the communities, particularly within young ponds. Analyses of pond sediment temperatures and thaw depths in relationship to broader vegetation categories based on dominant plot types (mosses, forbs, sparse) indicate that these categories differed in their capacity for insulation of pond sediments. In addition, factors related to vegetation were found to have negative relationships with sediment temperature and thaw. Broadly, moss-dominated thermokarst-pond plant communities insulated pond sediments to a greater degree than forb-dominated or sparsely vegetated communities. The moss communities also showed greater temperature stratification in the water column.

While the main objectives of this study (descriptions and characterization of common pond plant communities and analysis of their thermal impacts) were met, questions arose that could not be answered within the sampling framework of this study. For example, it was not possible to define a successional sequence of pond communities based on this data set or to predict if or how these communities may change in the future. Future studies should evaluate plant community composition and succession from a lens of degradation/stabilization stages, pond-formation history, and habitat variation within ponds.

References

- Abolt, C. J., Young, M. H., Atchley, A. L., Harp, D. R., & Coon, E. T. (2020). Feedbacks between surface deformation and permafrost degradation in ice wedge polygons, Arctic Coastal Plain, Alaska. *Journal of Geophysical Research: Earth Surface*, 125(3), e2019JF005349.
- Akasaka, M., & Takamura, N. (2011). The relative importance of dispersal and the local environment for species richness in two aquatic plant growth forms. *Oikos*, 120(1), 38–46.
- Alaska Climate Research Center, ACRC. (2020). *Data portal*. Alaska Climate Research Center. <https://akclimate.org/data/data-portal/>.
- AMAP. (2021). *Arctic Climate Change Update 2021*. Arctic Monitoring and Assessment Programme (AMAP).
- Andersen, M. R., Sand-Jensen, K., Iestyn Woolway, R., & Jones, I. D. (2017). Profound daily vertical stratification and mixing in a small, shallow, wind-exposed lake with submerged macrophytes. *Aquatic Sciences*, 79(2), 395–406.
- Barko, J. W., Gunnison, D., & Carpenter, S. R. (1991). Sediment interactions with submersed macrophyte growth and community dynamics. *Aquatic Botany*, 41(1–3), 41–65.
- Barko, J. W., & James, W. F. (1998). Effects of submersed aquatic macrophytes on nutrient dynamics, sedimentation, and resuspension. In *The Structuring Role of Submersed Macrophytes in Lakes* (Vol. 131, pp. 197–214). Springer Science and Business Media.
- Bates, D., Maechler, M., Bolker, B., & Walker, S. (2015). Fitting linear mixed-effects models using lme4. *Journal of Statistical Software*, 67(1), 1–48.
- Beckebanze, L., Rehder, Z., Holl, D., Wille, C., Mirbach, C., & Kutzbach, L. (2022). Ignoring carbon emissions from thermokarst ponds results in overestimation of tundra net carbon uptake. *Biogeosciences*, 19, 1225–1244.
- Billings, W. D., & Peterson, K. M. (1980). Vegetational change and ice-wedge polygons through the thaw-lake cycle in Arctic Alaska. *Arctic and Alpine Research*, 12(4), 413–432.
- Blok, D., Heijmans, M. M. P. D., Schaepman-Strub, G., van Ruijven, J., Parmentier, F. J. W., Maximov, T. C., & Berendse, F. (2011). The cooling capacity of mosses: Controls on water and energy fluxes in a Siberian tundra site. *Ecosystems*, 14(7), 1055–1065.
- Bornette, G., & Puijalon, S. (2009). Macrophytes: Ecology of aquatic plants. In *Encyclopedia of Life Sciences (ELS)*. John Wiley & Sons, Ltd.
- Bouyoucos, G. J. (1936). Directions for making mechanical analyses of soils by the hydrometer method. *Soil Science*, 42(3), 225–230.
- Capers, R. S., Selsky, R., & Bugbee, G. J. (2010). The relative importance of local conditions and regional processes in structuring aquatic plant communities. *Freshwater Biology*, 55(5), 952–966.

- Carpenter, S. R., & Lodge, D. M. (1986). Effects of submersed macrophytes on ecosystem processes. *Aquatic Botany*, 26, 341–370.
- Cook, C. D. K. (1999). The number and kinds of embryo-bearing plants which have become aquatic: A survey. *Perspectives in Plant Ecology, Evolution and Systematics*, 2(1), 79–102.
- Crowther, T., Todd-Brown, K., Rowe, C., Wieder, W., Carey, J., Machmuller, M., Snoek, B., Fang, S., Zhou, G., Allison, S., Blair, J., Bridgman, S., Burton, A., Carrillo, Y., Reich, P., Clark, J., Classen, A., Dijkstra, F., Elberling, B., & Bradford, M. (2016). Quantifying global soil carbon losses in response to warming. *Nature*, 540, 104–108.
- Dale, H. M., & Gillespie, T. J. (1977). The influence of submersed aquatic plants on temperature gradients in shallow water bodies. *Canadian Journal of Botany*, 55(16), 2216–2225.
- Daniëls, F. J. A. (1994). Vegetation classification in Greenland. *Journal of Vegetation Science*, 5(6), 781–790.
- Duarte, C. M., & Kalff, J. (1986). Littoral slope as a predictor of the maximum biomass of submerged macrophyte communities1,1. *Limnology and Oceanography*, 31(5), 1072–1080.
- Edvardsen, A., & Økland, R. H. (2006). Variation in plant species composition in and adjacent to 64 ponds in SE Norwegian agricultural landscapes. *Aquatic Botany*, 85(2), 92–102.
- Everett, K. R. (1980a). Distribution and properties of road dust along the northern portion of the Haul Road (eds Brown J, Berg R). *CRREL Report*, 80-19, p. 28. US Army Cold Regions Research and Engineering Laboratory.
- Everett, K. R. (1980b). Landforms. In *Geobotanical Atlas of the Prudhoe Bay Region, Alaska, CRREL Report*, 80-14, pp. 20–23. US Army Corps of Engineers, Cold Regions Research and Engineering Laboratory.
- Flora of North America Editorial Committee, eds. (1993). *Flora of North America North of Mexico* (Vol. 22). Oxford University Press.
- Fox, J., Weisberg, S., Price, B., Adler, D., Bates, D., Baud-Bovy, G., Bolker, B., Ellison, S., Firth, D., Friendly, M., Gorjanc, G., Graves, S., Heiberger, R., Krivitsky, P., Laboissiere, R., Maechler, M., Monette, G., Murdoch, D., Nilsson, H., ... Zeileis, A. (2021). *Companion to Applied Regression* (3.0-12). [Computer software]. <https://r-forge.r-project.org/projects/car/>.
- Gardner, W. H. (1986). Water content. In *Methods of Soil Analysis, Part 1. Physical and Mineralogical Methods* (2nd Edition, pp. 493–495). Soil Science Society of America.
- Gornall, J. L., Jónsdóttir, I. S., Woodin, S. J., & Van der Wal, R. (2007). Arctic mosses govern below-ground environment and ecosystem processes. *Oecologia*, 153(4), 931–941.
- Gould, W. A., Raynolds, M., & Walker, D. A. (2003). Vegetation, plant biomass, and net primary productivity patterns in the Canadian Arctic. *Journal of Geophysical Research: Atmospheres*, 108(D2).

- Green, A., Figuerola, J., & Sánchez, M. (2002). Implication of waterbird ecology for the dispersal of aquatic organisms. *Acta Oecologica*, 23, 177–189.
- Jones, B. M., Grosse, G., Farquharson, L. M., Roy-Léveillée, P., Veremeeva, A., Kanevskiy, M. Z., Gaglioti, B. V., Breen, A. L., Parsekian, A. D., Ulrich, M., & Hinkel, K. M. (2022). Lake and drained lake basin systems in lowland permafrost regions. *Nature Reviews Earth & Environment*, 3(1), 85–98.
- Jorgenson, M. T., Kanevskiy, M., Shur, Y., Moskalenko, N., Brown, D. R. N., Wickland, K., Striegl, R., & Koch, J. (2015). Role of ground ice dynamics and ecological feedbacks in recent ice wedge degradation and stabilization. *Journal of Geophysical Research: Earth Surface*, 120(11), 2280–2297.
- Jorgenson, M. T., Shur, Y. L., & Pullman, E. R. (2006). Abrupt increase in permafrost degradation in Arctic Alaska. *Geophysical Research Letters*, 33(2).
- Kade, A., & Walker, D. A. (2008). Experimental alteration of vegetation on nonsorted circles: Effects on cryogenic activity and implications for climate change in the Arctic. *Arctic, Antarctic, and Alpine Research*, 40(1), 96–103.
- Kallio, P., & Karenlampi, L. (1975). *Photosynthesis in mosses and lichens*. International Biome Programme No. 3, IBP Synthesis Meeting On the Functioning of Photosynthetic Systems in Different Environments, pp. 393–423.
- Kanevskiy, M., Shur, Y., Fortier, D., Jorgenson, M. T., & Stephani, E. (2011). Cryostratigraphy of late Pleistocene syngenetic permafrost (yedoma) in northern Alaska, Itkillik River exposure. *Quaternary Research*, 75(3), 584–596.
- Kanevskiy, M., Shur, Y., Jorgenson, M. T., Ping, C.-L., Michaelson, G. J., Fortier, D., Stephani, E., Dillon, M., & Tumskoy, V. (2013). Ground ice in the upper permafrost of the Beaufort Sea coast of Alaska. *Cold Regions Science and Technology*, 85, 56–70.
- Kanevskiy, M., Shur, Y., Jorgenson, T., Brown, D. R. N., Moskalenko, N., Brown, J., Walker, D. A., Raynolds, M. K., & Buchhorn, M. (2017). Degradation and stabilization of ice wedges: Implications for assessing risk of thermokarst in northern Alaska. *Geomorphology*, 297, 20–42.
- Kanevskiy, M., Shur, Y., Walker, D. A., Jorgenson, T., Raynolds, M. K., Peirce, J. L., Jones, B. M., Buchhorn, M., Matyshak, G., Bergstedt, H., Breen, A. L., Connor, B., Daanen, R. P., Liljedahl, A., Romanovsky, V. E., & Watson-Cook, E. (2022). The shifting mosaic of ice-wedge degradation and stabilization in response to infrastructure and climate change, Prudhoe Bay Oilfield, Alaska. *Arctic Science*, 8, 498–530.
- Lauridsen, T. L., Mønster, T., Raundrup, K., Nymand, J., & Olesen, B. (2019). Macrophyte performance in a low arctic lake: Effects of temperature, light and nutrients on growth and depth distribution. *Aquatic Sciences*, 82(1), 18.
- Le Moigne, A., Bartosiewicz, M., Schaeppman-Strub, G., Abiven, S., & Pernthaler, J. (2020). The biogeochemical variability of Arctic thermokarst ponds is reflected by stochastic and niche-driven microbial community assembly processes. *Environmental Microbiology*, 22(11), 4847–4862.

- Leffingwell, E. de K. (1919). *The Canning River Region, northern Alaska*. U.S. Government Printing Office.
- Lenth, R. V., Buerkner, P., Herve, M., Love, J., Miguez, F., Riebl, H., & Singmann, H. (2022). *Estimated marginal means, aka least-squares means* (1.7.2). [Computer software]. <https://github.com/rvlenth/emmeans>.
- Li, B., Heijmans, M. M. P. D., Blok, D., Wang, P., Karsanaev, S. V., Maximov, T. C., van Huissteden, J., & Berendse, F. (2017). Thaw pond development and initial vegetation succession in experimental plots at a Siberian lowland tundra site. *Plant and Soil*, 420(1), 147–162.
- Liljedahl, A. K., Boike, J., Daanen, R. P., Fedorov, A. N., Frost, G. V., Grosse, G., Hinzman, L. D., Iijima, Y., Jorgenson, J. C., Matveyeva, N., Necsoiu, M., Reynolds, M. K., Romanovsky, V. E., Schulla, J., Tape, K. D., Walker, D. A., Wilson, C. J., Yabuki, H., & Zona, D. (2016). Pan-Arctic ice-wedge degradation in warming permafrost and its influence on tundra hydrology. *Nature Geoscience*, 9(4), 312–318.
- Madsen, J. D., Wersal, R. M., & Woolf, T. E. (2007). A new core sampler for estimating biomass of submersed aquatic macrophytes. *Journal of Aquatic Plant Management*, 45, 31–34.
- Magnússon, R. Í., Limpens, J., Kleijn, D., van Huissteden, K., Maximov, T. C., Lobry, S., & Heijmans, M. M. P. D. (2021). Shrub decline and expansion of wetland vegetation revealed by very high resolution land cover change detection in the Siberian lowland tundra. *Science of The Total Environment*, 782, 146877.
- Magnússon, R., Limpens, J., Huissteden, J., Kleijn, D., Maximov, T., Rotbarth, R., Sassen-Klaassen, U., & Heijmans, M. M. P. D. (2020). Rapid vegetation succession and coupled permafrost dynamics in Arctic thaw ponds in the Siberian Lowland Tundra. *Journal of Geophysical Research: Biogeosciences*, 125(7).
- Måren, I. E., Kapfer, J., Aarrestad, P. A., Grytnes, J.-A., & Vandvik, V. (2018). Changing contributions of stochastic and deterministic processes in community assembly over a successional gradient. *Ecology*, 99(1), 148–157.
- McCune, B., & Grace, J. B. (2002). *Analysis of Ecological Communities*. MjM Software Design.
- McCune, B., & Mefford, M. J. (2018). *PC-ORD. Multivariate Analysis of Ecological Data* (7.08). Wild Blueberry Media.
- McLean, E. O. (1982). Soil pH and lime requirement. In *Methods of Soil Analysis, Part 2. Chemical and Microbiological Properties* (2nd Edition, pp. 199–224). ASA-SSSA.
- Mesquita, P. S., Wrona, F. J., & Prowse, T. D. (2010). Effects of retrogressive permafrost thaw slumping on sediment chemistry and submerged macrophytes in Arctic tundra lakes. *Freshwater Biology*, 55(11), 2347–2358.
- Minchin, P. R. (1987). An evaluation of the relative robustness of techniques for ecological ordination. *Vegetatio*, 69(1), 89–107.

- Mucina, L., Bültmann, H., Dierßen, K., Theurillat, J., Raus, T., Čarní, A., Šumberová, K., Willner, W., Dengler, J., García, R. G., Chytrý, M., Hájek, M., Di Pietro, R., Iakushenko, D., Pallas, J., Daniëls, F. J. A., Bergmeier, E., Santos Guerra, A., Ermakov, N., ... Tichý, L. (2016). Vegetation of Europe: Hierarchical floristic classification system of vascular plant, bryophyte, lichen, and algal communities. *Applied Vegetation Science*, 19(S1), 3–264.
- Mueller-Dombois, D., & Ellenberg, H. (1974). *Aims and Methods of Vegetation Ecology*. John Wiley & Sons, Ltd.
- Munsell Color. (1975). *Munsell soil color charts*. Macbeth Division of Kollmorgen Instruments Corporation, New Windsor, NY.
- Nauta, A. L., Heijmans, M. M. P. D., Blok, D., Limpens, J., Elberling, B., Gallagher, A., Li, B., Petrov, R. E., Maximov, T. C., van Huissteden, J., & Berendse, F. (2015). Permafrost collapse after shrub removal shifts tundra ecosystem to a methane source. *Nature Climate Change*, 5(1), 67–70.
- Nelson, F. E., Anisimov, O. A., & Shiklomanov, N. I. (2001). Subsidence risk from thawing permafrost. *Nature*, 410(6831), 889–890.
- O'Donnell, J. A., Romanovsky, V. E., Harden, J. W., & McGuire, A. D. (2009). The effect of moisture content on the thermal conductivity of moss and organic soil horizons from black spruce ecosystems in Interior Alaska. *Soil Science*, 174(12), 646–651.
- Page, A., Miller, R. H., & Keeney, D. R. (1982). Chemical and microbiological properties. In *Methods of Soil Analysis* (2nd ed., p. 24). Soil Science Society of America, Inc.
- Persson, I., & Jones, I. D. (2008). The effect of water colour on lake hydrodynamics: A modelling study. *Freshwater Biology*, 53(12), 2345–2355.
- Peters, D. B. (1965). Water Availability. In *Methods of Soil Analysis* (pp. 279–285). John Wiley & Sons, Ltd.
- Pienitz, R., Doran, P. T., & Lamoureux, S. F. (2008). Origin and geomorphology of lakes in the polar regions. In *Polar Lakes and Rivers* (pp. 25–41). Oxford University Press.
- Pisarenko, O. Y. (2020). New moss records from the Republic of Tuva. *Turczaninowia*, 23(2), 64–69.
- R Core Team. (2020). *R: A language and environment for statistical computing* (4.0.3). [Computer software]. R Foundation for Statistical Computing.
- Rautio, M., Dufresne, F., Laurion, I., Bonilla, S., Vincent, W. F., & Christoffersen, K. S. (2011). Shallow freshwater ecosystems of the Circumpolar Arctic. *Ecoscience*, 18(3), 204–222.
- Raynolds, M. K., Walker, D. A., Ambrosius, K. J., Brown, J., Everett, K. R., Kanevskiy, M., Kofinas, G. P., Romanovsky, V. E., Shur, Y., & Webber, P. J. (2014). Cumulative geoecological effects of 62 years of infrastructure and climate change in ice-rich permafrost landscapes, Prudhoe Bay Oilfield, Alaska. *Global Change Biology*, 20(4), 1211–1224.

- Raynolds, M. K., Walker, D. A., & Maier, H. A. (2006). *Alaska Arctic Tundra Vegetation Map* (Map No. 2) [Map]. U.S. Fish and Wildlife Service.
- Riis, T., Christoffersen, K. S., & Baattrup-Pedersen, A. (2014). Effects of warming on annual production and nutrient-use efficiency of aquatic mosses in a High Arctic lake. *Freshwater Biology*, 59(8), 1622–1632.
- Riis, T., Olesen, B., Katborg, C. K., & Christoffersen, K. S. (2010). Growth rate of an aquatic bryophyte (*Warnstorffia fluitans* (Hedw.) Loeske) from a High Arctic Lake: Effect of nutrient concentration. *Arctic*, 63(1), 100–106.
- Riis, T., & Sand-Jensen, K. (1997). Growth reconstruction and photosynthesis of aquatic mosses: Influence of light, temperature and carbon dioxide at depth. *Journal of Ecology*, 85(3), 359–372.
- Schneider, S. (2007). Macrophyte trophic indicator values from a European perspective. *Limnologica*, 37(4), 281–289.
- Schuur, E. A. G., Bockheim, J., Canadell, J. G., Euskirchen, E., Field, C. B., Goryachkin, S. V., Hagemann, S., Kuhry, P., Lafleur, P. M., Lee, H., Mazhitova, G., Nelson, F. E., Rinke, A., Romanovsky, V. E., Shiklomanov, N., Tarnocai, C., Venevsky, S., Vogel, J. G., & Zimov, S. A. (2008). Vulnerability of permafrost carbon to climate change: Implications for the global carbon cycle. *BioScience*, 58(8), 701–714.
- Schuur, E. A. G., McGuire, A. D., Schädel, C., Grosse, G., Harden, J. W., Hayes, D. J., Hugelius, G., Koven, C. D., Kuhry, P., Lawrence, D. M., Natali, S. M., Olefeldt, D., Romanovsky, V. E., Schaefer, K., Turetsky, M. R., Treat, C. C., & Vonk, J. E. (2015). Climate change and the permafrost carbon feedback. *Nature*, 520, 9.
- Sculthorpe, C. D. (1967). *Biology of aquatic vascular plants*. St. Martin's Press, New York, NY.
- Shur, Y., & Jorgenson, M. (2007). Patterns of permafrost formation and degradation in relation to climate and ecosystems. *Permafrost and Periglacial Processes*, 18, 7–19.
- Shur, Y., Jorgenson, M. T., & Kanevskiy, M. Z. (2011). Permafrost. In *Encyclopedia of Snow, Ice, and Glaciers* (pp. 841–848). Springer.
- Smith, S. L., O'Neill, H. B., Isaksen, K., Noetzli, J., & Romanovsky, V. E. (2022). The changing thermal state of permafrost. *Nature Reviews Earth & Environment*, 3(1), 10–23.
- Swanson, D. K. (2022, February 7). *A Tale of Three Lakes (that Drained)* [Presentation]. Alaska Native Plant Society, Arctic Inventory and Monitoring Network, National Park Service.
- Theurillat, J.-P., Willner, W., Fernández-González, F., Bueltmann, H., Čarni, A., Gigante, D., Mucina, L., & Weber, H. (2020). International Code of Phytosociological Nomenclature. 4th edition. *Applied Vegetation Science*, 24(1), e12491.
- Thiemer, K., Christiansen, D. M., Petersen, N. S., Mortensen, S. M., & Christoffersen, K. S. (2018). Reconstruction of annual growth in relation to summer temperatures and translocation of nutrients in the aquatic moss *Drepanocladus trifarius* from West Greenland. *Polar Biology*, 41(11), 2311–2321.

- Tichý, L., Chytry, M., & Bruelheide, H. (2006). Statistical determination of diagnostic species for site groups of unequal size. *Journal of Vegetation Science*, 17.
- van Breemen, N. (1995). How Sphagnum bogs down other plants. *Trends in Ecology & Evolution*, 10(7), 270–275.
- van Everdingen, R. (1998). *Multi-language glossary of permafrost and related ground-ice terms*. The Arctic Institute of North America.
- Viereck, L. A., Dyrness, C. T., Batten, A. R., & Wenzlick, K. J. (1992). The Alaska vegetation classification. *Gen. Tech. Rep., PNW-GTR-28*, 278. U.S. Department of Agriculture, Forest Service, Pacific Northwest Research Station.
- Vonk, J. E., Tank, S. E., Bowden, W. B., Laurion, I., Vincent, W. F., Alekseychik, P., Amyot, M., Billet, M. F., Canário, J., Cory, R. M., Deshpande, B. N., Helbig, M., Jammet, M., Karlsson, J., Larouche, J., MacMillan, G., Rautio, M., Walter Anthony, K. M., & Wickland, K. P. (2015). Reviews and syntheses: Effects of permafrost thaw on Arctic aquatic ecosystems. *Biogeosciences*, 12(23), 7129–7167.
- Walker, D. A. (1985). Vegetation and environmental gradients of the Prudhoe Bay Region, Alaska. *CRREL Report*, 85-14, 240. US Army Cold Regions Research and Engineering Laboratory, Hanover, NH.
- Walker, D. A., Buchhorn, M., Kanevskiy, M., Matyshak, G. V., Raynolds, M. K., Shur, Y. L., & Wirth, L. M. (2015). Infrastructure-Thermokarst-Soil-Vegetation interactions at Lake Colleen Site A, Prudhoe Bay, Alaska. *Alaska Geobotany Center Data Report, AGC 15-01*, 100. Institute of Arctic Biology, University of Alaska Fairbanks.
- Walker, D. A., Everett, K. R., Webber, P. J., & Brown, J. (1980). Geobotanical atlas of the Prudhoe Bay region, Alaska. *CRREL Report*, 80-14, 69. US Army Corps of Engineers, Cold Regions Research and Engineering Laboratory, Hanover, NH.
- Walker, D. A., & Everett, K. R. (1991). Loess ecosystems of northern Alaska: Regional gradients and toposequence at Prudhoe Bay. *Ecological Monographs*, 16, 437–464.
- Walker, D. A., Kanevskiy, M., Breen, A. L., Kade, A., Daanen, R. P., Jones, B. M., Nicolsky, D., Bergstedt, H., Watson-Cook, E., & Peirce, J. L. (in preparation). Observations in ice-rich permafrost systems, Prudhoe Bay Alaska, 2020-21. *Alaska Geobotany Center Data Report, AGC 22-01*. Institute of Arctic Biology, University of Alaska Fairbanks.
- Walker, D. A., Kanevskiy, M., Shur, Y. L., Raynolds, M. K., Buchhorn, M., & Wirth, L. M. (2016). Road effects at Airport Study Site, Prudhoe Bay, Alaska, Summer 2015. *Alaska Geobotany Center Data Report, AGC 16-01*, 76. Institute of Arctic Biology, University of Alaska Fairbanks.
- Walker, D. A., Kanevskiy, M., Shur, Y. L., Raynolds, M. K., Peirce, J. L., Buchhorn, M., Ermokhina, K., & Druckenmiller, L. A. (2018). 2016 ArcSEES Data Report: Snow, thaw, temperature, and permafrost borehole data from the Colleen and Airport sites, Prudhoe Bay, and photos of Quintillion fiber optic cable impacts, North Slope, Alaska. *Alaska Geobotany Center Data Report, AGC 18-01*, 74. Institute of Arctic Biology, University of Alaska Fairbanks.

- Walker, D. A., Reynolds, M. K., Kanevskiy, M. Z., Shur, Y. S., Romanovsky, V. E., Jones, B. M., Buchhorn, M., Jorgenson, M. T., Šibík, J., Breen, A. L., Kade, A., Watson-Cook, E., Matyshak, G. V., Bergstedt, H., Liljedahl, A. K., Daanen, R. P., Connor, B., Nicolsky, D., & Peirce, J. L. (2022). Cumulative impacts of a gravel road and climate change in an ice-wedge-polygon landscape, Prudhoe Bay, Alaska. *Arctic Science*, 00, 1-27.
- Walker, D. A., & Webber, P. J. (1980). Vegetation: Prudhoe Bay Region, Alaska, Area 3. *CRREL Report 80-14*. [Map]. US Army Corps of Engineers, Cold Regions Research and Engineering Laboratory, Hanover, NH.
- Wickham, H. (2016). *ggplot2: Elegant Graphics for Data Analysis*. Springer-Verlag. [Computer software]. <https://ggplot2.tidyverse.org/>.

Appendices

Appendix A. Environmental data summary, including mean, standard deviation (SD), and sample size (n) for each group of plots.

	Group Community n	1 <i>Calliergon richardsonii</i> 14	2 <i>Scorpidium scorpioides</i> 5	3 <i>Hippuris vulgaris</i> 7	4 <i>Pseudocalliergon turgescens</i> 2	5 <i>Ranunculus gmelini</i> 2	6 Sparsely vegetated A 4	7 Sparsely vegetated B 5							
Pond age	Age groups	C (n = 12), D (n = 2)	C (n = 3), B (n = 1), A (n = 1)	C (n = 5), B (n = 2)	C (n = 1), D (n = 1)	C (n = 2)	C (n = 4)	C (n = 5)							
		Mean	SD	Mean	SD	Mean	SD	Mean	SD						
	Species richness	3.00	1.57	4.00	2.35	3.57	1.51	3.50	0.71	2.50	2.12	3.25	0.96	2.60	1.34
% Cover (Live/Dead)	Erect dwarf shrub (D)	0.00	0.00	0.00	0.00	0.03	0.05	0.00	0.00	0.05	0.07	0.00	0.00	0.00	0.00
	Prostrate dwarf shrub (D)	0.00	0.00	0.00	0.00	0.01	0.04	0.00	0.00	0.00	0.00	0.10	0.00	0.04	0.05
	Evergreen shrub (D)	0.00	0.00	0.00	0.00	0.00	0.00	0.00	0.00	0.00	0.00	0.00	0.00	0.02	0.04
	Deciduous shrub (D)	0.00	0.00	0.00	0.00	0.01	0.04	0.00	0.00	0.00	0.00	0.10	0.00	0.04	0.05
	Erect forbs (L)	4.14	6.47	0.06	0.09	70.86	31.30	0.00	0.00	99.50	34.65	0.53	0.61	0.22	0.49
	Erect forbs (D)	0.72	2.67	0.00	0.00	5.43	8.70	0.00	0.00	0.05	0.07	0.00	0.00	0.02	0.04
	Non-tussock graminoid (L)	0.01	0.03	0.06	0.05	0.00	0.00	0.00	0.00	0.00	0.00	1.25	1.89	0.00	0.00
	Non-tussock graminoid (D)	0.01	0.03	1.02	2.23	0.01	0.04	0.00	0.00	0.00	0.00	0.83	1.45	0.44	0.87
	Tussock graminoid (D)	0.00	0.00	0.00	0.00	0.00	0.00	0.00	0.00	0.00	0.00	0.00	0.00	0.40	0.89
	Moss (L)	97.16	5.94	94.04	11.46	8.83	14.58	91.55	26.23	0.05	0.07	1.90	1.66	1.90	0.84
	Moss (D)	0.86	1.74	0.00	0.00	0.59	1.13	0.05	0.07	0.00	0.00	8.75	7.50	12.60	11.35
	Algae	26.16	37.02	17.06	32.67	24.34	33.67	11.00	15.56	0.05	0.07	0.10	0.00	0.02	0.04
Mean thickness (cm)	Rock	0.00	0.00	0.00	0.00	0.00	0.00	0.00	0.00	0.00	0.00	0.03	0.05	0.00	0.00
	Bare soil	0.00	0.00	0.00	0.00	2.14	5.67	0.00	0.00	0.00	0.00	17.75	8.66	7.20	8.07
	Marl	2.82	7.51	15.04	33.52	2.89	4.86	0.05	0.07	0.00	0.00	0.08	0.05	0.04	0.05
	Litter	100.00	0.00	100.00	0.00	95.71	7.87	12.55	17.61	100.00	0.00	82.50	12.58	93.00	7.58
	Total standing dead	0.96	1.71	3.04	4.44	6.07	8.77	0.00	0.00	0.05	0.07	9.68	7.15	13.12	11.95
	Shrub layer	0.00	0.00	0.00	0.00	0.00	0.00	0.00	0.00	0.00	0.00	6.25	1.89	3.93	5.54
Depth (cm)	Emergent layer	18.95	21.07	15.59	21.87	13.71	24.12	0.00	0.00	0.00	0.00	14.33	28.67	0.00	0.00
	Submergent layer	25.95	9.81	26.87	16.80	15.76	8.88	21.50	4.95	19.34	0.94	10.75	5.76	6.20	2.06
	Herb layer	13.24	17.41	22.59	23.98	22.38	14.73	0.00	0.00	19.34	0.94	13.42	16.92	1.60	3.58
	Live moss layer	26.13	9.92	27.80	16.00	5.05	2.67	21.50	4.95	2.50	3.54	5.67	2.23	6.87	2.89
	Dead moss layer	2.95	10.04	1.00	2.24	2.62	2.49	2.50	3.54	0.00	0.00	3.75	0.83	5.00	0.62
	Mean water July	40.53	11.16	49.56	9.16	48.49	8.03	28.15	5.16	41.10	5.52	49.90	3.71	45.36	6.72
Pond width (m)	Mean water Aug.	45.91	10.51	54.36	12.50	53.57	8.36	32.20	2.55	44.80	1.41	56.75	4.29	51.28	6.67
	Mean thaw July	34.70	4.32	36.60	4.69	40.89	4.08	30.25	4.24	43.50	1.41	40.56	1.82	45.70	2.31
	Mean thaw Aug.	44.20	5.04	43.44	6.63	50.83	4.47	40.10	2.97	53.30	0.99	49.40	4.06	55.92	3.44
	Maximum water July	44.21	11.96	55.40	10.88	55.43	7.46	31.50	3.54	49.50	6.36	57.25	2.87	54.00	6.28
	Maximum water Aug.	51.07	10.89	62.00	14.92	59.86	8.63	36.50	2.12	50.50	3.54	61.75	3.30	59.80	6.69
	Maximum width July	16.00	5.20	8.52	3.50	16.67	4.89	11.90	1.13	11.63	0.46	12.23	5.29	17.10	7.43
Water chemistry (pond bottom and surface)	Perpendicular to max July	6.83	2.38	5.16	1.17	5.37	1.88	5.45	0.07	8.40	1.56	6.13	2.70	7.20	2.05
	pH bottom	7.96	0.26	8.00	0.07	8.19	0.21	8.15	0.07	8.20	0.28	8.05	0.19	8.14	0.11
	pH surface	8.14	0.25	8.06	0.09	8.23	0.14	8.10	0.14	8.20	0.28	8.05	0.19	8.14	0.11
	Conductivity bottom (µS/cm)	300.42	64.24	366.80	69.52	317.27	60.08	264.40	9.33	259.50	36.91	377.20	55.94	284.06	45.81
	Conductivity surface (µS/cm)	296.69	62.85	371.56	69.04	312.79	59.98	269.55	12.23	258.35	35.57	381.20	58.58	282.04	47.28
	Salinity bottom (ppm)	0.19	0.05	0.20	0.00	0.19	0.04	0.20	0.00	0.15	0.07	0.20	0.00	0.16	0.05
Soil (organic horizon)	Salinity surface (ppm)	0.16	0.05	0.18	0.04	0.17	0.05	0.20	0.00	0.15	0.07	0.20	0.00	0.16	0.05
	Litter layer thickness (cm)	9.07	3.67	6.80	3.70	5.14	2.19	10.50	2.12	8.00	0.00	3.25	1.26	4.00	2.24
	Horizon thickness (cm)	14.14	5.22	22.20	6.42	17.29	5.15	7.00	0.00	9.50	0.71	21.00	6.00	13.80	5.76
	Gravimetric moisture (%)	174.85	61.66	128.34	33.26	118.16	26.09	141.06	5.03	113.00	21.76	124.46	10.61	125.75	28.96
	Volumetric moisture (%)	67.16	5.95	64.67	3.57	65.43	7.00	65.96	1.10	67.08	2.73	62.51	1.89	66.04	5.34
	Bulk density (g/cm³)	0.42	0.11	0.53	0.12	0.57	0.08	0.47	0.02	0.60	0.09	0.50	0.03	0.54	0.09
Soil (mineral horizon)	Organic matter (%)	22.33	6.45	20.10	6.09	17.82	2.15	20.99	4.43	19.98	4.01	19.68	3.08	16.98	2.25
	pH	7.42	0.16	7.34	0.29	7.46	0.18	7.33	0.01	7.39	0.34	7.29	0.12	7.47	0.16
	Horizon thickness (cm)	9.79	5.49	7.00	2.55	23.00	6.87	15.50	3.54	30.00	11.31	17.00	8.25	27.80	5.22
	Gravimetric moisture (%)	102.57	56.92	108.11	66.06	69.68	42.34	71.59	24.48	48.63	8.98	100.20	35.83	68.93	18.79
	Volumetric moisture (%)	58.36	19.54	59.16	9.52	55.55	11.42	56.33	8.04	52.49	5.63	62.46	9.97	55.66	11.67
	Bulk density (g/cm³)	0.61	0.29	0.70	0.33	0.93	0.26	0.82	0.17	1.09	0.08	0.65	0.12	0.82	0.07
Soil texture (%)	Organic matter (%)	16.13	6.89	15.94	2.92	14.99	6.12	17.76	6.22	10.62	1.27	19.16	5.43	16.17	3.96
	pH	6.85	1.98	7.48	0.20	7.45	0.21	7.17	0.08	7.45	0.01	7.34	0.19	7.32	0.15
	Sand	40.41	15.90	36.78	22.41	45.02	11.42	33.63	0.25	36.80	1.94	42.13	7.10	41.98	8.35
Biomass (g/m²)	Clay	6.55	2.48	5.22	3.14	7.97	2.85	6.74	3.08	10.56	0.00	7.97	0.96	7.69	1.20
	Silt	45.90	16.78	38.00	23.28	47.01	10.86	59.63	2.84	52.64	1.94	49.90	6.94	50.33	9.02
	Total	3079.05	1895.26	1638.62	1391.85	166.82	118.42	3134.98	586.51	274.93	215.92	172.00	104.19	428.27	168.35
	Moss	3031.83	1895.42	1629.62	1387.92	25.53	46.87	3129.76	590.77	40.02	49.62	124.31	108.31	243.85	195.19
	Shrub	10.06	21.21	0.33	0.49	11.75	23.54	0.00	0.00	29.33	37.60	7.68	2.72	21.60	16.54
Biomass (g/m²)	Forb	12.96	23.65	0.99	2.21	109.96	134.41	0.00	0.00	106.63	4.26	0.00	0.00	1.64	3.68
	Graminoid	24.20	40.37	7.68	11.49	4.86	7.48	5.21	4.26	25.49	20.55	21.79	12.00	33.22	20.40
	Litter	0.00	0.00	0.00	0.00	14.72	30.40	0.00	0.00	73.46	103.89	18.23	17.38	127.95	111.74
Mean temp. (°C, 19 July – 23 Aug. 2021)	Sediment	6.46	1.46	6.80	1.13	8.24	0.84	6.05	1.77	8.71	0.11	9.04	0.54	8.73	0.85
	Above vegetation layer	9.53	2.78	10.33	0.31	10.18	0.57	9.55	0.11	10.47	0.19	10.40	0.18	8.51	4.76
	Water surface	10.63	0.29	10.43	0.13	10.64	0.22	10.42	0.14	10.60	0.29	10.52	0.16	10.58	0.38
	Difference (water surface to sediment)	4.17	1.42	3.63	1.14	2.39	0.83	4.37	1.91	1.88	0.40	1.48	0.62	1.85	0.91

Appendix B. Species matrix, including percent cover values for each species in all 39 plots.

Taxon	Taxon code	21A-01	21A-02	21A-03	21A-04	21A-05	21A-06	21A-07	21A-08	21A-09	21A-10	21A-11	21A-12	21A-13	21A-14	21A-15	21A-16	21A-17	21A-18	21A-19	21A-21
<i>Calliergon richardsonii</i>	CALRIC	95	7	2	0	99	91	2	0.1	45	78	2	0.1	0	0	100	2	0.1	9	0.1	0.1
<i>Carex aquatilis</i>	CARAQU	0	0	0	0	0	0	0	0.1	0	0	0.1	4	0	0	0.1	0	0.1	1	0	0
<i>Hamatocaulis apponicus</i>	HAMLAP	0	0	0	0	0	0	2	0	0	0	0	0	0	0	0	0	0	0	0	0
<i>Hamatocaulis vermicosus</i>	HAMVER	0	0	0	0	0	0	0	0.1	0	0	0	0	0	0	0	0	0	0	0	16
<i>Hippuris vulgaris</i>	HIPVUL	12	0	80	0	15	4	12	0.1	0	0	0	0	90	1	0	1	3	0	0	0
<i>Meesia triquetra</i>	MESTRI	0	0	3	0	0	0	0	0	0	0	0	0	0	0	0	0	0	0	0	0
<i>Pedocalliergon</i> sp. 06-07	PSEUSP	0	0	0	0	0.1	0	0	0	0	0	0	0	0	0	0	0	0	0	0	0
<i>Pseudocalliergon</i> sp. 10-03	PSEUSP	0	0	0	0	0	0	0	0	0.1	0	0	0	0	0	0	0	0	0	0	0
<i>Pseudocalliergon</i> sp. 11-05	PSEUSP	0	0	0	0	0	0	0	0	0	0.1	0	0	0	0	0	0	0	0	0	0
<i>Pseudocalliergon turgescens</i>	PSETUR	0	0	0	0	0	0	0	0.1	0	0	0.1	0	0	0	0.1	0	0	0	0	94
<i>Ranunculus gemmifera</i>	RANGME	0	0	0	0	0	0	0	0	0	0	0	0	0	0	0	0.1	54	0	0	0
<i>Scorpidium cossonii</i>	SCOCOS	0	1	0	0	0	0	0	55	35	0	0	0.1	0	0	0	0	0	0	0	0
<i>Scorpidium revolutens</i>	SCOREV	0	0	0	0	0.1	0	0	0.1	0	0	0	0	0	0	1	0	0	0	0	0
<i>Scorpidium scorpoides</i>	SCOSCO	0	100	0	80	0	0	84	0	0	97	2	5	1	0	0	0	91	4	0	0
<i>Sparganium hyperboreum</i>	SPAHYP	0	0	0	0	0	0	0	0	0	0	0	0	0	0	0	0	0	0	0	0
<i>Utricularia vulgaris</i>	UTRVUL	0	0	15	0	0	5	5	0.1	0	0	0.1	1	0	0.1	1	0	67	0	0	0
Taxon	Taxon code	21A-22	21A-23	21A-24	21A-25	21A-26	21A-27	21A-28	21A-29	21A-30	21A-31	21A-32	21A-33	21A-34	21A-35	21A-36	21A-37	21A-38	21A-39	21A-40	
<i>Calliergon richardsonii</i>	CALRIC	0	91	2	10	100	1	0.1	96	2	0	0.1	100	100	1	104	100	0.1	100	0.1	
<i>Carex aquatilis</i>	CARAQU	0	0	0	0	0	0	0	0	0	0	0	0	0	0	0	0	0	0	0	
<i>Hamatocaulis apponicus</i>	HAMLAP	0	0	0	0	0	0	0	0	0	0	0	0	0	0	0	0	3	0.1	0	
<i>Hamatocaulis vermicosus</i>	HAMVER	0	0	0.1	0	0	0.1	0	0	0	7	0	0	0	0	0	0	0	0	0	
<i>Hippuris vulgaris</i>	HIPVUL	55	2	0	90	0	0	98	0	0	0	0	0	18	0	0	0	0	0	0	31
<i>Meesia triquetra</i>	MESTRI	0	0	0	0	0	0	0	0	0	0	0	0	0	0	0	0	0	0	0	
<i>Pedocalliergon</i> sp. 06-07	PSEUSP	0	0	0	0	0	0	0	0	0	0	0	0	0	0	0	0	0	0	0	
<i>Pseudocalliergon</i> sp. 10-03	PSEUSP	0	0	0	0	0	0	0	0	0	0	0	0	0	0	0	0	0	0	0	
<i>Pseudocalliergon</i> sp. 11-05	PSEUSP	0	0	0	0	0	0	0	0	0	0	0	0	0	0	0	0	0	0	0	
<i>Pseudocalliergon turgescens</i>	PSETUR	0	0	3	0	0	0	0	0	0	0	0	0	48	0	0	0	0	0	0	
<i>Ranunculus gemmifera</i>	RANGME	10	1	0	0	0	0	0	0	0	75	0	0	0	0	0	0	0	0	0	
<i>Scorpidium cossonii</i>	SCOCOS	0	0.1	0	0	0	0.1	0	2	0	0	0.1	0	0	0.1	0	0	0	0	0	
<i>Scorpidium revolutens</i>	SCOREV	0	0	0.1	0	0	0	0	0.1	0	0	1	0	0	0	0	0	0.1	0.1		
<i>Scorpidium scorpoides</i>	SCOSCO	0	4	0	0	0	0	0	0	0	0	0	0	0	0	0	0	0	0	0.1	
<i>Sparganium hyperboreum</i>	SPAHYP	0	0	0	0	0	0	0	0	0	0	0	0	0	0	0	0	0	0	0	
<i>Utricularia vulgaris</i>	UTRVUL	0	0	0	0	0	0	0	0	0	0	0	0	0	0	0	0	0	0	0	

Appendix C1. Environmental matrix, plots 21A-01 through 21A-21.

	Plot	21A-01	21A-02	21A-03	21A-04	21A-05	21A-06	21A-07	21A-08	21A-09	21A-10	21A-11	21A-12	21A-13	21A-14	21A-15	21A-16	21A-17	21A-18	21A-19	21A-21
Community/Cluster	CALRIC	SCOSCO	HIPVUL	SCOSCO	CALRIC	CALRIC	HIPVUL	SCOSCO	CALRIC	CALRIC	SCOSCO	Sparse A	HIPVUL	Sparse A	CALRIC	Sparse B	RANGME	SCOSCO	Sparse A	PSETUR	
Broad type	Moss	Moss	Forb	Moss	Moss	Moss	Sparse	Moss	Moss	Moss	Moss	Sparse	Forb	Sparse	Moss	Sparse	Forb	Moss	Sparse	Moss	
Site	JS	JS	JS	JS	JS	JS	JS	JS	JS	JS	JS	JS	JS	JS	JS	JS	JS	JS	NIRPO		
Latitude (decimal degrees)	70.23	70.23	70.23	70.23	70.23	70.23	70.23	70.23	70.23	70.23	70.23	70.23	70.23	70.23	70.23	70.23	70.23	70.23	70.23	70.23	
Longitude (decimal degrees)	-148.43	-148.43	-148.42	-148.42	-148.42	-148.42	-148.42	-148.42	-148.42	-148.42	-148.42	-148.42	-148.42	-148.42	-148.42	-148.42	-148.42	-148.42	-148.42	-148.45	
Pond age	Age group	C	C	C	A	C	C	C	B	D	D	C	C	B	C	C	C	C	C	C	
% Cover (Live/Dead)	Erect dwarf shrub (D)	0.0	0.0	0.1	0.0	0.0	0.0	0.0	0.0	0.0	0.0	0.0	0.0	0.0	0.0	0.0	0.0	0.0	0.0	0.0	0.0
	Prostrate dwarf shrub (D)	0.0	0.0	0.0	0.0	0.0	0.0	0.0	0.0	0.0	0.0	0.0	0.1	0.0	0.1	0.0	0.0	0.0	0.1	0.0	0.0
	Evergreen shrub (D)	0.0	0.0	0.0	0.0	0.0	0.0	0.0	0.0	0.0	0.0	0.0	0.0	0.0	0.0	0.0	0.0	0.0	0.0	0.0	0.0
	Deciduous shrub (D)	0.0	0.0	0.0	0.0	0.0	0.0	0.0	0.0	0.0	0.0	0.0	0.1	0.0	0.1	0.0	0.0	0.0	0.1	0.0	0.0
	Erect forbs (L)	12.0	0.0	95.0	0.0	15.0	9.0	17.0	0.2	0.0	0.0	0.1	1.0	90.0	1.1	1.0	1.1	124.0	0.0	0.0	0.0
	Erect forbs (D)	0.0	0.0	0.0	0.0	10.0	0.1	2.0	0.0	0.0	0.0	0.0	0.0	0.0	0.0	0.1	0.1	0.0	0.0	0.0	0.0
	Non-tussock graminoid (L)	0.0	0.0	0.0	0.0	0.0	0.0	0.1	0.0	0.0	0.1	4.0	0.0	0.0	0.1	0.0	0.0	0.1	0.1	0.0	0.0
	Non-tussock graminoid (D)	0.0	0.0	0.0	0.0	0.0	0.0	0.1	5.0	0.0	0.0	0.0	3.0	0.0	0.1	0.1	0.1	0.0	0.1	0.1	0.0
	Tussock graminoid (D)	0.0	0.0	0.0	0.0	0.0	0.0	0.0	0.0	0.0	0.0	0.0	0.0	0.0	0.0	0.0	0.0	0.0	0.0	0.0	0.0
	Moss (L)	95.0	107.0	6.0	80.0	99.0	93.3	2.2	84.1	100.0	78.3	99.1	2.1	40.1	1.2	100.2	3.1	0.1	100.0	4.1	110.1
Mean thickness (cm)	Moss (D)	0.0	0.0	0.0	0.0	0.0	0.0	0.0	3.0	0.0	0.0	4.0	0.0	5.0	0.0	5.0	0.0	5.0	0.0	5.0	0.1
	Algae	9.0	0.1	0.1	75.0	0.1	15.0	0.1	0.1	35.0	25.0	0.1	0.1	35.0	0.1	2.0	0.0	0.1	10.0	0.1	0.0
	Rock	0.0	0.0	0.0	0.0	0.0	0.0	0.0	0.0	0.0	0.0	0.0	0.0	0.0	0.0	0.0	0.0	0.0	0.0	0.0	0.0
	Bare soil	0.0	0.0	0.0	0.0	0.0	0.0	0.0	15.0	0.0	0.0	0.0	22.0	0.0	24.0	0.0	4.0	0.0	20.0	0.0	0.0
	Marl	0.1	0.1	0.0	75.0	0.0	0.0	0.1	0.0	0.0	0.1	0.1	0.1	10.0	0.1	0.1	0.1	0.0	0.0	0.0	0.0
	Litter	100.0	100.0	100.0	100.0	100.0	100.0	90.0	100.0	100.0	100.0	80.0	100.0	70.0	100.0	95.0	100.0	100.0	80.0	0.1	
	Total standing dead	0.1	0.0	0.2	10.0	1.0	0.1	5.1	5.0	0.0	4.0	0.1	8.1	0.0	5.2	0.1	5.2	0.1	5.2	0.0	0.0
	Shrub layer	0.0	0.0	0.0	0.0	0.0	0.0	0.0	0.0	0.0	0.0	0.0	0.0	0.0	0.0	0.0	0.0	0.0	0.0	0.0	0.0
	Emergent layer	39.7	45.7	0.0	0.0	47.0	0.0	0.0	0.0	0.0	0.0	0.0	32.3	57.3	58.0	0.0	35.0	0.0	0.0	0.0	0.0
	Submergent layer	22.7	43.7	14.0	13.3	39.7	35.7	7.7	13.7	19.0	12.0	17.0	8.0	25.3	12.3	28.3	7.3	20.0	46.7	18.0	25.0
Depth (cm)	Herb layer	39.7	0.0	15.7	0.0	47.0	32.0	9.7	23.7	0.0	14.3	32.3	4.0	19.7	12.0	28.7	8.0	20.0	57.0	37.7	0.0
	Live moss layer	22.7	43.7	6.3	13.3	39.7	26.7	8.3	18.3	19.0	12.0	17.0	7.7	4.3	3.0	34.7	10.7	5.0	46.7	7.3	25.0
	Dead moss layer	0.0	0.0	5.0	5.0	0.0	0.0	4.7	0.0	0.0	0.0	0.0	4.0	0.0	2.7	0.0	5.3	0.0	0.0	4.7	5.0
	Mean water July	35.2	48.2	50.0	61.8	44.4	53.2	51.6	48.0	40.6	59.8	36.6	49.8	58.6	54.8	45.0	34.4	45.0	53.2	49.2	31.8
	Mean water Aug	40.4	48.4	52.8	69.6	49.6	59.4	58.2	55.0	45.4	65.6	37.0	57.2	65.2	61.0	49.2	42.2	45.8	61.8	58.0	34.0
Depth (cm)	Mean July	35.5	29.0	43.5	36.5	35.0	34.3	41.3	41.8	37.8	37.0	38.3	40.0	35.5	41.8	43.0	47.0	42.5	37.5	38.3	27.3
	Mean Aug	45.6	38.2	54.4	39.0	37.6	40.8	50.0	50.6	48.4	45.6	50.8	47.0	45.4	52.0	54.2	58.0	54.0	38.6	45.0	38.0
	Maximum water July	37.0	48.0	55.0	71.0	48.0	57.0	60.0	55.0	41.0	62.0	43.0	54.0	65.0	61.0	54.0	46.0	54.0	60.0	57.0	34.0
	Maximum water Aug.	45.0	54.0	58.0	82.0	58.0	64.0	68.0	61.0	49.0	70.0	43.0	61.0	72.0	66.0	56.0	53.0	53.0	70.0	62.0	38.0
	Maximum width July	20.3	9.9	14.9	7.2	20.2	12.0	12.0	5.9	14.9	17.5	14.0	14.0	18.2	18.2	10.1	10.1	11.3	5.6	12.7	
Pond width (m)	Perpendicular to max July	8.2	6.3	8.2	6.1	7.3	4.7	4.7	3.6	3.3	4.1	5.5	5.5	4.6	6.2	6.2	7.3	4.3	4.3	5.5	
	pH bottom	8.2	8.0	8.1	7.9	8.0	7.8	8.0	8.0	8.2	8.2	8.1	8.2	8.2	8.2	8.2	8.3	8.4	8.0	7.8	8.2
	pH surface	8.3	8.2	8.2	8.0	8.1	8.0	8.1	8.0	8.3	8.2	8.1	8.2	8.2	8.2	8.2	8.3	8.4	8.0	7.8	8.2
	Conductivity bottom (µS/cm)	250.2	244.1	252.6	394.2	248.6	352.7	373.4	384.4	391.4	372.3	415.6	413.8	401.6	404.9	327.9	333.1	233.4	395.7	396.1	257.8
	Conductivity surface (µS/cm)	237.5	249.1	255.4	400.0	251.4	354.2	357.0	390.5	389.9	379.1	415.5	416.8	407.8	410.6	330.7	331.7	233.2	402.7	403.7	260.9
Soil (organic horizon)	Salinity bottom (ppm)	0.2	0.2	0.2	0.2	0.2	0.2	0.2	0.2	0.2	0.2	0.2	0.2	0.2	0.2	0.2	0.2	0.2	0.2	0.2	0.2
	Salinity surface (ppm)	0.1	0.1	0.1	0.2	0.1	0.2	0.2	0.2	0.2	0.2	0.2	0.2	0.2	0.2	0.2	0.2	0.2	0.2	0.2	0.2
	Litter layer thickness (cm)	7.0	10.0	4.0	1.0	4.0	16.0	6.0	6.0	6.0	6.0	7.0	7.0	2.0	3.0	3.0	11.0	3.0	8.0	10.0	3.0
	Horizon thickness (cm)	19.0	16.0	17.0	32.0	24.0	12.0	18.0	22.0	21.0	20.0	24.0	24.0	24.0	24.0	24.0	21.0	9.0	17.0	24.0	7.0
	Gravimetric moisture (%)	172.9	104.3	79.7	89.0	118.6	280.5	104.0	136.1	131.9	136.7	174.8	123.4	95.2	122.1	163.0	124.2	128.4	137.5	138.9	144.6
Soil (mineral horizon)	Volumetric moisture (%)	73.5	64.0	57.7	62.5	67.8	80.6	59.8	62.8	65.6	68.8	71.0	60.5	59.0	64.0	66.7	70.8	69.0	63.0	64.2	65.2
	Bulk density (g/cm³)	0.4	0.6	0.7	0.7	0.6	0.3	0.6	0.5	0.5	0.5	0.4	0.5	0.6	0.5	0.4	0.6	0.5	0.5	0.5	0.5
	Organic matter (%)	23.2	13.5	15.2	18.2	19.0	29.2	16.9	19.3	18.7	22.3	30.1	21.5	20.9	18.7	21.0	20.7	17.1	19.4	22.7	24.1
	pH	7.5	7.6	7.6	7.8	7.4	7.5	7.7	7.4	7.2	7.2	6.9	7.4	7.2	7.2	7.5	7.3	7.6	7.5	7.2	7.3
	Horizon thickness (cm)	7.0	6.0	29.0	7.0	8.0	0.0	19.0	11.0	9.0	8.0	7.0	16.0	14.0	16.0	4.0	26.0	38.0	4.0	8.0	13.0
Soil texture and color	Gravimetric moisture (%)	169.9	96.8	40.9	112.1	119.6	-	55.6	51.1	58.1	73.9	62.8	96.9	153.7	74.0	190.2	91.7	42.3	217.7	151.8	88.9
	Volumetric moisture (%)	81.3	63.4	44.9	72.1	77.1	-	52.8	53.7	57.5	61.3	59.4	65.8	74.9	57.9	74.7	66.1	48.5	47.1	74.6	62.0
	Organic matter (%)	18.0	12.9	11.7	16.4	13.3	-	18.4	13.8	12.7	16.4	16.2	17.2	23.0	20.5	16.2	19.2	9.7	20.4	25.9	22.2
	Field color	7.4	7.6	7.6	7.8	7.4	-	7.3	7.4	7.2	7.2	7.3	7.4	7.2	7.3	7.6	7.2	7.3	7.1	7.1	
	Sand (%)	54.2	36.2	33.4	38.2	36.2	-	48.0	38.0	40.0	37.3	38.0	46.0	56.7	44.0	37.3	58.4	51.3	-	50.0	61.6
Biomass (

Appendix C2. Environmental matrix, plots 21A-22 through 21A-40.

	Plot	21A-22	21A-23	21A-24	21A-25	21A-26	21A-27	21A-28	21A-29	21A-30	21A-31	21A-32	21A-33	21A-34	21A-35	21A-36	21A-37	21A-38	21A-39	21A-40
Community/Cluster	HIPVUL	CALRIC	Sparse B	HIPVUL	CALRIC	Sparse B	HIPVUL	CALRIC	Sparse B	RANGME	PSETUR	CALRIC	Sparse B	CALRIC	CALRIC	Sparse A	CALRIC	HIPVUL		
Broad type	Forb	Moss	Sparse	Forb	Moss	Sparse	Forb	Moss	Sparse	Forb	Moss	Moss	Sparse	Moss	Sparse	Moss	Sparse	Moss	Forb	
Site	NIRPO	NIRPO	NIRPO	NIRPO	NIRPO	NIRPO	NIRPO	NIRPO	NIRPO	NIRPO	NIRPO	NIRPO	NIRPO	NIRPO	NIRPO	NIRPO	NIRPO	NIRPO	NIRPO	
Latitude (decimal degrees)	70.23	70.23	70.23	70.23	70.23	70.23	70.23	70.23	70.23	70.23	70.23	70.23	70.23	70.23	70.23	70.23	70.23	70.23	70.23	
Longitude (decimal degrees)	-148.45	-148.45	-148.45	-148.45	-148.45	-148.45	-148.45	-148.45	-148.45	-148.45	-148.45	-148.45	-148.45	-148.45	-148.45	-148.45	-148.45	-148.45	-148.45	
Pond age	Age group	C	C	C	B	C	C	C	C	C	D	C	C	C	C	C	C	C	C	
% Cover (Live/Dead)	Erect dwarf shrub (D)	0.0	0.0	0.0	0.0	0.0	0.0	0.1	0.0	0.0	0.1	0.0	0.0	0.0	0.0	0.0	0.0	0.0	0.0	0.0
	Prostrate dwarf shrub (D)	0.0	0.0	0.1	0.1	0.0	0.1	0.0	0.0	0.0	0.0	0.0	0.0	0.0	0.0	0.1	0.0	0.0	0.0	0.0
	Evergreen shrub (D)	0.0	0.0	0.0	0.0	0.0	0.1	0.0	0.0	0.0	0.0	0.0	0.0	0.0	0.0	0.0	0.0	0.0	0.0	0.0
	Deciduous shrub (D)	0.0	0.0	0.1	0.1	0.0	0.1	0.0	0.0	0.0	0.0	0.0	0.0	0.0	0.0	0.0	0.1	0.0	0.0	0.0
	Erect forbs (L)	65.0	3.0	0.0	90.0	0.0	0.0	98.0	0.0	0.0	75.0	0.0	0.0	18.0	0.0	0.0	0.0	0.0	0.0	41.0
	Erect forbs (D)	0.0	0.0	0.0	0.0	0.0	0.0	20.0	0.0	0.0	0.0	0.0	0.0	0.0	0.0	0.0	0.0	0.0	0.0	16.0
	Non-tussock graminoid (L)	0.0	0.0	0.0	0.0	0.0	0.0	0.0	0.0	0.0	0.0	0.0	0.0	0.0	0.0	0.0	0.0	0.0	0.0	0.0
	Non-tussock graminoid (D)	0.0	0.0	2.0	0.0	0.0	0.0	0.0	0.0	0.1	0.0	0.0	0.0	0.0	0.0	0.0	0.1	0.0	0.0	0.0
	Tussock graminoid (D)	0.0	0.0	2.0	0.0	0.0	0.0	0.0	0.0	0.0	0.0	0.0	0.0	0.0	0.0	0.0	0.0	0.0	0.0	0.0
	Moss (L)	0.0	95.1	2.1	13.1	100.1	1.1	0.1	98.1	2.1	0.0	73.0	101.1	100.0	1.1	100.0	100.0	2	100.1	0.3
	Moss (D)	0.0	0.0	25.0	0.0	0.0	25.0	0.1	0.1	5.0	0.0	0.0	0.0	3.0	3.0	0.0	5.0	20.0	0.0	1.0
	Algae	85.0	90.0	0.0	50.0	0.1	0.1	95.0	0.0	0.0	22.0	1.0	1.0	0.0	0.1	90.0	0.1	3.0	0.1	0.1
	Rock	0.0	0.0	0.0	0.0	0.0	0.0	0.0	0.0	0.0	0.0	0.0	0.0	0.0	0.0	0.0	0.1	0.0	0.0	0.0
	Bare soil	0.0	0.0	10.0	0.0	0.0	0.0	0.0	0.0	2.0	0.0	0.0	0.0	0.0	0.0	20.0	0.0	5.0	0.0	0.0
	Marl	0.0	0.0	0.0	0.0	0.1	0.0	0.1	0.1	0.1	0.0	5.0	6.0	0.0	0.0	0.0	0.1	28.0	10.0	0.0
	Litter	100.0	100.0	95.0	100.0	100.0	100.0	100.0	100.0	100.0	100.0	25.0	100.0	100.0	80.0	100.0	100.0	100.0	100.0	80.0
	Total standing dead	0.0	0.0	27.1	0.1	0.0	25.2	20.1	0.1	5.1	0.0	0.0	0.0	3.0	3.0	0.0	5.0	20.2	0.0	17.0
Mean thickness (cm)	Shrub layer	0.0	0.0	8.0	0.0	0.0	11.7	0.0	0.0	0.0	0.0	0.0	0.0	0.0	0.0	0.0	9.0	0.0	0.0	0.0
	Emergent layer	0.0	0.0	0.0	0.0	43.0	0.0	38.0	0.0	0.0	0.0	17.0	50.7	0.0	33.0	0.0	0.0	0.0	0.0	0.0
	Submergent layer	14.3	23.3	7.3	8.3	42.4	3.7	30.7	23.3	8.3	18.7	18.0	16.8	37.3	4.3	30.4	16.7	4.7	15.7	10.0
	Herb layer	14.3	23.7	0.0	11.3	0.0	0.0	38.0	0.0	0.0	18.7	0.0	0.0	0.0	0.0	0.0	0.0	0.0	0.0	48.0
	Live moss layer	0.0	24.7	7.3	4.3	43.0	3.7	5.0	23.3	8.3	0.0	18.0	17.0	37.8	4.3	33.0	16.7	4.7	15.7	7.0
	Dead moss layer	0.0	0.0	4.0	0.0	0.0	5.7	5.0	0.0	5.0	0.0	0.0	0.0	37.7	5.0	0.0	3.7	3.7	0.0	3.7
Depth (cm)	Mean water July	43.0	51.0	52.8	54.2	42.4	47.4	34.0	38.8	46.0	37.2	24.5	16.8	42.0	46.2	30.4	42.6	45.8	25.2	48.0
	Mean water Aug	48.6	49.4	61.0	59.8	49.4	50.8	39.8	44.0	51.8	43.8	30.4	24.6	48.2	50.6	35.6	50.2	50.8	31.8	50.6
	Mean thaw July	48.3	37.8	42.5	39.5	31.8	47.8	38.3	34.3	47.3	44.5	33.3	31.5	27.3	44.0	27.3	34.5	42.3	39.0	40.0
	Mean thaw Aug.	58.2	51.8	53.6	51.6	38.8	53.2	46.2	46.4	53.8	52.6	42.2	40.6	40.0	61.0	38.8	45.2	53.6	45.0	50.0
	Maximum water July	47.0	57.0	63.0	58.0	45.0	56.0	44.0	43.0	54.0	45.0	29.0	19.0	43.0	51.0	33.0	51.0	57.0	29.0	59.0
	Maximum water Aug.	52.0	52.0	70.0	61.0	58.0	59.0	47.0	50.0	62.0	48.0	35.0	28.0	53.0	55.0	46.0	52.0	58.0	34.0	61.0
Pond width (m)	Maximum width July	26.7	28.3	28.3	16.2	14.7	14.7	15.9	11.8	11.8	12.0	11.1	11.1	20.6	20.6	12.5	11.1	11.1	18.9	12.8
	Perpendicular to max July	3.9	8.5	8.5	7.4	10.0	10.0	3.0	4.8	4.8	9.5	5.4	8.0	6.5	6.5	9.9	10.1	10.1	4.0	5.8
	pH bottom	8.6	7.8	8.1	8.1	8.0	8.0	8.0	8.1	8.0	7.6	8.1	8.2	8.2	8.2	7.7	8.0	7.4	8.3	
	pH surface	8.5	8.1	8.1	8.2	8.3	8.0	8.3	8.1	8.1	8.0	8.0	7.7	8.2	8.2	8.7	7.9	8.0	7.8	8.1
	Conductivity bottom (µS/cm)	273.5	298.6	300.1	252.8	226.1	232.3	316.0	317.7	315.9	285.6	271.0	317.2	231.3	238.9	187.9	294.5	294.0	389.5	351.0
	Conductivity surface (µS/cm)	273.5	298.4	297.9	247.7	227.1	231.4	295.0	317.0	316.1	283.5	278.2	315.8	231.3	232.3	180.7	294.0	293.7	346.6	351.1
Soil (organic horizon)	Salinity bottom (ppm)	0.2	0.2	0.2	0.1	0.1	0.2	0.2	0.2	0.2	0.2	0.2	0.2	0.1	0.1	0.1	0.2	0.2	0.3	0.2
	Salinity surface (ppm)	0.2	0.2	0.2	0.1	0.1	0.2	0.2	0.2	0.2	0.2	0.2	0.2	0.1	0.1	0.1	0.2	0.2	0.2	0.2
	Litter layer thickness (cm)	6.0	8.0	3.0	7.0	5.0	3.0	2.0	16.0	8.0	8.0	9.0	8.0	11.0	3.0	7.0	11.0	5.0	10.0	8.0
	Horizon thickness (cm)	17.0	17.0	15.0	12.0	12.0	13.0	23.0	12.0	15.0	10.0	7.0	15.0	8.0	5.0	11.0	8.0	12.0	10.0	10.0
	Gravimetric moisture (%)	129.3	133.9	108.3	136.1	281.8	101.4	128.1	196.1	119.9	97.6	137.5	160.3	281.0	175.0	119.8	151.3	113.5	120.0	154.7
	Volumetric moisture (%)	67.3	64.4	65.4	65.8	70.2	63.3	73.1	64.3	58.9	65.2	66.7	65.5	58.1	71.8	68.4	61.2	56.5	75.3	
Soil (mineral horizon)	Bulk density (g/cm³)	0.5	0.5	0.6	0.5	0.2	0.6	0.6	0.3	0.5	0.7	0.5	0.4	0.2	0.4	0.6	0.5	0.5	0.5	0.5
	Organic matter (%)	19.1	16.9	16.3	16.2	36.4	15.2	16.5	20.8	15.4	22.8	17.9	23.9	31.7	17.3	16.2	21.3	15.8	12.0	20.0
	pH	7.6	7.4	7.5	7.4	7.4	7.6	7.4	7.4	7.3	7.2	7.3	7.1	7.5	7.7	7.7	7.4	7.6	7.3	
	Horizon thickness (cm)	32.0	11.0	26.0	25.0	6.0	29.0	16.0	6.0	22.0	22.0	18.0	11.0	14.0	36.0	15.0	20.0	28.0	18.0	26.0
	Gravimetric moisture (%)	36.2	70.8	59.0	59.2	200.4	59.5	98.0	65.6	48.6	55.0	54.3	95.9	114.0	86.0	113.0	122.4	78.1	42.0	44.3
	Volumetric moisture (%)	42.5	61.9	48.7	58.9	64.9	64.5	58.8	40.4	56.5	50.6	63.1	54.4	68.1	59.4	54.0	51.5	44.0	50.4	
Soil texture and color	Biomass (g/m²)	1.1	3082.6	188.6	2.7	4702.0	327.8	3.3	6037.0	100.9	75.1	2712.0	1491.7	6346.7	60.9	3733.9	694.6	47.7	3498.2	28.5
	Shrub	0.0	0.0	39.5	3.8	6.0	9.3	1.6	0.0	13.7	55.9	0.0	40.6	6.0	39.5	0.0	2.2	7.7	0.0	0.0
	Forb	166.1	0.0	0.0	89.4	0.0	0.0	390.9	0.0	8.2	109.6	0.0	0.0	58.1	0.0	0.0	0.0	0.0	0.0	36.2
	Graminoid	0.0	3.3	48.8	9.3	13.2	48.2	0.0	36.7	42.2	40.0	8.2	5.5	0.0	0.5	0.5	6.0	8.8	139.8	19.7
	Litter	0.0	0.0	261.0	21.9	0.0	100.9	0.0	0.0	225.3	146.9	0.0								

Appendix D. Soils data.

Plot	21A-01	21A-02	21A-03	21A-04	21A-05	21A-06	21A-07	21A-08	21A-09	21A-10	21A-11	21A-12	21A-13	21A-14	21A-15	21A-16	21A-17	21A-18	21A-19	21A-21	
Community/Cluster	CA1RIC	SCOSCO	HIPVUL	SCOSCO	CA1RIC	HIPVUL	SCOSCO	CA1RIC	SCOSCO	Spars A	CALRIC	HIPVUL	Spars A	CALRIC	Spars A	BANGME	SCOSCO	Spars A	PSETUR		
Broad type	Moss	Moss	Forb	Moss	Moss	Moss	Moss	Moss	Moss	Forb	Forb	Moss	Moss	Forb	Moss	Forb	Moss	Moss	Moss		
Site	JS	JS	JS	JS	JS	JS	JS	JS	JS	JS	JS	JS	JS	JS	JS	JS	JS	JS	JS		
Litter layer thickness (cm)	7.0	10.0	4.0	1.0	4.0	16.0	6.0	6.0	6.0	7.0	7.0	2.0	3.0	3.0	11.0	3.0	8.0	10.0	3.0	12.0	
Horizon thickness (cm)	19.0	16.0	17.0	32.0	24.0	12.0	18.0	22.0	21.0	20.0	24.0	24.0	24.0	24.0	9.0	21.0	9.0	17.0	24.0	7.0	
Gravimetric moisture (%)	172.9	104.3	79.7	89.0	118.6	280.5	104.0	136.1	131.9	136.7	174.8	123.4	95.2	122.1	163.0	124.2	128.4	137.5	138.9	144.6	
Soil (organic horizon)	Volumetric moisture (%)	73.5	64.0	57.7	62.5	67.8	80.6	59.8	62.8	65.6	68.8	71.0	60.5	59.0	64.0	66.7	70.8	69.0	63.0	64.2	65.2
Bulk density (g/cm³)	0.4	0.6	0.7	0.7	0.6	0.3	0.6	0.5	0.5	0.5	0.5	0.5	0.4	0.5	0.6	0.5	0.4	0.6	0.5	0.5	
Organic matter (%)	23.2	13.5	15.2	18.2	19.0	29.2	16.9	19.3	18.7	22.3	30.1	21.5	20.9	18.7	21.0	20.7	17.1	19.4	22.7	24.1	
pH	7.5	7.6	7.6	7.4	7.5	7.5	7.7	7.4	7.2	7.2	6.9	7.4	7.2	7.2	7.5	7.3	7.6	7.5	7.2	7.3	
Horizon thickness (cm)	7.0	6.0	29.0	7.0	8.0	0.0	19.0	11.0	9.0	8.0	7.0	16.0	14.0	16.0	4.0	26.0	38.0	4.0	8.0	13.0	
Gravimetric moisture (%)	169.9	96.8	40.9	112.1	119.6	-	55.6	51.1	58.1	73.9	62.8	96.9	133.7	74.0	190.2	91.7	42.3	217.7	151.8	88.9	
Soil (mineral horizon)	Volumetric moisture (%)	81.3	63.4	44.9	72.1	77.1	-	52.8	53.7	57.5	61.3	59.4	65.8	74.9	57.9	74.7	66.1	48.5	47.1	74.6	62.0
Bulk density (g/cm³)	0.5	0.7	1.1	0.6	0.6	-	0.9	1.1	1.0	0.8	0.9	0.7	0.5	0.8	0.4	0.7	1.1	0.2	0.5	0.7	
Organic matter (%)	18.0	12.9	11.7	16.4	13.3	-	18.4	13.8	12.7	16.4	16.2	17.2	23.0	20.5	16.2	19.2	9.7	20.4	25.9	22.2	
pH	7.4	7.6	7.6	7.8	7.4	-	7.3	7.4	7.2	7.3	7.4	7.2	7.3	7.6	7.2	7.4	7.3	7.1	7.1	7.1	
Sand (%)	54.2	36.2	33.4	38.2	36.2	-	48.2	56.2	56.2	56.9	53.4	45.5	37.4	47.8	54.2	35.4	38.2	-	43.5	33.8	
Clay (%)	6.2	5.8	9.8	5.8	7.8	-	3.8	5.8	3.8	5.8	3.8	8.6	8.6	5.8	8.2	8.6	6.2	10.6	-	6.6	
Silt (%)	39.6	58.0	56.7	56.0	56.0	-	48.0	38.0	40.0	37.3	38.0	46.0	56.7	44.0	37.3	38.4	51.3	-	50.0	61.6	
Soil texture and color	sandy	silt loam	silt loam	silt loam	silt loam	-	sandy	sandy	sandy	sandy	loam	loam	sandy	sandy	loam	silt loam	silt loam	-	sandy	silt loam	
Field color	very dark brown	very dark gray	very dark gray	very dark gray	very dark gray	black	very dark brown	black													
Plot	21A-22	21A-23	21A-24	21A-25	21A-26	21A-27	21A-28	21A-29	21A-30	21A-31	21A-32	21A-33	21A-34	21A-35	21A-36	21A-37	21A-38	21A-39	21A-40		
Community/Cluster	HIPVUL	CA1RIC	Spars B	HIPVUL	CA1RIC	Spars B	HIPVUL	CA1RIC	Spars B	HIPVUL	CA1RIC	Spars B	HIPVUL	CA1RIC	Spars B	CALRIC	CA1RIC	Spars A	CALRIC	HIPVUL	
Broad type	Forb	Moss	Spars	Forb	Moss	Spars	Forb	Moss	Spars	Forb	Moss	Spars	Forb	Moss	Spars	Moss	Moss	Moss	Forb		
Site	NIRPO	NIRPO	NIRPO	NIRPO	NIRPO	NIRPO	NIRPO	NIRPO	NIRPO	NIRPO	NIRPO	NIRPO	NIRPO	NIRPO	NIRPO	NIRPO	NIRPO	NIRPO	NIRPO	NIRPO	
Litter layer thickness (cm)	6.0	8.0	3.0	7.0	5.0	3.0	2.0	16.0	8.0	8.0	9.0	8.0	11.0	3.0	7.0	11.0	5.0	10.0	8.0		
Horizon thickness (cm)	17.0	17.0	15.0	12.0	12.0	13.0	23.0	12.0	15.0	10.0	7.0	15.0	8.0	11.0	8.0	12.0	10.0	10.0	10.0		
Gravimetric moisture (%)	129.3	133.9	108.3	136.1	281.8	101.4	128.1	196.1	119.9	97.6	137.5	160.3	281.0	175.0	198	151.3	113.5	120.0	154.7		
Soil (organic horizon)	67.3	64.4	65.4	65.8	63.3	73.1	64.3	58.9	65.2	66.7	65.5	58.1	71.8	68.4	69.8	61.2	56.5	75.3			
Bulk density (g/cm³)	0.5	0.5	0.6	0.5	0.2	0.6	0.3	0.5	0.7	0.5	0.4	0.2	0.4	0.2	0.4	0.5	0.5	0.5	0.5		
Organic matter (%)	19.1	16.9	16.3	16.2	36.4	15.2	16.5	20.8	15.4	22.8	17.9	23.9	31.7	17.3	16.2	21.3	15.8	12.0	20.0		
pH	7.6	7.4	7.5	7.4	7.4	7.6	7.6	7.4	7.3	7.2	7.3	7.1	7.5	7.7	7.7	7.4	7.6	7.3	7.3		
Horizon thickness (cm)	32.0	11.0	26.0	25.0	6.0	29.0	16.0	6.0	22.0	22.0	18.0	11.0	14.0	36.0	15.0	20.0	28.0	18.0	26.0		
Gravimetric moisture (%)	36.2	70.8	59.0	59.2	200.4	59.5	98.0	65.6	48.6	55.0	54.3	95.9	114.0	86.0	113.0	122.4	78.1	42.0	44.3		
Soil (mineral horizon)	Volumetric moisture (%)	42.5	61.9	48.7	58.9	69.8	54.9	64.5	58.8	40.4	56.5	50.6	63.1	54.4	68.1	59.4	54.0	51.5	44.0	50.4	
Bulk density (g/cm³)	1.2	0.9	0.8	1.0	0.3	0.9	0.7	0.9	0.8	1.0	0.9	0.7	0.8	0.5	0.8	0.5	0.4	1.0	1.1		
Organic matter (%)	78	15.6	15.5	14.3	26.1	15.7	21.4	11.2	10.2	11.5	13.4	19.4	25.8	20.2	20.3	22.0	13.0	8.8	8.3		
pH	7.8	7.4	7.4	7.3	7.6	7.3	7.4	7.6	7.5	7.5	7.2	7.1	7.1	7.7	7.4	7.6	7.5	7.6	7.6		
Sand (%)	53.8	52.2	50.2	41.8	35.4	33.4	35.4	53.4	51.4	35.4	33.5	35.5	31.4	39.4	27.4	29.4	31.8	43.5	65.1		
Clay (%)	8.6	5.8	8.6	12.6	6.6	8.6	8.6	6.6	8.6	10.6	8.9	8.6	6.6	6.6	8.2	6.6	10.6	6.6	6.6		
Silt (%)	37.6	42.0	41.3	45.6	58.0	58.0	56.0	40.0	40.0	54.0	57.6	56.0	62.0	54.0	64.4	64.0	59.6	46.0	28.4		
Soil texture and color	sandy	sandy	loam	loam	loam	loam	loam	loam	loam	loam	loam	loam	loam	loam	loam	loam	loam	loam	loam		
Field color	very dark gray	very dark gray	very dark gray	very dark gray	grayish brown	black	very dark gray	very dark gray	black	very dark gray											

Appendix E. Biomass data.

Plot	21A-01	21A-02	21A-03	21A-04	21A-05	21A-06	21A-07	21A-08	21A-09	21A-10	21A-11	21A-12	21A-13	21A-14	21A-15	21A-16	21A-17	21A-18	21A-19	21A-21	
Community/Cluster	CALRIC	SCOSCO	HIPVUL	SCOSCO	CALRIC	CALRIC	HIPVUL	SCOSCO	CALRIC	CALRIC	HIPVUL	Sparse A	HIPVUL	Sparse A	CALRIC	Sparse B	RANGMI	SCOSCO	Sparse A	PSETUR	
Broad type	Moss	Moss	Forb	Moss	Moss	Moss	Forb	Moss	Moss	Moss	Forb	Sparse	Moss	Sparse	Forb	Moss	Sparse	Forb	Moss	Moss	
Site	JS	JS	JS	JS	JS	JS	JS	JS	JS	JS	NIRPO										
Total	237.9	2609.0	121.7	225.9	1075.6	2215.3	234.1	324.0	2146.8	4277.7	3394.6	107.5	37.3	177.6	3248.7	573.4	122.3	1639.7	316.9	3549.7	
Moss	165.6	2607.9	13.2	220.9	2183.0	1042.2	129.4	310.8	2017.4	4205.9	3368.8	57.0	0.6	111.3	3244.9	541.1	4.9	1639.7	281.2	3547.5	
Biomass (g/m ²)	Shrub	3.3	1.1	64.1	0.0	0.0	7.1	12.6	0.5	74.0	0.0	0.0	3.8	0.0	9.9	1.6	6.0	2.7	0.0	9.3	0.0
Forb	69.1	0.0	44.4	4.9	28.0	26.3	6.0	0.0	0.0	0.0	0.0	0.0	0.0	0.0	0.0	0.0	0.0	0.0	0.0	0.0	
Graminoid	0.0	0.0	0.0	0.0	4.4	0.0	4.9	12.6	55.4	71.8	25.8	36.2	0.0	15.9	2.2	26.3	11.0	0.0	26.3	2.2	
Litter	0.0	0.0	0.0	0.0	0.0	0.0	81.1	0.0	0.0	0.0	0.0	10.4	0.0	40.6	0.0	0.0	0.0	0.0	0.0	0.0	
Plot	21A-22	21A-23	21A-24	21A-25	21A-26	21A-27	21A-28	21A-29	21A-30	21A-31	21A-32	21A-33	21A-34	21A-35	21A-36	21A-37	21A-38	21A-39	21A-40		
Community/Cluster	HIPVUL	CALRIC	Sparse B	HIPVUL	CALRIC	Sparse B	HIPVUL	CALRIC	Sparse B	HIPVUL	CALRIC	CALRIC	Sparse B	CALRIC	CALRIC	Sparse A	CALRIC	HIPVUL	CALRIC	Sparse A	
Broad type	Forb	Moss	Sparse	Forb	Moss	Sparse	Forb	Moss	Sparse	Forb	Moss	Moss	Moss	Moss	Moss	Moss	Moss	Moss	Moss	Forb	
Site	NIRPO	NIRPO	NIRPO	NIRPO	NIRPO	NIRPO	NIRPO	NIRPO	NIRPO	NIRPO	NIRPO										
Total	167.2	3085.9	53.7.8	127.2	4721.2	486.3	395.8	6073.7	390.3	427.6	2720.3	1537.7	6410.8	153.5	3734.4	702.8	86.1	3638.0	84.4		
Moss	1.1	3082.6	188.6	2.7	4702.0	327.8	3.3	6037.0	100.9	75.1	2712.0	1491.7	6346.7	60.9	3733.9	694.6	47.7	3498.2	28.5		
Biomass (g/m ²)	Shrub	0.0	0.0	39.5	3.8	6.0	9.3	1.6	0.0	13.7	55.9	0.0	40.6	6.0	39.5	0.0	2.2	7.7	0.0	0.0	
Forb	166.1	0.0	0.0	89.4	0.0	0.0	390.9	0.0	8.2	109.6	0.0	0.0	58.1	0.0	0.0	0.0	0.0	0.0	36.2		
Graminoid	0.0	3.3	48.8	9.3	13.2	48.2	0.0	36.7	42.2	40.0	8.2	5.5	0.0	0.5	6.0	8.8	139.8	19.7			
Litter	0.0	0.0	261.0	21.9	0.0	100.9	0.0	0.0	225.3	146.9	0.0	0.0	52.6	0.0	0.0	21.9	0.0	0.0	0.0		

Appendix F. Species list.

Mosses (n = 11)

- Calliergon richardsonii*, (Mitt.) Kindb, Calliergonaceae
Hamatocaulis lapponicus, (Norrlin) Hedenas, Calliergonaceae
Hamatocaulis vernicosus, (Mitt.) Hedenas, Calliergonaceae
Meesia triquetra, (H. Richter) Aongstr, Meesiaceae
Pseudocalliergon turgescens, (T. Jensen) Loeske, Amblystegiaceae
Pseudocalliergon sp. 1, (Limprecht) Loeske, Amblystegiaceae
Pseudocalliergon sp. 2, (Limprecht) Loeske, Amblystegiaceae
Pseudocalliergon sp. 3, (Limprecht) Loeske, Amblystegiaceae
Scorpidium cossonii, (Schimper) Hedenas, Calliergonaceae
Scorpidium revolvens, (Swartz) Rubers, Calliergonaceae
Scorpidium scorpioides, (Hedwig) Limprecht, Calliergonaceae

Forbs (n = 4)

- Hippuris vulgaris*, L., Plantaginaceae
Ranunculus gmelini, DC., Ranunculaceae
Sparganium hyperboreum, Laest. Ex Beurl., Sparganiaceae
Utricularia vulgaris, L., Lentibulariaceae

Sedges (n = 1)

- Carex aquatilis*, Wahlenb., Cyperaceae

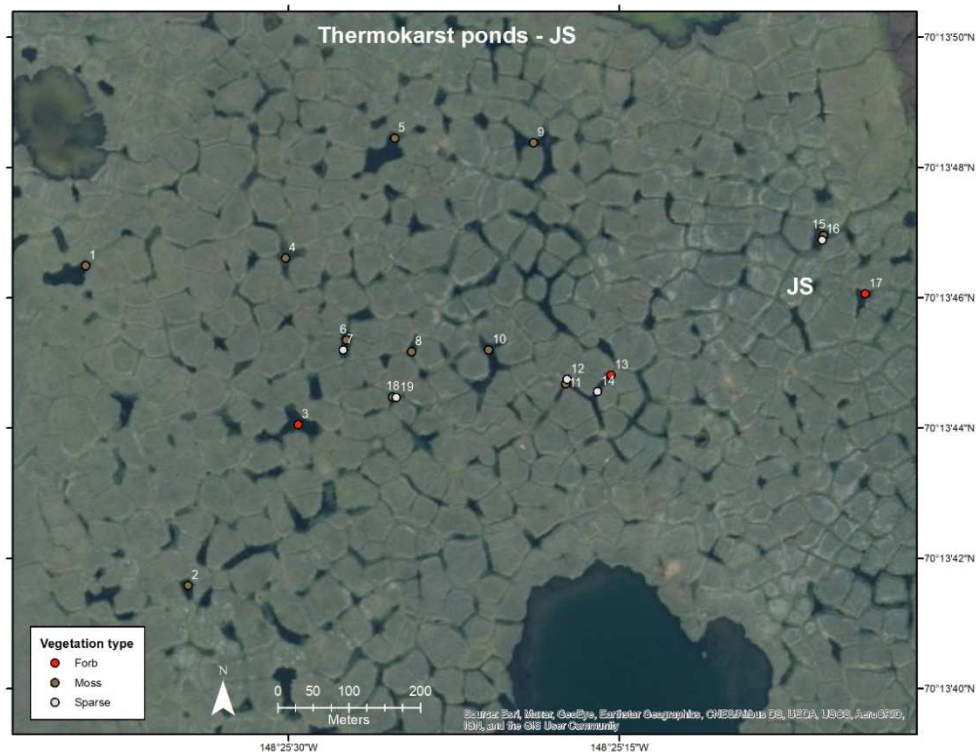
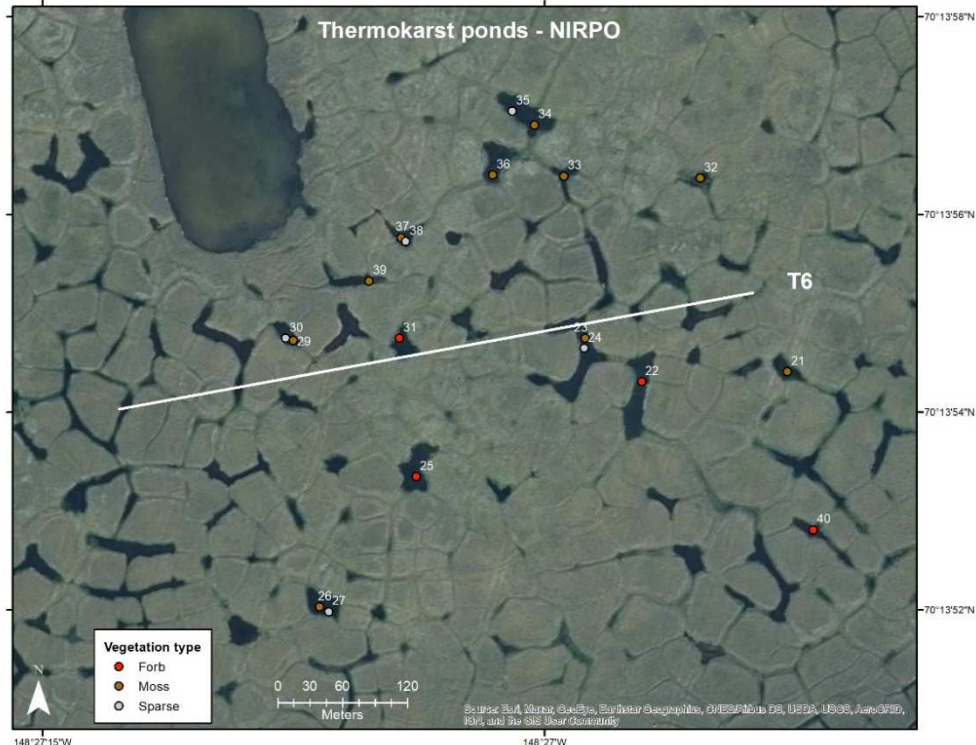
Total species richness = 16

Mosses = 68.75%

Forbs = 25.0%

Sedges = 6.25%

Appendix G. Additional plot maps of NIRPO and JS sites. Points represent plots of various vegetation types (moss, forb, sparse) within thermokarst ponds, with associated plot numbers shown. Each plot is co-located with a PVC pole containing temperature sensors. Images from Google Earth.



ProQuest Number: 29996504

INFORMATION TO ALL USERS

The quality and completeness of this reproduction is dependent on the quality
and completeness of the copy made available to ProQuest.



Distributed by ProQuest LLC (2022).

Copyright of the Dissertation is held by the Author unless otherwise noted.

This work may be used in accordance with the terms of the Creative Commons license
or other rights statement, as indicated in the copyright statement or in the metadata
associated with this work. Unless otherwise specified in the copyright statement
or the metadata, all rights are reserved by the copyright holder.

This work is protected against unauthorized copying under Title 17,
United States Code and other applicable copyright laws.

Microform Edition where available © ProQuest LLC. No reproduction or digitization
of the Microform Edition is authorized without permission of ProQuest LLC.

ProQuest LLC
789 East Eisenhower Parkway
P.O. Box 1346
Ann Arbor, MI 48106 - 1346 USA